การศึกษาพิษของบาราคอลต่อตับในหนูถีบจักร

นางวัชราภรณ์ เทวกุล ณ อยุธยา

วิทยานิพนธ์นี้เป็นส่วนหนึ่งของการศึกษาตามหลักสูตรปริญญาวิทยาศาสตรดุษฎีบัณฑิต
สาขาเภสัชศาสตร์ชีวภาพ
คณะเภสัชศาสตร์ จุฬาลงกรณ์มหาวิทยาลัย
ปีการศึกษา 2546

ISBN 974-17-5193-1

HEPATOTOXICITY STUDIES OF BARAKOL IN MICE

Mrs. Watcharaporn Devakul Na Ayutthaya

A Dissertation Submitted in Partial Fulfillment of the Requirements

for the Degree of Doctor of Philosophy Program in Biopharmaceutical Sciences

Faculty of Pharmaceutical Sciences

Chulalongkorn University

Academic Year 2003

ISBN 974-17-5193-1

Thesis Title	HEPATOTOXICITY STUDIES OF BARAKOL IN MICE
By	Mrs. Watcharaporn Devakul Na Ayutthaya
Field of Study	Ph.D. Program in Biopharmaceutical Sciences
Thesis Advisor	Associate Professor Pornpen Pramyothin, Ph.D.
Thesis Co-advisor	Professor Pawinee Piyachaturawat, Ph.D.
	Wichai Ekataksin, M.D., Ph.D.

Accepted by the Faculty of Pharmaceutical Sciences, Chulalongkorn University in Partial Fulfillment of the Requirements for the Doctor's Degree.

…….. Dean of the Faculty of Pharmaceutical Sciences
(Associate Professor Boonyong Tantisira, Ph.D.)

THESIS COMMITTEE

……Chairman
(Assistant Professor Niyada Kiatying-Angsulee, Ph.D.)

……Thesis Advisor
(Associate Professor Pornpen Pramyothin, Ph.D.)

……Thesis Co-advisor
(Professor Pawinee Piyachaturawat, Ph.D.)

……Member
(Associate Professor Thitima Pengsuparp, Ph.D.)

……Member
(Associate Professor Major General Dhasanai Suriyachan, Ph.D.)

……Member
(Associate Professor Anudep Rungsipipat, D.V.M., Ph.D.)

วัชราภรณ์ เทวกุล ณ อยุธยา: การศึกษาพิษของบาราคอลต่อตับในหนูถีบจักร (HEPATOTOXICITY STUDIES OF BARAKOL IN MICE) อาจารย์ที่ปรึกษา: รศ.ดร.พรเพ็ญ เปรมโยธิน, อาจารย์ที่ปรึกษาร่วม: ศ.ดร.ภาวิณี ปิยะจตุรวัฒน์ และ นพ.ดร.วิชัย เอกทักษิณ 141 หน้า. ISBN 974-17-5193-1.

ทำการศึกษาพิษเฉียบพลันและพิษกึ่งเฉียบพลันต่อตับของบาราคอลในหนูถีบจักร ตัวแปรที่ใช้พิจารณาความเป็นพิษต่อตับเป็นค่าชีวเคมีคลินิก (ระดับซีรั่ม AST และ ALT, total bilirubin, cholesterol, triglyceride และ glucose) และผลทางจุลพยาธิวิทยา ให้บาราคอลครั้งเดียว (100, 200, 300 และ 400 มก. ต่อ กก. ทางปาก) และในขนาดต่อเนื่อง (100, 200 และ 300 มก. ต่อ กก. ต่อ วัน ทางปาก เป็นเวลา 28 วัน) กับหนูถีบจักร ผลการศึกษาพิษเฉียบพลันและกึ่งเฉียบพลันต่อตับพบการเพิ่มขึ้นของ total bilirubin ระดับของ AST และ ALT และการลดลงของ cholesterol, triglyceride และ glucose ซึ่งสอดคล้องกับผลทางจุลพยาธิวิทยา มีการบวมน้ำของเซลล์ตับ จาก necrosis และ apoptosis กระจายรอบบริเวณ central vein และขยายไปจนถึงบริเวณ periportal และความรุนแรงของการเกิดพิษต่อตับจากบาราคอลขึ้นกับขนาดที่ได้รับและระยะเวลาที่ให้ กลไกที่เกี่ยวข้องน่าจะมาจากการกระตุ้นให้เกิด coagulative necrosis และ apoptosis เป็นผลให้การทำงานของเซลล์ตับเสียไป ผลสุดท้ายของการเกิดพิษต่อตับโดยบาราคอลขึ้นอยู่กับความสมดุลย์ระหว่างความยาวนานของการตายและกระบวนการซ่อมแซมของเซลล์ตับ พบเซลล์ตับมีการซ่อมแซมและกลับสู่สภาพเดิมในการให้บาราคอลทุกขนาด การลดระดับของ total cytochrome P450 โดยที่การแสดงออกของโปรตีนจากยีน CYP 3A1 และ 2E1 ไม่เปลี่ยนแปลง การยับยั้งการหายใจของ mitochondria และการแตกของเม็ดเลือดแดงน่าจะเกี่ยวข้องกับการเกิดพิษต่อตับจากบาราคอล

สาขาวิชาเภสัชศาสตร์ชีวภาพ ลายมือชื่อนิสิต .....

ปีการศึกษา 2546 ลายมือชื่ออาจารย์ที่ปรึกษา .....

ลายมือชื่ออาจารย์ที่ปรึกษาร่วม .....

ลายมือชื่ออาจารย์ที่ปรึกษาร่วม .....

4276959833 MAJOR: BIOPHARMACEUTICAL SCIENCES

KEYWORDS: BARAKOL / HEPATOTOXICITY / NECROSIS / APOPTOSIS / CYTOCHROME P450 / MITOCHONDRIA / MICE

WATCHARAPORN DEVAKUL NA AYUTTHAYA: HEPATOTOXICITY STUDIES OF BARAKOL IN MICE. THESIS ADVISOR: ASSOC. PROF. PORNPEN PRAMYOTHIN, THESIS CO-ADVISORS: PROF. PAWINEE PIYACHATURAWAT AND DR. WICHAI EKATAKSIN, 141 PP. ISBN 974-17-5193-1.

Acute and subacute hepatotoxicity induced by barakol were investigated in mice. Blood clinical biochemistry parameters including serum aspartate aminotransferase (AST), alanine aminotransferase (ALT), total bilirubin, cholesterol, triglyceride, glucose and histopathological examination were used as indices of liver injury. Barakol in a single dose (100, 200, 300, and 400 mg/kg, po) and repeated doses (100, 200, and 300 mg/kg/day, po, 28 days) were given to mice for acute and subacute toxicity studies. The acute and subacute hepatotoxic findings included the increase in total bilirubin, AST and ALT levels and the decrease in cholesterol, triglyceride and glucose concentrations which corresponded to the histopathological examination showing hydropic degeneration, centrilobular and invaded to periportal necrosis and apoptosis. The degree of severity from barakol-induced liver injury was dose- and time-dependent. The mechanisms involved may be the induction of coagulative necrosis and apoptosis resulting in the disturbance of normal liver cell function. The ultimate outcome of hepatotoxicity by barakol depended on the balance between the extent of damage and repair processes. There were signs of liver regeneration and recovery in all doses of barakol treatment. Reduction of total cytochrome P450 contents with unchanged protein on expression of CYP 3A1 and 2E1, inhibition of mitochondrial respiration and hemolysis of red blood cells may involve in barakol-induced hepatotoxicity.

Field of study Biopharmaceutical Sciences

Academic year 2003

Student's signature ……..

Advisor's signature ……..

Co-advisor's signature …….

Co-advisor's signature …….

ACKNOWLEDGEMENTS

I would like to express my deepest gratitude and sincere appreciation to my advisor, Assoc. Prof. Dr. Pornpen Pramyothin for her advice, guidance, excellent encouragement, kindness and support throughout my study. My great appreciation is also expressed to my co-advisors, Prof. Dr. Pawinee Piyachaturawat and Dr. Wichai Ekataksin, RBD-TGIST Distinguished Fellow, for their guidance, help, support, comments and suggestions on my research field and laboratory work. My great appreciation is also extended to Asst. Prof. Dr. Niyada Kiatying-Angsulee, Assoc. Prof. MG. Dr. Dhasanai Suriyachan, Assoc. Prof. Dr. Thitima Pengsuparp and Assoc. Prof. Dr. Anudep Rungsipipat, D.V.M., who are the committee members, for their useful comments and suggestions on this thesis.

I sincerely thank Assoc. Prof. Chaiyo Chaichantipyuth for providing barakol in this study. My appreciation is also expressed to Mrs Pranee Chavalittumrong, Dr. Songpol Chivapat, D.V.M., and Dr. Raywadee Butraporn, D.V.M., Asst. Prof. Withaya Janthasoot, Assoc. Prof. Dr. Supatra Srichairat, Assoc. Prof. Nuansri Niwattisaiwong, Prof. Dr. Sukhum Bunyaratvey, Asst. Prof. Dr. Kulawee Sujarit and Dr. Kanokpan Wongprasert for their help, support, kind assistance, technical guidance and suggestions.

I wish to thank all staff members at many places as follows: Institute of Medicinal Plant Research, Department of Medical Science and animal care facility, National Institute of Health, Ministry of Health; Department of Pharmacology, Physiology, Biochemistry and Pharmacognosy, Faculty of Pharmaceutical Sciences, Chulalongkorn University; Department of Pharmacology and Pathology, Faculty of Veterinary Science, Chulalongkorn University; Department of Pathology, Faculty of Medicine, Chulalongkorn University; Department of Physiology and Anatomy, Faculty of Science, Mahidol University; Department of Clinical Tropical Medicine, Faculty of Tropical Medicine, Mahidol University for their kind assistances.

My special thanks also extend to my classmates, all my friends and laboratory members (many places as above) for their help, sincerity, kindness and friendship.

This study was supported partly by the Graduate Research Funds from the Ministry of University Affairs and the Graduate School, Chulalongkorn University, Grant to support High Potential Research Unit, Ratchadaphiseksomphot Endowment Fund and Rangsit University.

Finally, I wish to express my deepest appreciation and infinite gratitude to my father, mother, sisters and especially my husband for their love, encouragement, understand and support that they are deserved to be mentioned as a part of my success.

CONTENTS

page

CONTENTS (cont.)

page

CONTENTS (cont.)

page

CONTENTS (cont.)

page

LIST OF TABLES

LIST OF TABLES (cont.)

page

LIST OF FIGURES

LIST OF FIGURES (cont.)

page

LIST OF FIGURES (cont.)

page

LIST OF FIGURES (cont.)

page

LIST OF FIGURES (cont.)

page

LIST OF FIGURES (cont.)

page

CHAPTER I

INTRODUCTION

Background and Rationale

Barakol is an active constituent of *Cassia siamea* or Cassod tree found in tropical zone of Asia including India, Laos, Burma, and Thailand. This plant has been used as an ingredient in Thai food such as Khi-lek curry. It is also used in Thai traditional medicine for the treatment of insomnia. In the current economic situation, alternative therapy using Thai traditional medicine is becoming attractive due to its diversity and availability. *Cassia siamea* has been prepared in tablet form to treat anxiety and insomnia since 1997. In 2001, adverse effects of *Cassia siamea* tablet were first reported with the induction of hepatitis in patients (สมบัติ ตรีประเสริฐสุข, มงคล หงษ์ศิรินิรชร และ อนุชิต จูฑะพุทธิ, 2543). The mechanism of liver inflammation associated with *Cassia siamea* remains unknown. Therefore, the present study aims to investigate the effect of barakol, active constituent in young leaves and flowers of *Cassia siamea*, on the induction of liver injury and its possible mechanisms of action *in vivo*, *ex vivo*, and *in vitro* models.

Literature Review

***Cassia siamea* Lamk.**

Cassia *siamea* (Leguminosae) or Khi-lek tree can be found mainly in tropical countries in Asia such as India, Malasia, and the Philippines. It is widely distributed throughout Thailand with different local names such as Khi-lekban

(ขี้เหล็กบ้าน), Khi-lekluang (ขี้เหล็กหลวง), Khi-lekyai (ขี้เหล็กใหญ่), Ya-ha (ยะหา) (ป่าไม้, กรม, 2491; พร้อมจิต ศรลัมพ์ และคณะ, 2532; ภูมิพิชญ์ สุธาวรรณ, 2535).

The medium sized tree of *Cassia siamea* has compound leaves and bright yellow flowers (Fig. 1). The leaves have 6-12 pairs of leaflets (15-30 cm long), elliptic-round in shape. Petals are middle sized and have bright yellow colors. Pod is nearly straight and flat shape (Chaichantipyuth, 1979). *Cassia siamea* leaves and flowers have been used as vegetable in many countries. In Thai traditional medicine, young leaves are prescribed for the treatment of insomnia, hypertension, constipation and diabetes mellitus, whereas root for fever and bark for skin disease (พร้อมจิต ศรลัมพ์ และคณะ, 2532; ภูมิพิชญ์ สุธาวรรณ, 2535). Anhydrobarakol, anthraquinone, and alkaloids are biological constituents reported in young leaves and flowers of *Cassia siamea* (Rai, 1977; Wagner *et al*., 1978).

Fig. 1. Leaves and flowers of *Cassia siamea*.

Barakol

In 1969, barakol ($C_{13}H_{12}O_4$) was first isolated from leaves and flowers of *Cassia siamea* by Hassanali-Walji, King, and Wallwork, and was identified as 3a, 4-dihydro-3a, 8-dihydroxy-2, 5-dimethyl-1, 4-dioxaphenalene. Its structure (Fig. 2) and a proposed synthetic procedure were described by Bycroft *et al.* (1970).

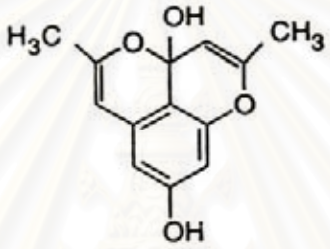

Fig. 2. Chemical structure of barakol (3a, 4-dihydro-3a, 8–dihydroxy-2, 5-dimethyl-1, 4-dioxaphenalene).

Barakol is stable in hydroxylic solvent or in a moist atmosphere but anhydrobarakol is not (Hassanali-Walji *et al*., 1969; Bycroft *et al*., 1970). It is rapidly degraded by base, but stable with strong acid in the form of anhydro-salt. The conversion reaction is described in Fig. 3 (Bycroft *et al*., 1970; Thongsaard *et al*., 2001). Therefore, anhydrobarakol changes to barakol after administration. This barakol solution remained stable for 24 hours after preparation and should be protected from light (Thongsaard *et al*., 2001). Chloroform extract from young leaves yielded 0.1 % barakol as an active constituent (Chaichantipyuth, 1979).

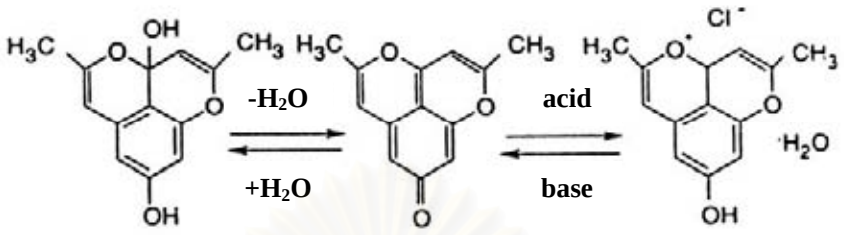

Barakol Anhydrobarakol Anhydrobarakol hydrochloride

Fig. 3. The conversion reaction of barakol, anhydrobarakol and anhydrobarakol hydrochloride (Thongsaard *et al*., 2001).

The Action of *Cassia siamea*

Pharmacological studies of *Cassia siamea* were first conducted in the experimental animals by Arunluksana (1949). Water and alcohol extracts of young leaves decreased locomotor activity and increased tension in smooth muscle in rats. It also had sedative effect in human without causing any toxicity (Arunluksana, 1949).

The effect of barakol on CNS was investigated and reported by Jantarayota (1987) that barakol had no protective effect against convulsion induced by chemicals (picrotoxin, bicucullin, and strychnine) in mice. Barakol at low dose (10-100 mg/kg, ip) decreased locomotion (Jantarayota, 1987; Sukma *et al*., 2002). At higher doses (100-200 mg/kg), barakol had analgesic effect in hot plate test by increasing nociceptive threshold. Barakol (25-100 mg/kg, ip) reduced head shake behavior in rats by suppressing serotoninergic system. Barakol may have dopaminergic effect at the doses of 75-150 mg/kg. Administration of barakol (25 mg/kg and 100 mg/kg, ip) induced sleeping behavior in rats (Bulyalert, 1992). Barakol (50-100 mg/kg, ip) prolonged thiopental-induced sleeping time in a dose-dependent manner (Sukma *et al*., 2002).

Barakol (10 mg/kg, ip) produced sedative effect with a behavioral profile similar to that of diazepam except for the increase in locomotor and exploratory behavior using elevated plus-maze model (Thongsaard *et al.*, 1995, 1996). Its mechanism of action involved dopamine agonist-like effect by acting at dopamine D2-like receptors. It inhibited the K^+-stimulated endogenous dopamine release from striatal slices with selective effects on the newly synthesized dopamine without changing the dopamine uptake (Thongsaard, Bennett, and Marsden, 1995; Thongsaard *et al*., 1997).

Barakol (0.5-15 mg/kg, iv) has hypotensive effect on blood pressure in a dose-related manner in rats and cats. Barakol (10^{-5}-10^{-3} M) reduced the phenylephrine-induced contraction of the isolated rat thoracic aorta. The mechanism involved may be its action similar to that of endothelium-derived relaxing factor (EDRF) (Suwan *et al*., 1992).

In addition, barakol has antimicrobial action against bacteria (Gritsanapan, Mekmanee, and Chulasiri, 1989). Water extract of *Cassia siamea* leaves also showed antimalarial effect on the growth of *Plasmodium falciparum* (Gbeassor *et al*., 1989).

The hexane, chloroform and methanol extracts of *Cassia siamea* leaves and flowers had antimutagenic activity against aflatoxin B_1–induced mutagenesis (Kusamran, Tepsuwan, and Kupradinum, 1998). Feeding rats with 5 % dietary of *Cassia siamea* for 14 days decreased the activities of some chemical carcinogen-activating enzymes such as aniline hydroxylase (ANH), aminopyrine-N-demethylase (AMD) as well as the capacity of S9 fractions. It also induced detoxification enzymes (glutathione-S-transferase, GST; UDP-glucuronyltransferase, UGT) (Tepsuwan and Kusamran, 1997; Tepsuwan, Kupradinum, and Kusamran, 1999). It has been suggested that barakol may have an anticarcinogenic activity.

In 2002, Maniratanachote *et al*. reported that normal diet- and high cholesterol diet-fed rats treated with barakol (30 mg/kg/day, po) for 90 days had decreased serum triglyceride but increased bilirubin levels. High cholesterol diet-fed rats treated with barakol found to decrease alkaline phosphatase (ALP) levels compared to that of barakol-treated normal diet-fed rats. There were no effects of barakol in both dietary conditions on aspartate aminotransferase (AST), alanine aminotransferase (ALT), other blood biochemistry profile, and hematological parameters. High cholesterol diet-fed rats had higher AST, ALT, ALP, and total cholesterol levels than those of normal diet-fed rats. These findings may indicate different types of liver injury caused by barakol and hypercholesterolemic condition (Maniratanachote *et al*., 2002).

Various concentrations of barakol (0.025-0.15 mM) increased aminopyrine N-demethylase and glutathione S-transferase activities with the reduction in UDP-glucuronyltransferase activity in isolated rat hepatocytes. Only high concentrations of barakol (0.1, 0.15 mM) increased the AST, ALT, and glutathione (GSH) contents with no change in malondialdehyde (MDA) formation. Cytotoxicity induced by high concentrations of barakol may involve certain xenobiotic-metabolizing enzymes (phase I and phase II), not lipid peroxidation reaction (Chirdchupunsare, Pramyothin, and Chaichantipyuth, 2003).

Toxicity

Toxicity of *Cassia siamea* is low in guinea-pigs and rats after receiving 70 and 76 g/kg of dried leaves, respectively (Arunluksana, 1949). In clinical trial, consumption of *Cassia siamea* (6-15 g) in volunteers produced no observable adverse effect (Arunluksana, 1949). Toxicity could not be observed in rats taking 10 g/kg of 50 % ethanol extract administered orally and intraperitoneally (Mokkhasmit, Sawasdimongkol, and Sartravaha, 1971).

Barakol at the dose of 10-100 mg/kg, ip, decreased locomotor activity, while at the dose of 100-200 mg/kg, barakol increased nociceptive threshold. Median convulsant dose (CD50) and median lethal dose (LD50) were 296.71 mg/kg and 324.09 mg/kg, respectively, in mice treated with barakol intraperitoneal (Jantarayota, 1987).

Acute hepatitis was reported in pateints at Phramongkutklao and Chulalongkorn Memorial Hospitals when 1-4 capsules/day of *C. siamea* leaves (400 mg dried leaves/capsule) were taken for 7-60 days. All patients had no history of chronic liver diseases. However, this hepatotoxic effect in human has not clearly been investigated whether acute hepatitis was induced by barakol or other constituents in *C. siamea* leaves (สมบัติ ตรีประเสริฐสุข และคณะ, 2543; Hongsirinirachorn, Threeprasertsuk, and Chutaputti, 2001). Chronic toxicity study of *C. siamea* tablets (1.19% anhydrobarakol/tablet) in rats was reported in 2001. *C. siamea* (20, 200, 2000 mg/kg) caused degeneration and necrosis of hepatocytes after feeding rats for 6 months. Fatty liver appearance and increased in relative liver weight were found in rats treated with 2,000 mg/kg/day of *C. siamea* corresponding to 100 folds of human therapeutic dose. The severity of the lesion was dose-dependent (Chivapat *et al*., 2001).

In 2003, adverse effects of barakol extracted from old leaves and flowers of *Cassia siamea* in 12 healthy Thai patients were reported by Hongsirinirachorn's groups (Hongsirinirachorn *et al*., 2003). The subjects took 20-40 mg/day of barakol (2-4 tablets) for 3-180 days. Eight of them had anorexia and jaundice for 4-60 days before admission. The results showed no relationship between degree of symptom and dosage/duration of barakol intake. The levels of total bilirubin and liver function test suggested moderate to severe hepatitis with no viral markers detected. Histopathological findings in 3 cases were compatible with interface hepatitis.

Liver

Liver is the largest organ in the abdomen. It consists of hepatic lobules, each of which is made up of hepatic cell plates (hepatocytes or parenchymal cells) that ultimately arranged with sinusoids. The sinusoids contain Kupffer cells whose role is to engulf and destroy materials such as bacteria and aged erythrocytes. The arachnocytes (Ekataksin and Kaneda, 1999) (also known as stellate cells, fat-storing cells, or Ito cells) are located in the perisinusoidal spaces of Disse. Liver receives blood supplies from two sources. The main blood supply derives from the portal vein which carries nutrient-rich blood from the gut, and another source is from hepatic artery that supplies oxygen-rich blood. The portal vein and hepatic artery branch together along with biliary tract system to form portal triad. Lymphatic and sympathetic nerve bundles are also found. The blood circulates from the periportal region through the sinusoids and is collected in the central vein. In contrast, the bile flows in the opposite direction from center to periphery of the lobule (Treinen-Moslen, 2001; Kierazenbaum, 2002).

From functional point of view, the hepatic lobular profile is perceived with 3 concentric zones. A peripheral zone (periportal zone) is the area close to the portal tract and periphery of the lobule. An intermediate zone is the area between periportal zone and pericentral zone. The latter is located centrilobularly surrounding the initial segment of hepatic vein system. There are structural differences and functional distinction in the lobular zones, known as the hepatic heterogeneity (Zimmerman, 1999; Meyer and Kulkarni, 2001; Treinen-Moslen, 2001). For instance, mitochondria are larger and more numerous, and lysosomes and Golgi apparatus are more abundant in periportal zone. Smooth endoplasmic reticulum is more abundant in pericentral zone. Dominant processes in periportal zone are fatty acid oxidation, gluconeogenesis, cholesterol synthesis, protein synthesis and bile acid secretion. Glycolysis and lipogenesis occur mainly in pericentral zone. Pericentral zone is also the site of high activities of enzymes-involved in the bioactivation and detoxification of xenobiotics. Glutathione is rich

in periportal zone, but low in pericentral zone (Smith *et al*., 1979). The amounts of cytochrome P450 proteins such as CYP 2E1 are also rich in pericentral zone of rat liver induced by ethanol (Tsutsumi *et al*., 1989). These enzymes are located in the endoplasmic reticulum. Therefore, agents that induce cytochrome P450 function increase the smooth endoplasmic reticulum in pericentral zone. The concentrations of bile salts are efficiently extracted by hepatocytes in periportal zone with little bile salts left in the blood that flow over hepatocytes in pericentral zone.

The liver performs many crucial functions, some of which are carried out by the hepatocytes, while the others are done by the nonparenchymal cell types (Laskin, 1990; Treinen-Moslen, 2001). These functions include synthesis, accumulation, detoxification, and transportation (Table 1).

Table 1. Major functions of the liver (Treinen-Moslen, 2001).

Recognized functions	Descriptions
Hepatocytic	
Metabolism of nutrients	carbohydrate, protein, lipid
Synthesis of plasma proteins	albumin, clotting factors, lipoproteins
Biotransformation and detoxification of xenobiotic agents	drugs, chemicals, ethanol
Formation and secretion of biliary compounds	bile acids, bilirubin and cholesterol
Nonhepatocytic	
Circulatory reservoir	sinusoidal bed, arterial vascular bed
Lymph production	endothelial fenestration
Immune modulation	Kupffer cells, NK cells, T lymphocytes
Storage	arachnocytes (retinol-storing cells)

Classification of Chemically Induced Liver Injury

Liver is the first organ to be perfused by chemicals that are absorbed in the gut. Biotransformation of chemicals may produce reactive metabolites that can induce lesions in the liver. Therefore, liver is the target organ for chemical-induced injury by drugs and xenobiotics. Toxicity produced by these agents can be divided into two broad categories: predictable (direct toxicity) and unpredictable (idiosyncratic toxicity) (Dahm and Jones, 1996; Zimmerman, 1999). Liver damaged by hepatotoxic agents in the former group is predictable interms of dose-dependent, and testing reproducibility. In contrast, idiosyncratic hepatotoxins-induced liver injuries or lesions are variable, non-dose-related manner, and testing are not reproducible in experimental animals. The patterns of liver injury occur within minutes or require several hours to develop depending on many factors such as type of toxic agents, severity of intoxication, and route of exposures. Various forms of cell injury can be recognized under the light microscope and are discussed briefly as follows:

Patterns of acute cell injury

Cellular swelling is the first manifestation of almost all forms of cell injury. It appears whenever cells are incapable of maintaining ionic and fluid homeostasis. Cell swelling is not severe and is generally reversible. This form of nonlethal and reversible injury is sometimes called hydropic change or vacuolar degeneration (Cooper, 2002).

Cell necrosis is a degenerative process leading to cell death. The most common form of necrosis found is coagulative necrosis. It occurs in the setting of irreversible exogenous injury, and this form may be localized and effected a few hepatocytes (focal necrosis) or it may involve an entire lobe (massive necrosis). It involves abrupt disruption of cell homeostasis resulting in loss of osmotic stability, cell and organelles swelling, failure of cellular energetic, and membrane leakage

with release of cytoplasmic contents (Fig. 4) (Wyllie *et al*., 1980; Gores, Herman, and Lemasters, 1990; Zimmerman, 1999; Cooper, 2002). Changes in enzyme levels in blood can be used as indicators of liver damage when plasma membrane leak. The activities of aspartate aminotransferase (AST) and alanine aminotransferase (ALT) are used to detect liver damage. Suggested mechanisms involve the irreversibility of necrotic changes, including the release of lysosomal enzymes, activation of membrane-active proteases, and phospholipases, impairment of ion homeostasis, and generations of biological reactive intermediates.

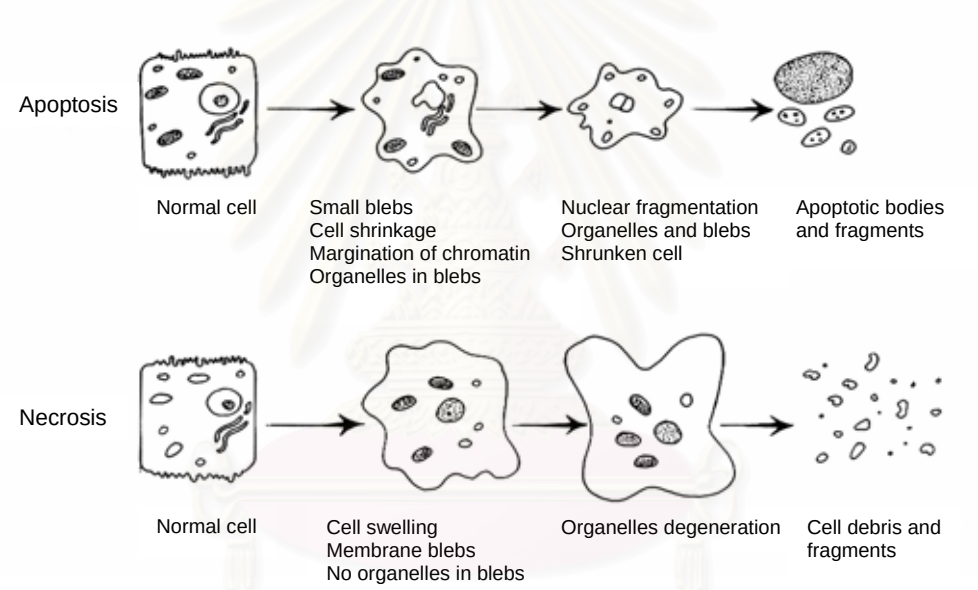

Fig. 4. Morphological changes of necrosis and apoptosis (Zimmerman, 1999).

Apoptosis is a normal physiologic process in which individual cells are activated through a controlled death program. It involves single cell or clusters of cells that appear on hematoxylin and eosin (H&E) stained sections as round or oval masses with intensely eosinophilic cytoplasm characterized by a series of morphological changes (Fig. 4). Initially, there is a decrease or shrinkage in cell volume (cytoplasmic condensation), generation of a pyknotic nucleus and chromatin condensation along the nuclear membrane. Then, there are loss of nuclear membrane, fragmentation of the nuclear chromatin and subsequent

formation of multiple fragments of condensed nuclear material along with cytoplasm, called apoptotic bodies. These features may appear on cell surface as vesicles or blebs. Finally, these fragments are phagocytosed or degraded to prevent the release of intracellular components into the surrounding area and avoid the inflammatory response (Wyllie *et al*., 1980; Zimmerman, 1999; Cooper, 2002; Jaeschke and Lemasters, 2003). Apoptosis can be distinguished from necrosis by morphological criterias, using either light or electron microscopy.

Although there are advances in the understanding of hepatotoxicity, the mechanisms by which certain chemicals- or drugs- induced liver injury or alter its function remain largely unknown. Many compounds cause cellular damage through metabolic activation to reactive intermediates. These reactive metabolites bind covalently to cellular macromolecules such as nucleic acids, proteins, and lipids, thereby changing their biological properties (Cascales *et al*., 1994; Zimmerman, 1999; Plaa, 2000). Disruption of cellular calcium, phospholipases, proteases, and endonucleases as the results of impairment of cell homeostasis may lead to cell death. Increased cytosolic calcium in turn activates function. Mitochondria and endoplasmic reticulum have been proposed as a key determinant of cell death (Corcoran and Ray, 1992; Plaa, 2000). An event now recognized to be important in both cellular necrosis and apoptosis is mitochondrial changes in membrane integrity, involving both inner and outer membranes. It leads to rapid change of permeability associated with mitochondrial permeability transition (MPT) causing membrane depolarization and release of pro-apotosis intermembrane proteins such as cytochrome c in the cytosol (Petit *et al*., 1996; Green and Reed, 1998; Lemasters *et al*., 1998, 1999; Jaeschke and Lemasters, 2003). Induction of MPT is sufficient to induce chromatin condensation and internucleosomal DNA fragmentation, which involve chromatin condensation factors such as caspase-activating factor (caspase 3) and apoptosis-inducing factor (a flavoprotein) (Kroemer *et al*., 1995, 1997, 1998; Susin *et al*., 1999; Daugas *et al*., 2000; Jaeschke and Lemasters, 2003). The Bcl-2 family of proteins is implicated in controlling the integrity of the mitochondria (Susin *et al*., 1996).

CHAPTER II

MATERIALS AND METHODS

Materials

Animals

Adult male ICR mice (weighing 25-30 g) were obtained from the National Laboratory Animal Center, Mahidol University, Salaya, Nakornpathom, Thailand. The protocols in this experiment were ethically approved by the Ethical Committee on Animal and Human Research Studies, Faculty of Pharmaceutical Sciences, Chulalongkorn University. All animals were housed in groups of two in stainless steel cages with wood shavings as bedding under controlled environmental conditions (room temperature 25 ± 1 °C with 12-hour light/dark cycle, humidity of approximately 60 %). They were given free standard mouse pellets (C.P. Mice feed, Pokphand Animal Fed Company, Limited, Bangkok) and tap water *ad libitum*. They were kept for seven days before the experiment to acclimatized into the animal care facility at Institute of Health Building, Ministry of Public Health. All experiments followed a similar time sequence between 08.00 a.m. - 06.00 p.m. each day.

Barakol Extraction and Derivative Preparation

Barakol (anhydrobarakol hydrochloride) was extracted and identified by Associate Professor Chaiyo Chaichantipyuth, Department of Pharmacognosy, Faculty of Pharmaceutical Sciences, Chulalongkorn University. The procedures of extraction and derivative preparation were done according to the scheme on page 14

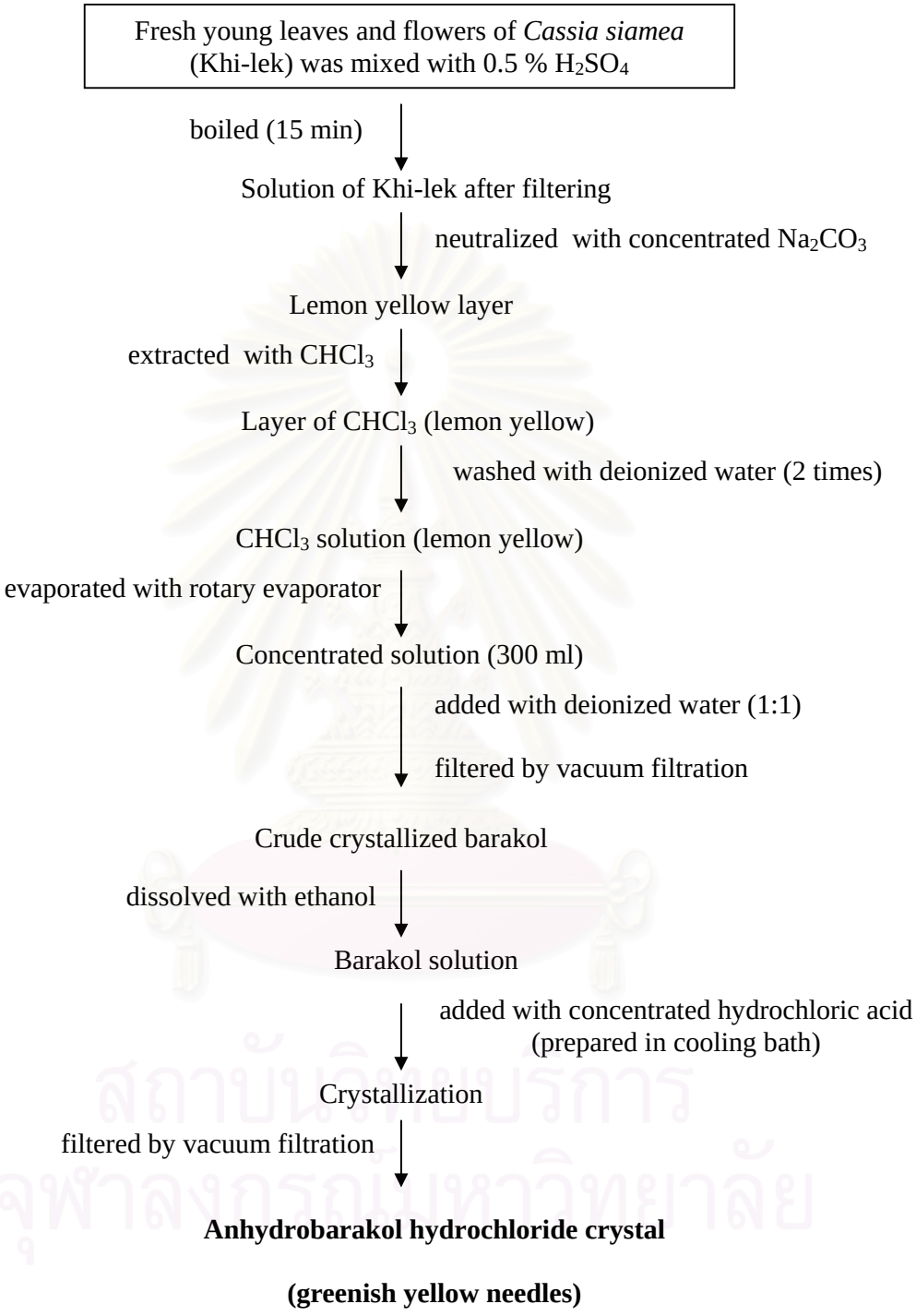

Fig. 5. The sequences of barakol extraction and derivative preparation from *Cassia siamea* leaves and flowers.

(Fig. 5). Briefly, fresh young leaves and flowers of Khi-lek were obtained from a local Bangkok market. First, they were cut into small pieces and mixed with 0.5 % sulfuric acid (H_2SO_4). Next, they were boiled for 15 minutes and filtered. The solution was kept until the temperature reach room temperature. After that, the solution was mixed with concentrated sodium carbonate (Na_2CO_3). The lemon yellow layer of the mixture was extracted with chloroform in seperating funnel. The solution was washed with deionized water, filtered, concentrated and added deionized water (1:1). Finally, the solution was filtered by vacuum filtration and crude crystallized barakol was stored in refrigerator until hydrochloride salt was prepared. For derivative preparation, the crystal was diluted in ethanol until it became colourless. Concentrated hydrochloric acid was added to obtain barakol hydrochloride. The mixture was kept at 4 $^{\circ}$C to form crystal and filtered by vacuum filtration. Finally, greenish yellow needles was identified by ultraviolet spectroscopy (UV) and thin layer chromatography (TLC). It was kept in the bottle that protected from light in the desiccator.

In this experiment, barakol solution was freshly prepared by dissolving anhydrobarakol hydrochloride crystal in distilled water and wrapped with aluminium foil.

Chemicals

Clinical biochemistry kits and tissue sections were provided by Institute of Medicinal Plant Research, Department of Medical Sciences, Ministry of Public Health.

Primary antibodies of cytochrome P450 were kindly provided by Dr. Frank J Gonzalez, National Institute of Health, National Cancer Institute, Bethesda, Maryland, USA. Secondary antibodies, Horseradish peroxidase conjugated goat anti-rabbit immunoglobulin, was purchased from Chemicon International Incorporation, USA.

Bovine serum albumin (BSA), DNAse I, Folin & Ciocalteu's phenol reagent, glycine, glycerol, propidium iodine, sodium citrate, sucrose, Trisma® base, and Tween 20 were purchased from Sigma Chemical Company, USA.

Sodium dithionite was purchased from Fluka Chemic, Japan.

Ethanol, methanol, formalin, glutaraldehyde, and xyline were purchased from Merck, Germany.

SDS-polyacrylamide, N,N,N,N,-tetramethylethylenediamine (TEMED), ammonium persulfate (APS), and non-fat dried milk were purchased from Bio-Rad, Richmon, USA.

Polyvinylidine difluoride (PVDF) sheets were purchased from Amersham, Buckinghamshire, England.

Enhanced chemiluminescence (ECL), anti-fade solution kit was purchased from Boehinger Mannheim, Germany.

Apoptosis detection kit (TUNEL assay) was purchased from Promega Corporation, USA.

Carbon monoxide gas was purchased from Thai Industrial Gases Public Company, Limited, Thailand.

All other chemicals and solvents used throughout this investigation were of analytical grade and commercially obtained.

Instruments

Instruments employed in these studies include autopipettes, surgical equipments, pH meter, vortex mixer, sonicater, incubator, centrifuge, homoginizer with pestle, glass homogenizing vessel (Heidolph), refrigerated superspeed centrifuge (Hitachi), refrigerated ultracentrifuge (Beckman), UV-160A spectrophotometer (Shimadzu), reaction chamber (Gilson), Clark oxygen electrode, amplifier, recorder (Gilson), mini Trans-Blot Electrophoretic Transfer cell (Bio-Rad), scanning densitometer, light microscopy, fluorescence microscopy, and ultra-low temperature freezer (Forma Scientific).

Methods

Part A : Dose-Time Course Effect of Barakol on Liver Injury *In Vivo* Study

Animal Treatment

Experiment I. Acute Toxicity Study

Mice were randomly divided into 5 groups (n=8) and the procedures in this study were shown at the diagram on page 18 (Fig. 6). Each animal was weighed at the beginning of the experiment. In group I, mice received distilled water only. The other groups received various single doses of barakol (100, 200, 300, and 400 mg/kg, po). They were sacrificed under light ether anesthesia at various time points (24, 48, 72, and 96 hours) after treatment. Blood samples were collected from the inferior vena cava to determine clinical biochemistry parameters. The livers from all groups were removed, weighed and divided into 2 parts. First, two-third of the liver was wrapped with aluminum foil and placed on ice for the determination of total cytochrome P450 contents in *ex vivo* study. Second, small parts of the liver were preserved in 3.7 % formaldehyde solution in phosphate buffer saline (PBS) for histopathological examination (light microscopy). The livers of mice treated

Group I	Control (distilled water)
Group II	Barakol 100 mg/kg (B100)
Group III	Barakol 200 mg/kg (B200)
Group IV	Barakol 300 mg/kg (B300)
Group V	Barakol 400 mg/kg (B400)

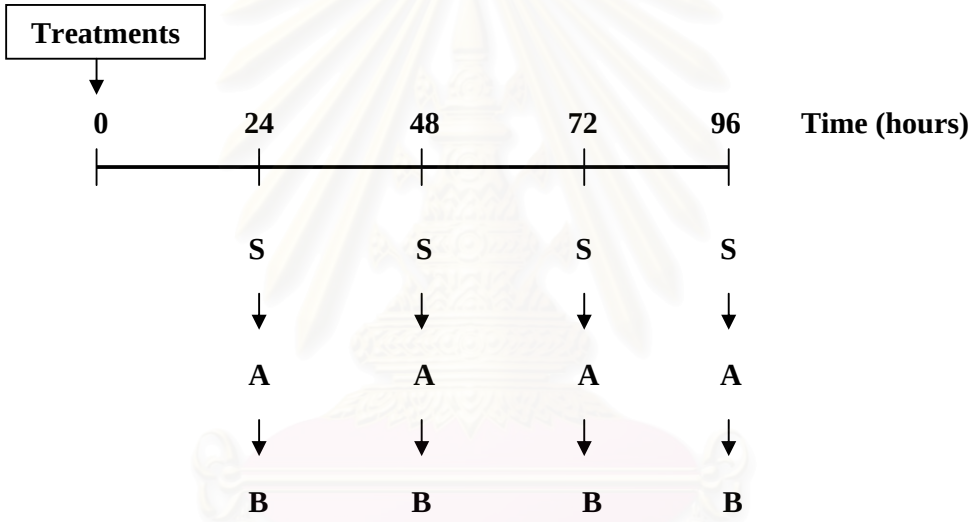

S = sample collection
A = blood and liver collection
B = clinical biochemistry analysis, and histopathological examination

Fig. 6. Schematic diagram showing dose-time course of treatment and sample collection in acute toxicity study.

with high doses (200-400 mg/kg) of barakol after 48 hours were also examined by electron microscopy for the ultrastructure of organelles.

Experiment II. Subacute Toxicity Study

Mice were randomly divided into 4 groups (n=8) and the protocal for this experiment followed the diagram on page 20 (Fig. 7). Briefly, mice in group I was given distilled water, and the remaining three groups were given the assigned doses of barakol from acute study (100, 200, and 300 mg/kg) by daily gavage for 28 days. The body weight and food consumption were recorded throughout the experiment. They were sacrificed under light ether anesthesia at 2, 4, 7, 14, 21, and 28 days after treatment. Blood samples were collected from the inferior vena cava to determine clinical biochemistry parameters. Livers were weighed and harvested (two-third of liver) for the determination of the total cytochrome P450 contents. Small samples of the liver were preserved in 3.7 % formaldehyde solution in PBS for histopathological examination. The liver samples, after treated for 14 days, were randomly selected for other special stainings and TUNEL assay.

Group I	Control (distilled water)
Group II	Barakol 100 mg/kg/day (B100)
Group III	Barakol 200 mg/kg/day (B200)
Group IV	Barakol 300 mg/kg/day (B300)

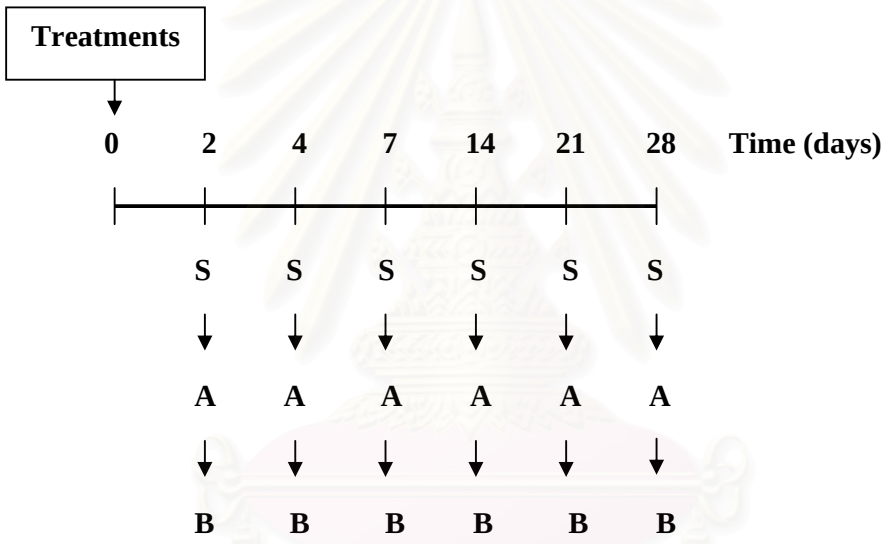

S = sample collection
A = blood and liver collection
B = clinical biochemistry analysis, and histopathological examination

Fig. 7. Schematic diagram showing dose-time course of treatment and sample collection in subacute toxicity study.

Blood Sampling for Clinical Biochemistry Analysis

At various time points, mice were slightly anesthesized with diethyl ether. The abdomen was opened and the lower abdominal inferior vena cava was exposed. Through a needle puncture, blood was collected from inferior vena cava. The blood samples were allowed to clot in ice-bath and centrifuged to obtain the serum that was stored at –20 °C until further assay. The clinical biochemistry parameters, the activities of aspartate and alanine aminotransferases (AST and ALT), the levels of cholesterol, triglyceride, total bilirubin, and glucose were measured by automatic chemistry analyzer (Hitachi 912, Roche®) at Clinical Laboratory, Institute of Medicinal Plant Research, Department of Medical Sciences, Ministry of Public Health.

Histopathological Findings

Hematoxylin and Eosin Staining

Small portions of the liver in acute and subacute studies were fixed in 3.7 % formaldehyde solution in PBS and processed by standard histological methods. Paraffin embedded specimens were cut at 5 μm thickness by a sliding microtome (Pteratome CRM 440, Sakura Seiki, Japan); the facility was rendered possible by the Liver Research Unit, Department of Anatomy, Faculty of Science, Mahidol University. The slides were deparaffinized in xylene and hydrated in serial dilution of ethanol and running tab water. Then, they were stained with hematoxylin and eosin (H&E). Parts of the paraffin embedded specimens were prepared by a colleague at Institute of Medicinal Plant Research, Department of Medical Sciences, Ministry of Public Health. To evaluate intralobular changes, the lobular field was divided with three imaginary concentric zones and described as a peripheral (periportal) zone, an intermediate zone, and a centrilobular (pericentral) zone. Some tissue sections were evaluated by examining the distribution of apoptotic bodies and demonstrated by mapping method. Apoptotic mapping index

(AMI) was conducted by a Nikon Cosmozone 1SA on an NEC 9801RX2, inputted through a digitizer tablet (Graphtec KD-5050).

Sudan III Staining

To study fat accumulation, small pieces of mouse liver from all groups at 14 days of treatment were fixed in 3.7 % formaldehyde solution in PBS. These tissue samples were washed in tap water and immersed in 50 % sucrose and kept at 4 $^{\circ}$C for 48 hours. Tissue blocks were cut at 10 μm thickness using a cryomicrotome and placed on poly-L-lysine coated microscopic glass slides. These slides were stained with Sudan III solution (30 min) and washed in 50 % alcohol. Then, slides were stained with hematoxylin and washed with distilled water. These tissue sections were examined for fat deposit at the Liver Research Unit, Department of Anatomy, Faculty of Science, Mahidol University.

Turnbull Blue Method

To observe iron deposit, mouse liver dosed with high doses of barakol in subacute study were fixed in 3.7 % formaldehyde solution in PBS and embedded in paraffin. Tissue sections (5 μm thickness on special coated microscope slides) were cut from paraffin blocks. These sections were deparaffinized in xylene and washed in distilled water. Then they were treated with ammonium sulfide (1 hour) and washed in distilled water. They were immersed in equal parts of potassium ferricyanide and hydrochloric acid (freshly prepared) and rinsed in distilled water. Finally, they were stained with safranin and rinsed in 40 % ethanol. These tissue sections were evaluated for iron pigment at Department of Pathology, Faculty of Veterinary Science, Chulalongkorn University.

Tissues Specially Stained for Fragmented DNA of Apoptotic Cells

The selected mouse livers from subacute study were evaluated for apoptotic bodies using the terminal deoxynucleotidyl transferase-mediated deoxyuridine triphosphate (dUTP) nick-end labeling (TUNEL) method. This specific assay used terminal deoxynucleotidyl transferase (TdT) to attach fluorescein-12-deoxyuridine triphosphate (dUTP) to free 3'-OH DNA ends. The fluorescein-12-dUTP-labelled DNA was then visualized under fluorescent microscopy. The TUNEL assay was performed using a test kit from Promega according to the manufacturer's instructions.

Liver samples were fixed in 3.7 % formaldehyde solution in PBS and embedded in paraffin. Tissue sections were cut at 5 μm thickness by a sliding microtome (Pteratome CRM 440, Sakura Seiki, Japan); the facility was rendered possible by the Liver Research Unit, Department of Anatomy, Faculty of Science, Mahidol University and placed on poly-L-lysine coated microscopic glass slides. They were deparaffinized in xylene and hydrated in absolute ethanol and running tab water. They were washed in distilled water and then wash in freshly prepared PBS pH 7.4 for 5 min. These slides were fixed with freshly prepared 4 % paraformaldehyde in PBS for 15 min and washed with PBS again. Then, the liquid was removed and tissues were incubated with 100 μl of proteinase K (20 μg/ml) in 10 nmol/l Tris buffer, pH 7.4, containing 5 nmol/l EDTA for 15 min at 37 $^{\circ}$C. Tissues were washed in PBS for 5 min, post-fixed with 4 % paraformaldehyde in PBS (5 min) and washed in PBS (5 min). The sections (positive and negative control) were included to avoid false-positive and false-negative results. The positive control slides were treated with 100 μl of DNAse-I (20 μg/ml) to digest the nuclear DNA into fragments. Then, these slides were washed 3 times for 5 min each with autoclaved water. The negative control slides consisted of identically treated tissue without the enzyme for the TdT reaction. The slides were covered with 100 μl of equilibration buffer for 10 min. Then, they were covered with 50 μl of TdT incubation buffer (45 μl of equilibration buffer, 5 μl of nucleotide mix and

1 μl of TdT enzyme), and incubated for 1 hour at 37 °C in a humidified chamber. Tissues were covered with plastic cover slip to ensure distribution of the reagent and the chamber was covered with aluminum foil to protect the tissues from direct light during subsequent steps. After incubation, the reaction was terminated by immersing the slides in 2X SSC (15 min). They were washed 3 times for 5 min each with fresh PBS to remove unincorporated fluorescein-12-dUTP. Then, they were counter-stained with fresh propidium iodide solution (1 mg/ml in PBS) for 15 min, in the dark. They were washed 3 times for 5 min each with deionized water and mounted with 1 drop of the anti-fade solution before immediate observation under fluorescence microscope with a fluorescein filter set.

Transmission Electron Microscopy (TEM)

Liver samples were selected from acute study for electron microscopy by Scientific and Technological Research Equipment Center, Chulalongkorn University. The livers were quickly cut into small fragments and immediately fixed in 2.5 % glutaraldehyde in PBS. After postfixation in 1 % OsO_4, tissues were dehydrated and embedded in resin. Ultrathin sections were cut by an ultramicrotome and examined under the electron microscope for ultrastructure changes of hepatocytes.

Part B : Possible Mechanisms of Barakol-Induced Hepatotoxicity, *Ex Vivo* and *In Vitro* Studies.

Animal Treatment

Mouse Liver Microsomes Preparation (*Ex Vivo* Study)

Liver microsomes were prepared using method described by Lake (1987) with some modifications. The glassware, glass homogenizer, centrifuge tubes,

medium, and microsomal suspension were maintained at 4 °C throughout the period of the experiment.

Liver (from *in vivo* study) was cut into small pieces by fine scissors and washed with PBS, pH 7.4, for 2-3 times to remove blood. It was suspended in PBS and homogenized in a Heidolph glass homogenizer equipped with a motor-driven Teflon pestle to break the cell membrane.

After centrifugation at 10,000 g for 30 min at 4 °C using a Hitachi superspeed refrigerated centrifuge, the supernatant was collected into ultracentifuge tubes and centrifuged at 100,000 g for an hour at 4 °C. The microsomal pellets were resuspended in 0.1 M PBS containing 20 % glycerol, pH 7.4 (1.5 ml) by gentle manual homogenization. Microsomal preparation was aliquoted into 2-3 microtubes and stored at –80 °C until protein and total cytochrome P450 content analysis.

Mouse Liver Mitochondria Preparation (*In Vitro* Study)

Mitochondria were purified as described (Hogeboom, 1955; Myers, and Slater, 1957). The glassware, glass homogenizer, centrifuge tubes, and medium were kept in ice-box throughout the period of preparation.

Mice were sacrificed by cervical dislocation. The peritoneal cavity was opened and the liver was quickly removed. It was minced into small pieces (<1cm) using scissors in an ice-cold small beaker and washed 2-3 times with 0.25 M sucrose to remove blood. The liver was suspended in ice-cold 0.25 M sucrose and homogenized in a Heidolph glass homogenizer equipped with a motor-driven Teflon pestle to break the cell membrane.

A postnuclear supernatant was obtained by centrifugation at 600 g for 5 min at 4 °C, using superspeed refrigerated centrifuge. The postnuclear supernatant

was collected and centrifuged at 4,500 g for 10 min. Mitochondrial pellets were further purified by sucrose gradient centrifugation (13,000 g, 10 min). The pellets from final spin consisted of two distinct layers, the lower brown layer of tightly packed mitochondria and the upper pink layer of loosely packed microsomes. The microsomes were washed with 0.25 M sucrose for 3 times. The final mitochondrial pellets were resuspended in 0.25 M sucrose (2 ml) by gentle manual homogenization. The mitochondrial suspension was kept on ice-bath during the experimental period. The suspension (50 μl) was aliquoted into a microtube and stored at –20 $^{\circ}$C until protein analysis. The final yield was approximately 30-60 mg mitochondrial protein per ml, and the respiratory control index (RCI) value more than 4 at 37 $^{\circ}$C with glutamate plus malate as substrates.

Determination of Protein Concentration

Liver protein concentration was determined by the method modified from Lowry *et al*. (1951) with bovine serum albumin as protein standard. Briefly, protein was reacted with copper in alkali and folin-phenol reagent. Later the original yellow color of the phosphomolybdate disappeared. Finally, the mixture developed the blue color and the absorbance was measured.

Determination of Total Cytochrome P450 Contents

Total cytochrome P450 contents in liver microsomal samples were determined spectrophotometrically by the method of Omura, and Sato (1964). Briefly, the quantity of cytochrome P450 was calculated from the absorbance difference (450-490 nm) when reduced by sodium dithionite and bubbled with carbon monoxide. The extinction coefficient of 91 $mM^{-1}cm^{-1}$ was used. The spectra were recorded on UV–160A spectrophotometer.

Western Blot Analysis (CYP 3A1 and CYP 2E1)

The cytochrome P450 protein in hepatic microsome was determined by Western blot analysis according to the method of Laemmli (1970); the facility was rendered possible by Department of Physiology, Faculty of Science, Mahidol University. The microsomal suspension was diluted in phosphate buffer and denatured at 95 °C for 3 min. Then, 20 μg of microsomal protein was loaded on to 15 % SDS-polyacrylamide gels. After electrophoresis, the protein was transferred to Polivinylidine difluoride (PVDF) membrane in Tris/glycine/methanol buffer run at 100 V at 4 °C.

The membrane was blocked with 5 % non-fat dried milk in non-specific binding overnight at 4 °C without shaking. It was washed for 15 min (2 times) with Tris buffered saline–Tween 20 (TBST) at room temperature. The primary antibodies of cytochrome P450 3A1 and 2E1 were incubated at 1:5000 and 1:2000 dilutions, respectively, in blocking buffer overnight at 4 °C. The membrane was subsequently washed 4 times for 15 min each with TBST at room temperature and the secondary antibody (1:10,000 dilutions), horseradish peroxidase-conjugated goat anti-rabbit immunoglobulin (IgG), was applied in blocking buffer for 45 min with shaking. The membrane was washed as described above (TBST 3 times, TBS 1 time), and the bands were revealed using the enhanced chemiluminescence (ECL) detection system on Kodak X-OMAT X-ray film. All blots were produced in triplicate, and the relative intensity of immunoreactive bands was determined by Scanning Densitometer Image Processing Scan Analysis. The final result for a sample was defined as the mean of three immunoblots performed on an identical microsomal extract.

Measurement of Mitochondrial Oxidative Phosphorylation

Mitochondrial oxygen consumption rates were assessed with a polarographic Clark type oxygen electrode in a Gilson reaction chamber connected

with YSI oxygen monitor and recorder (Fig. 8). The phosphorylative capacity was measured from the polarographic tracing (Sordahl *et al*., 1971; Masini *et al*., 1997).

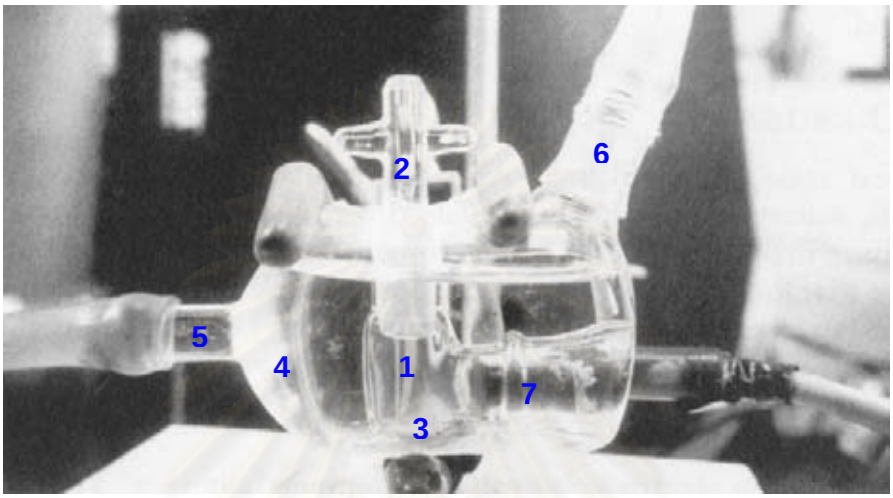

1 = reaction chamber 2 = stopper 3 = magnetic stirrer
4 = water jacket 5 = water intake 6 = water outlet
7 = oxygen electrode

Fig. 8. Gilson reaction chamber (Hinkle, 1995).

The chamber was about 2 ml in volume. It composed of water jacket encompassed the chamber and a hollow glass stopper through which the substrates and reagents were injected into the chamber. The temperature in the chamber was controlled at 37 °C by circulating water bath, and the reaction chamber was equipped with a Clark oxygen electrode that connected to an amplifier (YSI model 53). The signal was recorded on a stripchart recorder (Gilson model N2), which provided tracings called “oxygraph” or “polarographic” tracings.

The standard incubation medium used for this measurement consisted of 40 mM HEPES buffer pH 7.2, 2 mM $MgCl_2$, and 92 mM KCl, which is isotonic with the mitochondria. The medium (1.75 ml) and mitochondrial suspension (50 µl) were incubated in the reaction chamber with other substrates and various

concentrations of barakol (0.075, 0.15, 0.3, 0.6, 1.2, and 3 mM), which were agitated by a small rotating magnet. The electrode was calibrated with ultrapure water saturated with air at 37 °C. The amounts of oxygen dissolved in water (1 ml) at 37 °C can be calculated as follow.

Determination of The Respiratory Control Index (RCI)

Classification of mitochondrial metabolic states as shown in Table 2, and the method used for calculating the RCI value was described by Chance and Williams (1956).

Table 2. Classification of mitochondrial metabolic states.

State	Condition
1	Oxygen only
2	Oxygen and ADP
3	Oxygen, ADP and substrates
3u	Uncoupler
4	Oxygen and substrates
5	Substrate only
6	The respiration is inhibited by excess calcium

$$\text{RCI} = \frac{\text{Rate of state 3 respiration}}{\text{Rate of state 4 respiration (after state 3)}}$$

or

$$\text{RCI} = \frac{\text{Slope of the tracing in state 3 respiration}}{\text{Slope of the tracing in state 4 respiration}}$$

or (from Fig. 9. on page 31)

$$\text{RCI} = \frac{Y1/X}{Y2/X} = \frac{Y1}{Y2}$$

Y1 = the length of line Y1

Y2 = the length of line Y2

The tightness of the coupling mechanism or the substrate oxidation is tightly coupled to ATP synthesis is indicated by the RCI. Therefore, good intact mitochondria should have RCI more than 4 at 37 °C with glutamate plus malate as substrates. Only mitochondrial preparations that demonstrated a RCI value above 4 were used in this study.

Determination of P/O Ratio (ADP/O)

The P/O ratio is the number of ATP molecules synthesized per one oxygen atom consumed during state 3 respiration. This value can be calculated according to Estabrook (1967) as follows:

$$\text{P/O} = \frac{\text{n moles of ATP synthesized}}{\text{ng atoms of oxygen consumed in state 3 respiration}}$$

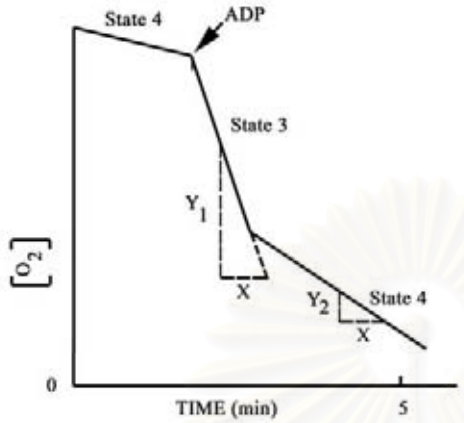

Fig. 9. An oxygraph tracing illustrating the measurement of RCI value.

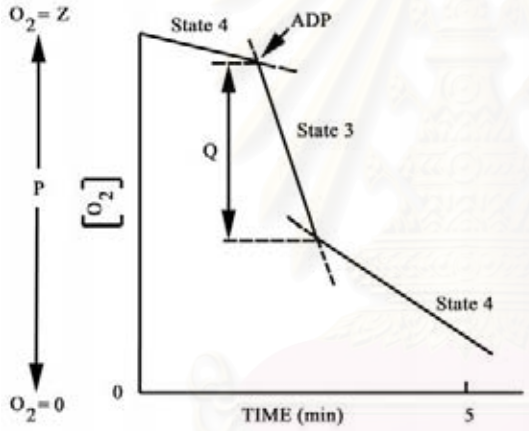

Fig. 10. An oxygraph tracing illustrating the measurement of P/O ratio.

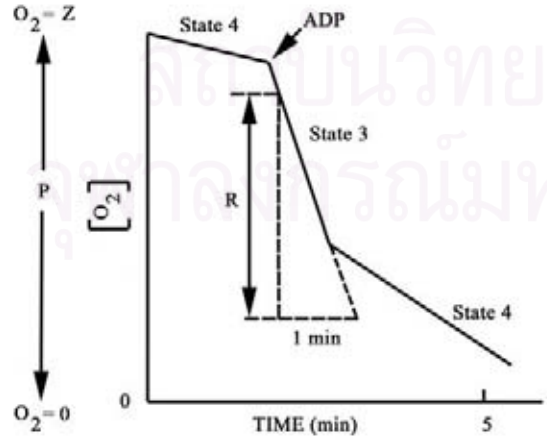

Fig. 11. An oxygraph tracing illustrating the measurement of oxygen consumption rates.

The n moles of ATP synthesized is equal to nmoles of ADP added to the reaction chamber or is calculated from the concentration and volume of ADP added.

The ng atoms of oxygen consumed in state 3 respiration are (Q/P) x Z, calculated from oxygraph tracing on page 31 (Fig. 10). P and Q are the length of line P and Q, respectively. Z are ng atoms of oxygen initially dissolved in the reaction mixture.

Z value depends on volume of the reaction mixture and temperature. If volume of the mixture is high and temperature is low, the more oxygen will be dissolved in the reaction.

$$Z = A \times \text{total volume of reaction mixture}$$

A = the amount of oxygen dissolved in water (1 ml) at 37 °C can be calculated from the following formula which is 444.9 ng atoms O/ml after substituting the value of all parameters as follow:

$$A = (S/V)(P/100) \times N \times 10^9 \quad \text{ng atoms O/ml}$$

S = absorption coefficient at 37 °C (volume of oxygen reduced at 0 °C and 760 mmHg, absorbed by one volume of water when the pressure of gas itself amounted to 760 mmHg) = 0.02373

P = percentage of oxygen in atmostpheric air = 21 %

N = number of atom in a molecule of oxygen = 2

V = volume of gas (at 0 °C and 760 mmHg) corresponding to 1g mole = 22,400 ml

Rates of Oxygen Consumption Calculation

Rates of oxygen consumption in various metabolic states can be calculated from oxygraph tracing as shown on page 31 (Fig. 11).

Method 1

Rate of oxygen consumption in state 3 = (R/P) x Z ng atoms O/min

Method 2

Rate of oxygen consumption in state 3 = (R/P) x A ng atoms O/min/ml

R = the length of line R

P = the length of line P

Z = ng atoms oxygen initially dissolved in the reaction mixture

A = ng atoms oxygen dissolved in water 1 ml

Oxygen consumption rates, calculated from method 1, can be divided by mitochondrial protein used in the reaction and the unit of which becomes ng atoms O/min/mg protein.

Data Collection and Data Analysis

Statistical analysis was carried out using SPSS/PC^{+} 11.0 software. All data were expressed as mean ± standard error of mean (SEM). These experimental data from different groups were compared by one-way analysis of variance (ANOVA) coupled with Tukey test. A p value less than 0.05 (p<0.05) was considered significant.

CHAPTER III

RESULTS

Part A : Dose-Time Course Effect of Barakol on Liver Injury *In Vivo* Study

Experiment I. Acute Toxicity Study

Blood Sampling for Clinical Biochemistry Analysis

In mice, the levels of aspartate aminotransferase (AST), alanine aminotransferase (ALT) and total bilirubin in blood increased after a single dose of barakol (200, 300 and 400 mg/kg), measured at 24, 48, and 72 hours. At 96 hours after barakol, AST and ALT values declined to normal values, while total bilirubin also declined but still higher than that of control values (Figs. 12-14). Total bilirubin also increased in mice treated with a single dose of 100 mg/kg barakol, while other parameters were similar to those in control. The concentrations of cholesterol, triglyceride and glucose decreased in barakol-treated mice measured at 24 hours after treatment. At 48 and 72 hours, triglyceride and glucose levels returned to normal. Cholesterol also decreased especially in mice treated with high doses of barakol (300 and 400 mg/kg) (Figs. 15-17). The severity of hepatic injury induced by barakol was dose-dependent.

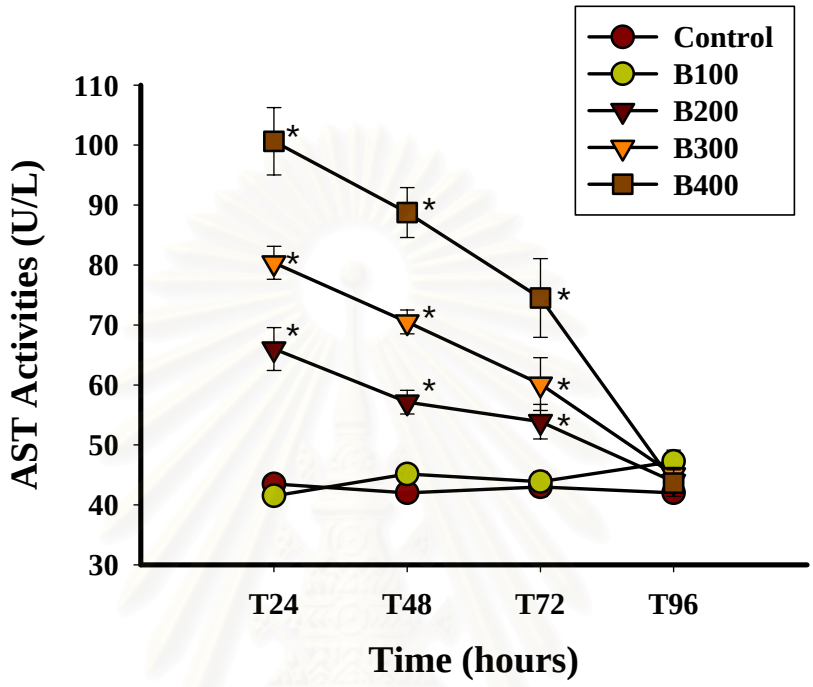

Fig. 12. Effect of barakol on aspartate aminotransferase (AST) activity in acute toxicity study.

Mice received single dose of barakol (100, 200, 300, and 400 mg/kg) and blood was collected at different time points (24, 48, 72, and 96 hours). Results are expressed as mean ± SEM (* $p < 0.05$).

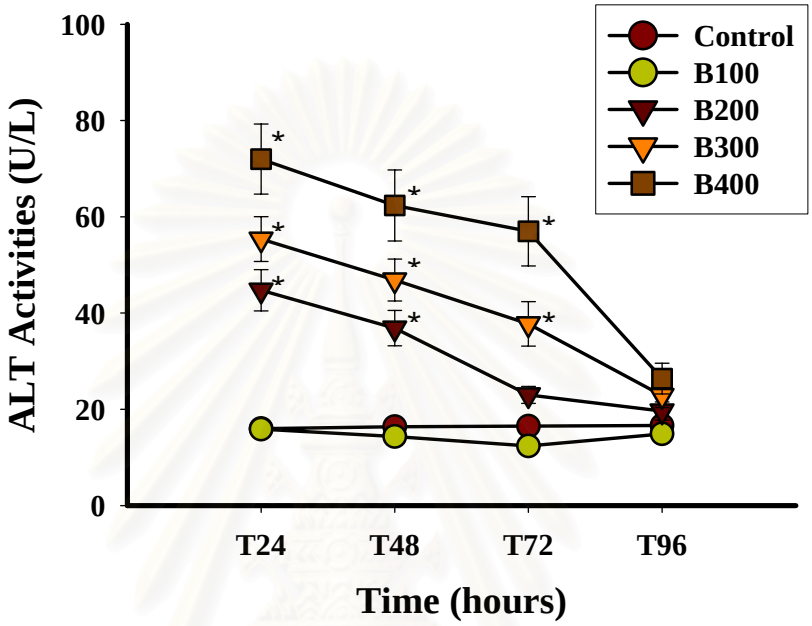

Fig. 13. Effect of barakol on alanine aminotransferase (ALT) activity in acute toxicity study.

Mice received single dose of barakol (100, 200, 300, and 400 mg/kg) and blood was collected at different time points (24, 48, 72, and 96 hours). Results are expressed as mean ± SEM (* $p < 0.05$).

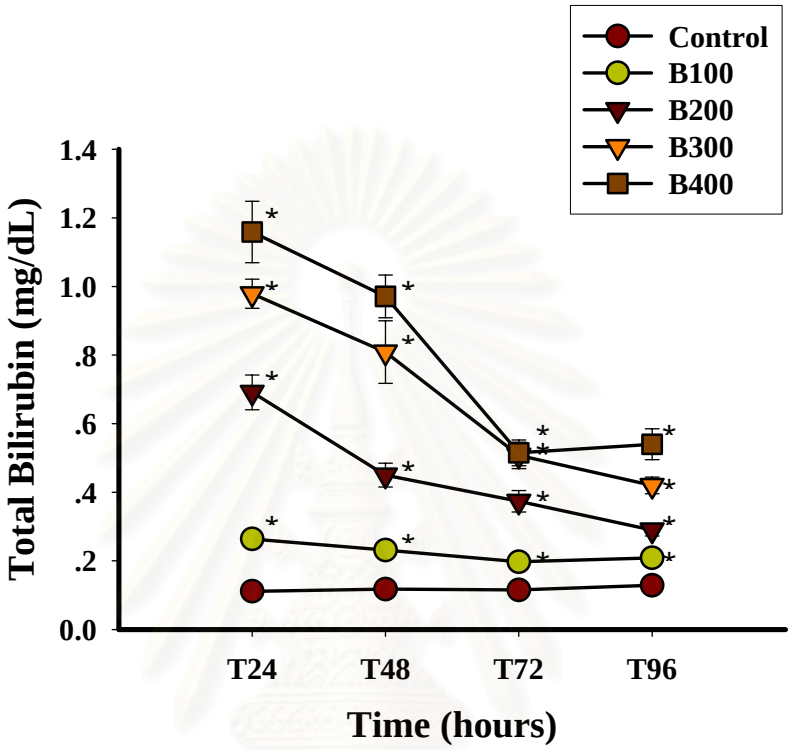

Fig. 14. Effect of barakol on total bilirubin level in acute toxicity study.

Mice received single dose of barakol (100, 200, 300, and 400 mg/kg) and blood was collected at different time points (24, 48, 72, and 96 hours). Results are expressed as mean ± SEM (* $p < 0.05$).

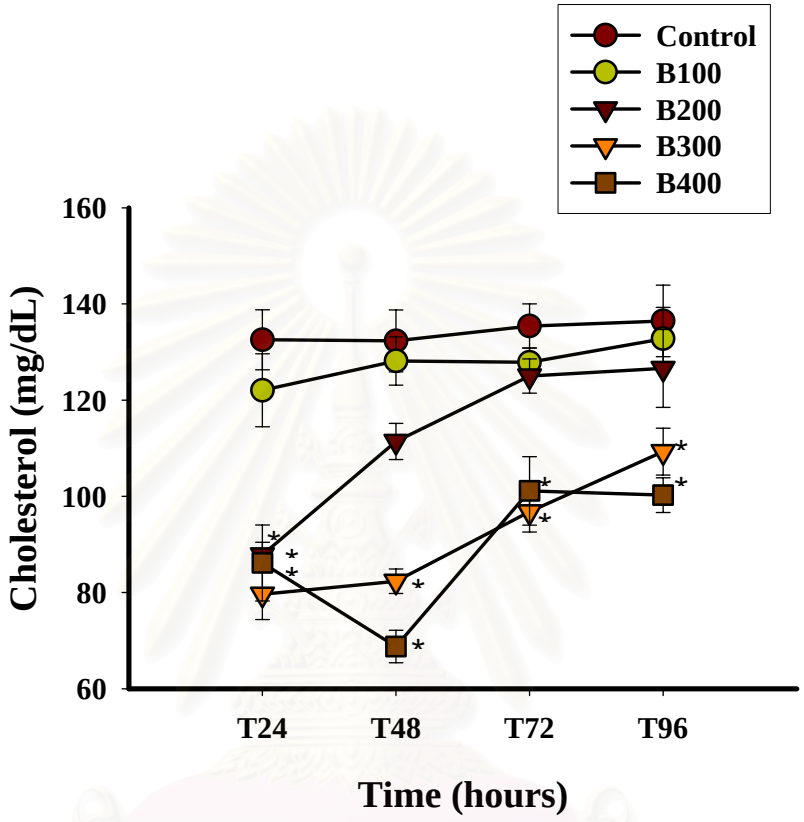

Fig. 15. Effect of barakol on cholesterol level in acute toxicity study.

Mice received single dose of barakol (100, 200, 300, and 400 mg/kg) and blood was collected at different time points (24, 48, 72, and 96 hours). Results are expressed as mean ± SEM (* $p < 0.05$).

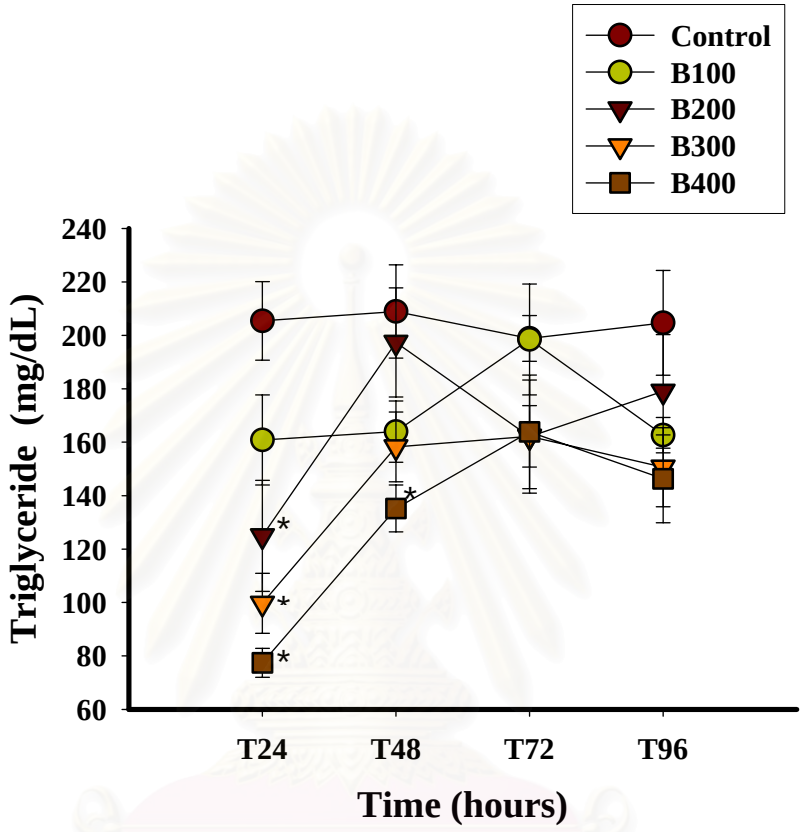

Fig. 16. Effect of barakol on triglyceride level in acute toxicity study.

Mice received single dose of barakol (100, 200, 300, and 400 mg/kg) and blood was collected at different time points (24, 48, 72, and 96 hours). Results are expressed as mean ± SEM (* $p < 0.05$).

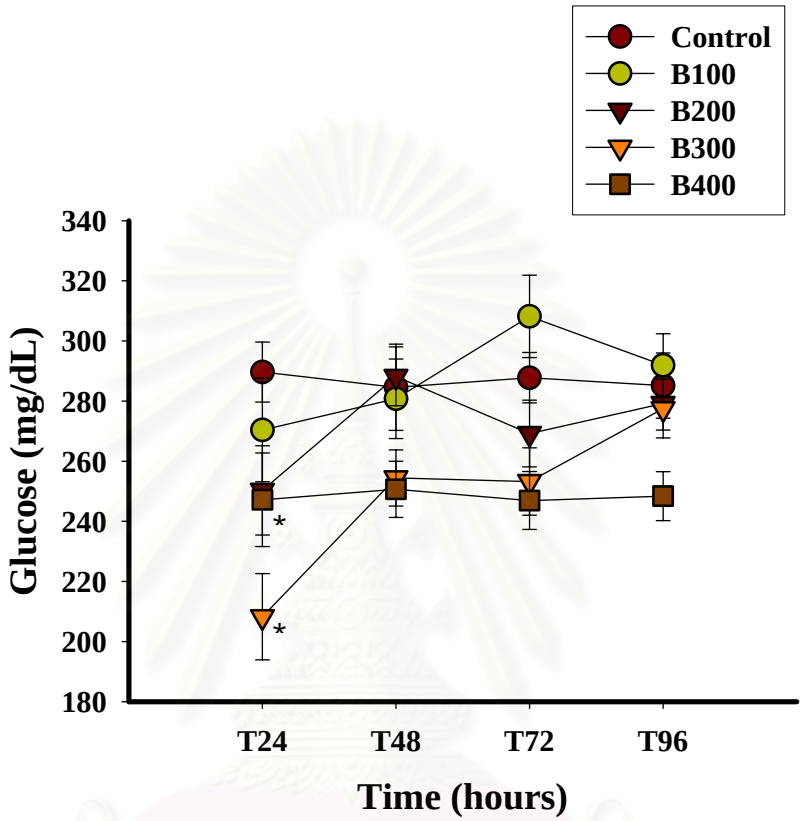

Fig. 17. Effect of barakol on glucose level in acute toxicity study.

Mice received single dose of barakol (100, 200, 300, and 400 mg/kg) and blood was collected at different time points (24, 48, 72, and 96 hours). Results are expressed as mean ± SEM (* $p < 0.05$).

Histopathological Findings

Histopathological analysis of liver sections iss summarized in Table 3. The lobular architecture was intact. Portal tract showed no evidence of inflammation in all treated groups at all different time points. In 100 mg/kg barakol-treated mice, there was diffused centrilobular hepatic necrosis at 24 hours (Fig. 20) compared with control group (Fig. 18). From pericentral zone to intermediate zone there were swelling of hepatocytes and scattered degree of necrosis presented by neutrophil infiltration in 200, 300, and 400 mg/kg barakol-treated mice at 24 hours. The degree of hydropic degeneration of hepatocytes increased with dose of barakol. In 200-400 mg/kg barakol-treated mice, the hydropic degeneration recovered after 48 hours but scattered necrosis of liver cells were still detected at 72 hours in 400 and 600 mg/kg barakol-treated groups (Figs. 21-23).

Transmission electron microscopy (TEM) examination showed mild degeneration of mitochondria and cisternae of endoplasmic reticulum, especially in mice treated with high doses of barakol. In addition, hepatocytes in barakol-treated groups exhibited fatty degeneration (Figs. 25 and 26).

Table 3. Histopathological findings of mouse liver after treating with various single doses of barakol at different time points in acute toxicity study.

Single Dose of Barakol (mg/kg)	Histopathological Findings									
	Necrosis	Hydropic Degeneration			Apoptotic Body			Iron Pigment		
		C	I	P	C	I	P	C	I	P
Control (Fig. 18)	-	-	-	-	-	-	-	-	-	-
Barakol 50 mg/kg (Fig. 19)										
24 h	-	-	-	-	-	-	-	-	-	-
Barakol 100 mg/kg (Fig. 20)										
24 h	±	-	-	-	-	-	-	-	-	-
48 h	-	-	-	-	-	-	-	-	-	-
72 h	-	-	-	-	-	-	-	-	-	-
96 h	-	-	-	-	-	-	-	-	-	-
Barakol 200 mg/kg (Fig. 21)										
24 h	+	+	-	-	-	-	-	-	-	-
48 h	+	-	-	-	-	-	-	-	-	-
72 h	-	-	-	-	-	-	-	-	-	-
96 h	-	-	-	-	-	-	-	-	-	-
Barakol 300 mg/kg (Fig. 22)										
24 h	+	+	+	-	-	-	-	-	-	-
48 h	+/M	+	-	-	-	-	-	-	-	-
72 h	-	-	-	-	-	-	-	-	-	-
96 h	-	-	-	-	-	-	-	-	-	-
Barakol 400 mg/kg (Fig. 23)										
24 h	+	+	+	-	-	-	-	-	-	-
48 h	+/M	+	-	-	-	-	-	-	-	-
72 h	+/M	-	-	-	-	-	-	-	-	-
96 h	-	-	-	-	-	-	-	-	-	-
Barakol 600 mg/kg (Fig. 24)										
24 h	+	+	+	+	-	-	-	-	-	-

Mice received single dose of barakol (100, 200, 300, and 400 mg/kg). Liver was taken at different time points (24, 48, 72, and 96 hours) for histopathological examination. C, pericentral zone; P, peripheral zone; I, intermediate zone; +, present; -, not present; ±, present in some specimens; +/M, present with mitotic figure.

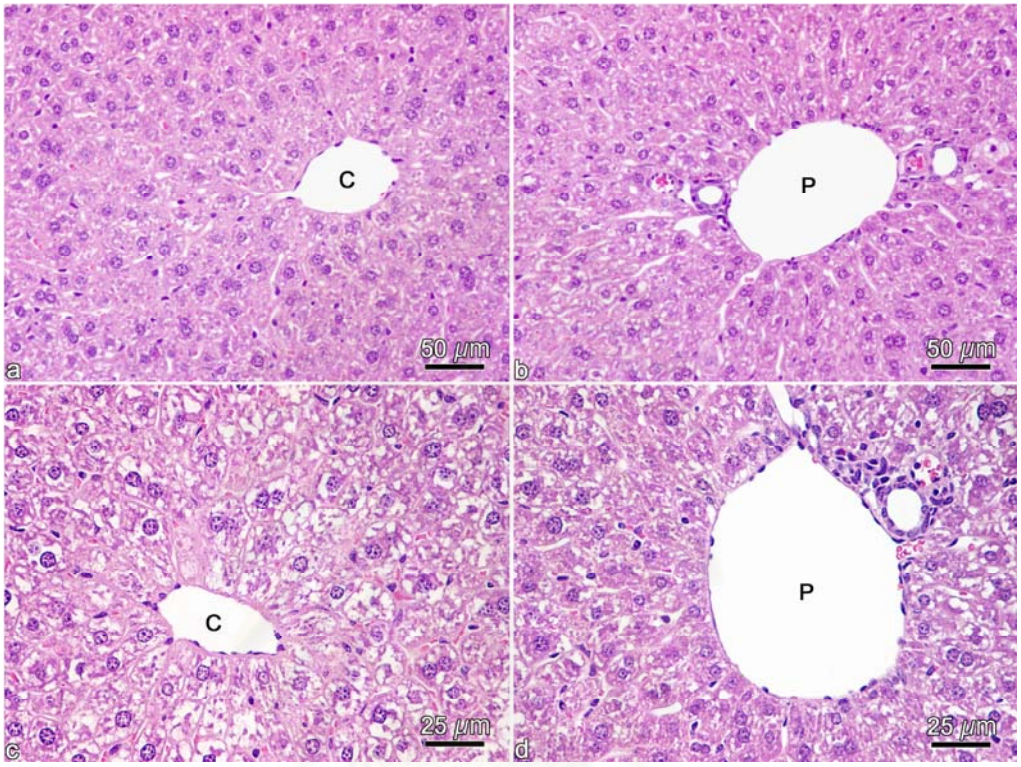

Fig. 18. Light micrographs of control mouse liver stained with H&E.

Mice received distilled water only. No remarkable lesion on hepatocytes (a-d).

C, central vein; P, portal vein.

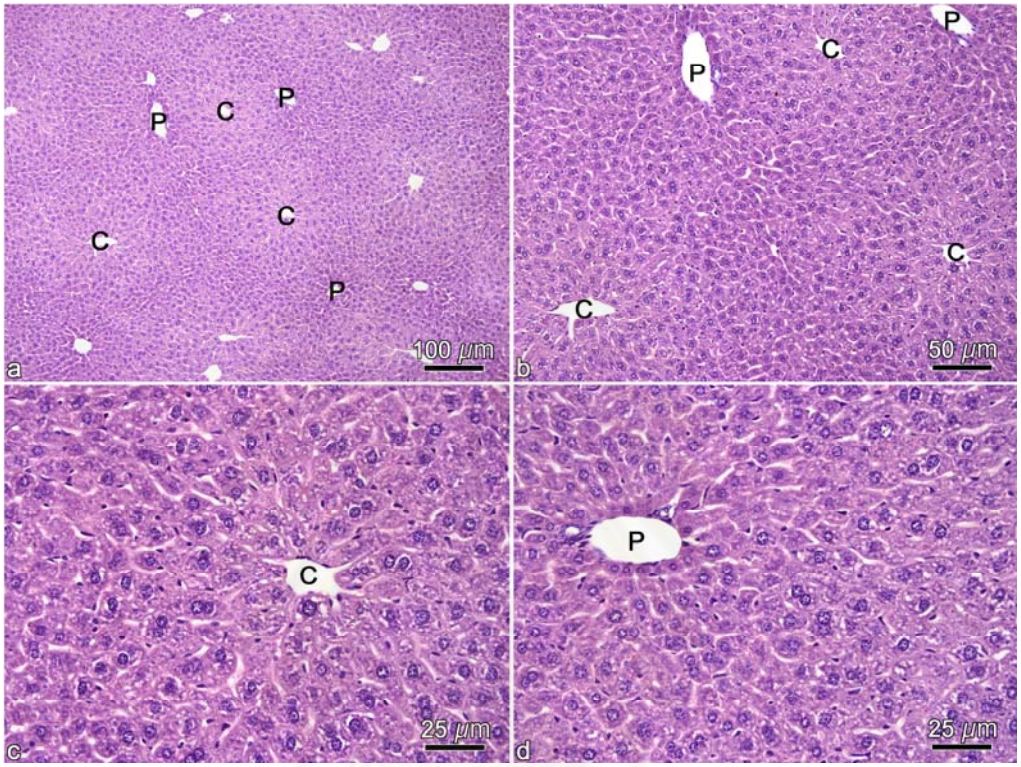

Fig. 19. Light micrographs of mouse liver treated with a single dose of 50 mg/kg barakol at 24 hours and stained with H&E.

a-d At 24 hours, no remarkable lesion on hepatocytes.
C, central vein; P, portal vein.

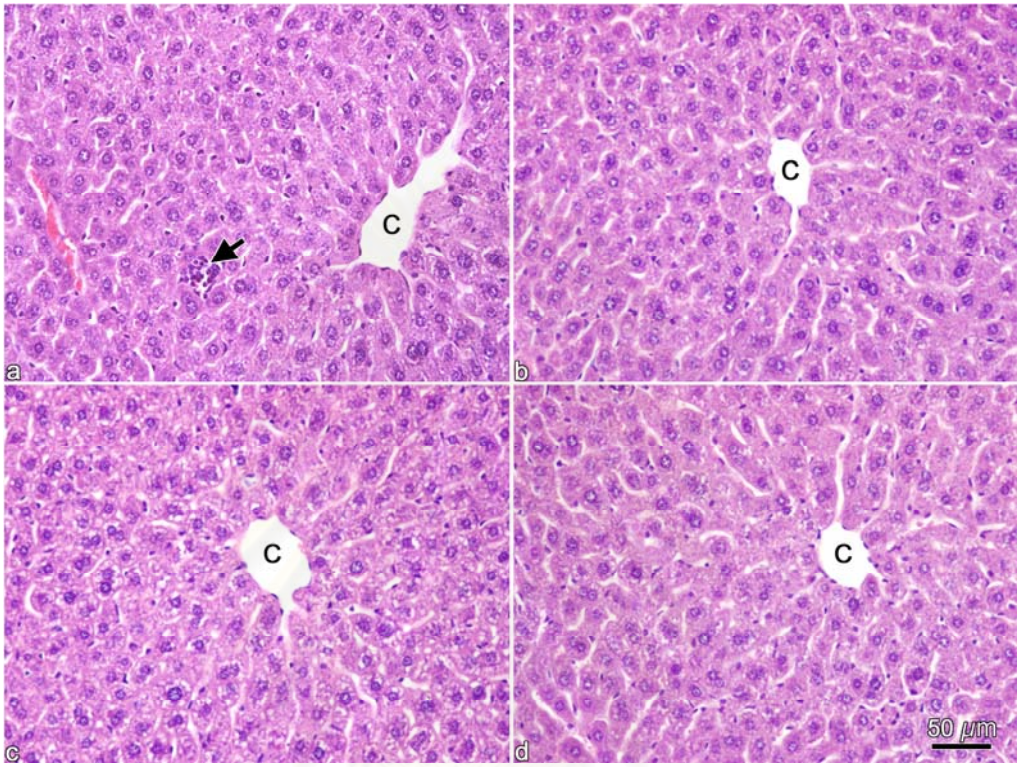

Fig. 20. Light micrographs of mouse liver treated with a single dose of 100 mg/kg barakol at different time points and stained with H&E.

a Mouse liver, treated with barakol at 24 hours, showed scattered necrosis at periportal zone as indicated by occasional neutrophil accumulation (arrow).

c-d Mouse livers after treating with barakol at 48, 48, and 72 hours, respectively, showed normal lobular structure.

C, central vein; P, portal vein.

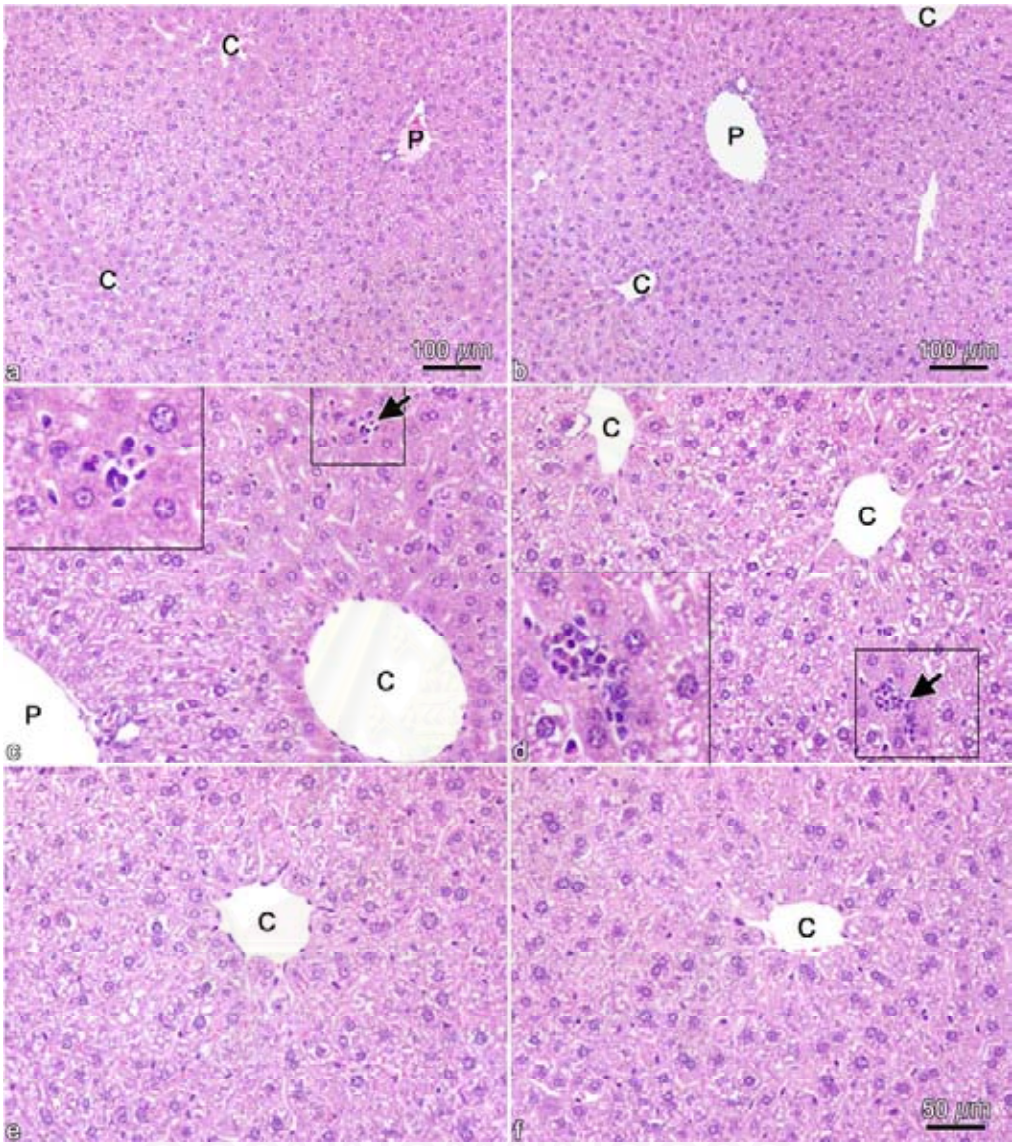

Fig. 21. Light micrographs of mouse liver treated with a single dose of 200 mg/kg barakol at different time points and stained with H&E.

a, c At 24 hours, hydropic degeneration occurred in pericentral zone.

b, d At 48 hours, hydropic degeneration disappeared but hepatocytic necrosis was found instead (arrow).

e, f At 72 and 96 hours, respectively, the hepatocytic plates recovered.

C, central vein; P, portal vein.

Fig. 22. Light micrographs of mouse liver treated with a single dose of 300 mg/kg barakol at different time points and stained with H&E.

a, c At 24 hours, hepatocytic necrosis was found from pericentral zone to intermediate zone (arrow) and hydropic degeneration from pericentral zone to peripheral zone.

b, d At 48 hours, hepatocytic necrosis was observed in pericentral zone with hydropic degeneration (arrow).

e At 48 hours, the light micrograph showed centrilobular hydropic degeneration.

f At 48 hours, the light micrograph showed liver regeneration (arrowhead).

g, h At 72 and 96 hours, respectively, the lobule nearly resumed to normal structure.

C, central vein; P, portal vein.

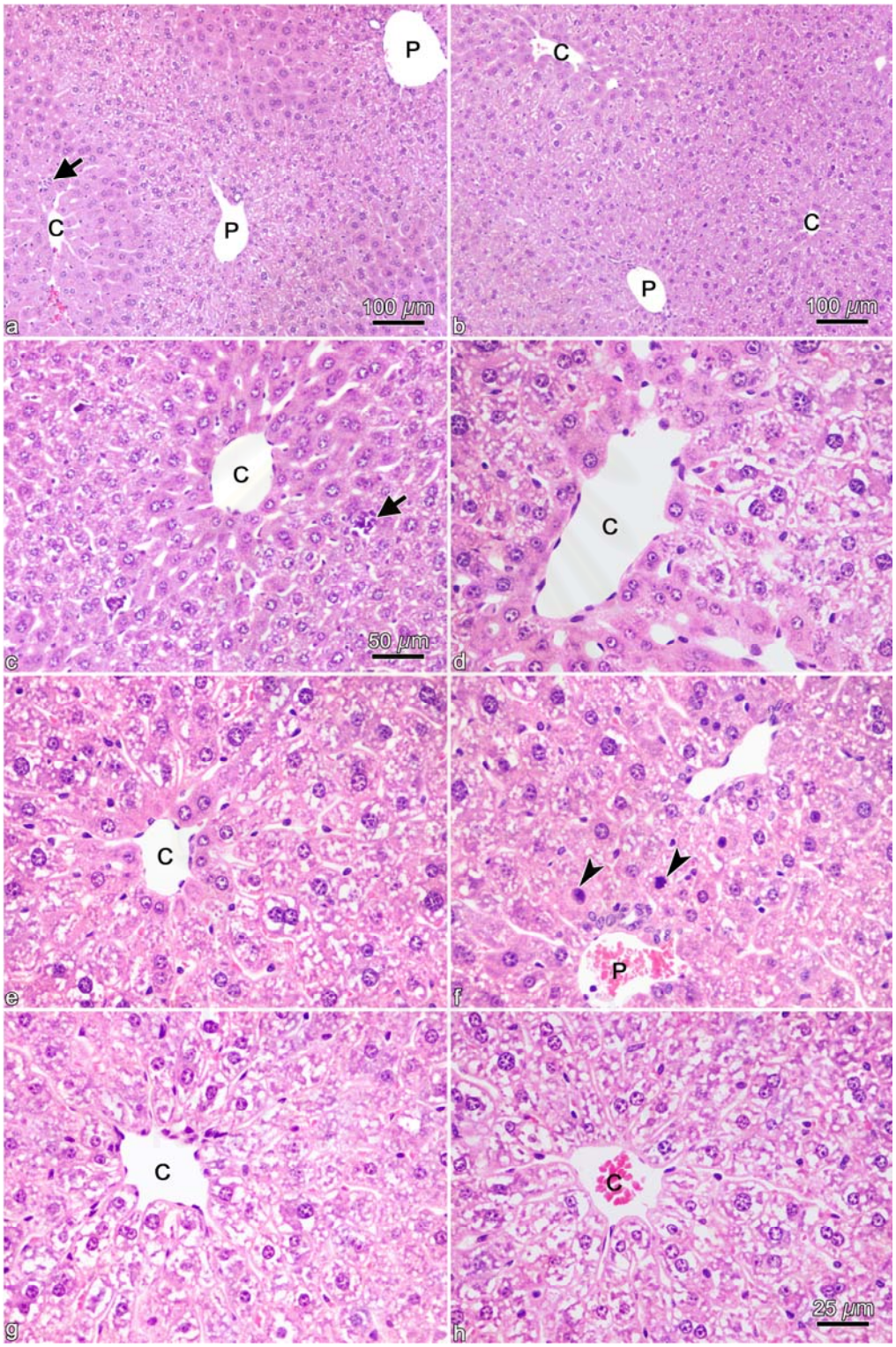
P
C
P
100 µm
a
C
C
P
100 µm
b
C
50 µm
c
C
d
C
e
P
f
C
g
C
25 µm
h

Fig. 23. Light micrographs of mouse liver treated with a single dose of 400 mg/kg barakol at different time points and stained with H&E.

a and b At 24 hours, hepatocytic necrosis was found from pericentral zone to intermediate zone (arrow) and hydropic degeneration from pericentral zone to peripheral zone.

c At 48 hours, the light micrograph showed centrilobular hydropic degeneration.

d At 48 hours, hepatocyte undergone nuclear division was observed (arrowhead).

e At 72 hours, hydropic degeneration disappeared but hepatocytic necrosis was found instead in pericentral zone (arrow).

f At 96 hours, the lobule nearly resumed to normal structure.

C, central vein; P, portal vein.

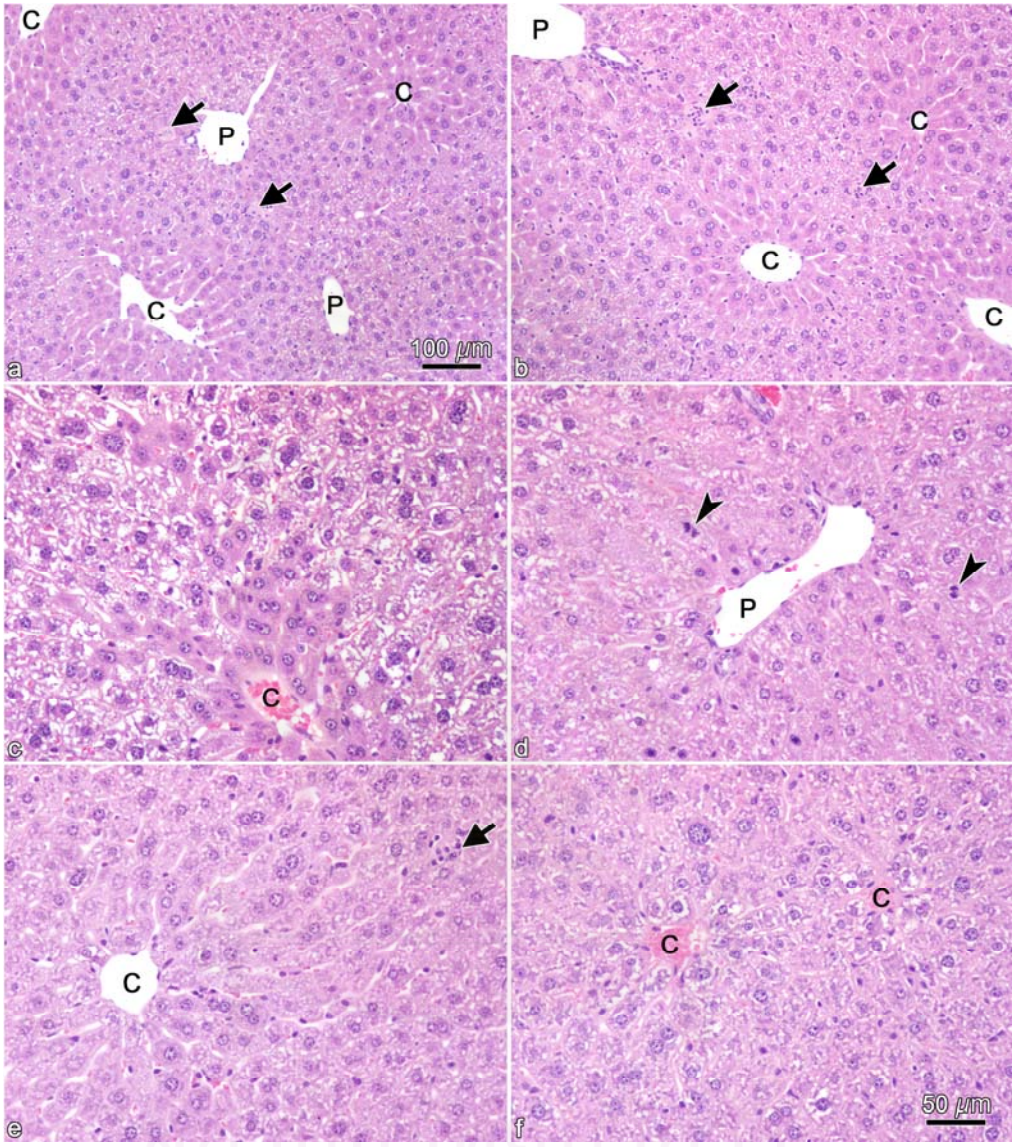

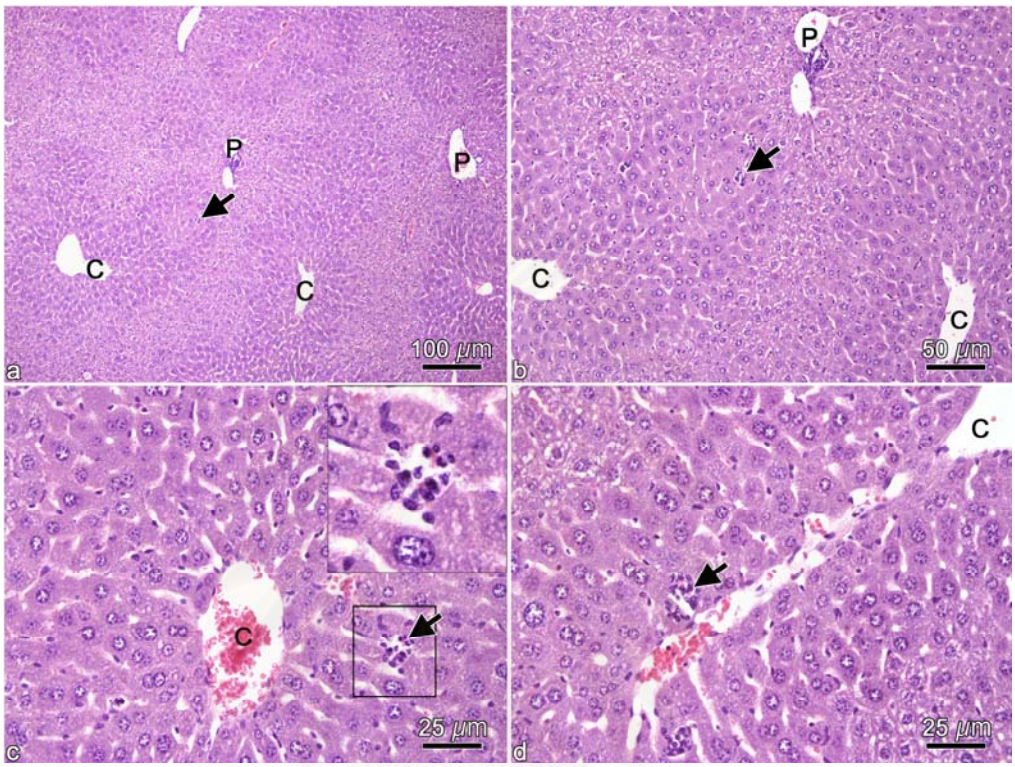

Fig. 24. Light micrographs of mouse liver treated with a single dose of 600 mg/kg barakol at 24 hours and stained with H&E.

a-d Mouse liver after treated with barakol at 24 hours showing hydropic degeneration at intermediate zone and scattered necrosis of liver cells (arrow).

Fig. 25. Electron micrographs of mouse liver treated with a single dose of 200, 300, and 400 mg/kg barakol at 48 hours.

a Normal ultrastructure of hepatocyte in control mouse.

b At 200 mg/kg barakol, mitochondria became swollen and enlarged with light electron density.

c At 300 mg/kg barakol, mitochondria became largely swollen.

d The degree of mitochondrial swelling was mild in mouse with 400 mg/kg barakol.

a-b Magnification X 5,100; c Magnification X 6,800; d Magnification X 5,400; M, mitochondria; N, nucleus; L, lipid.

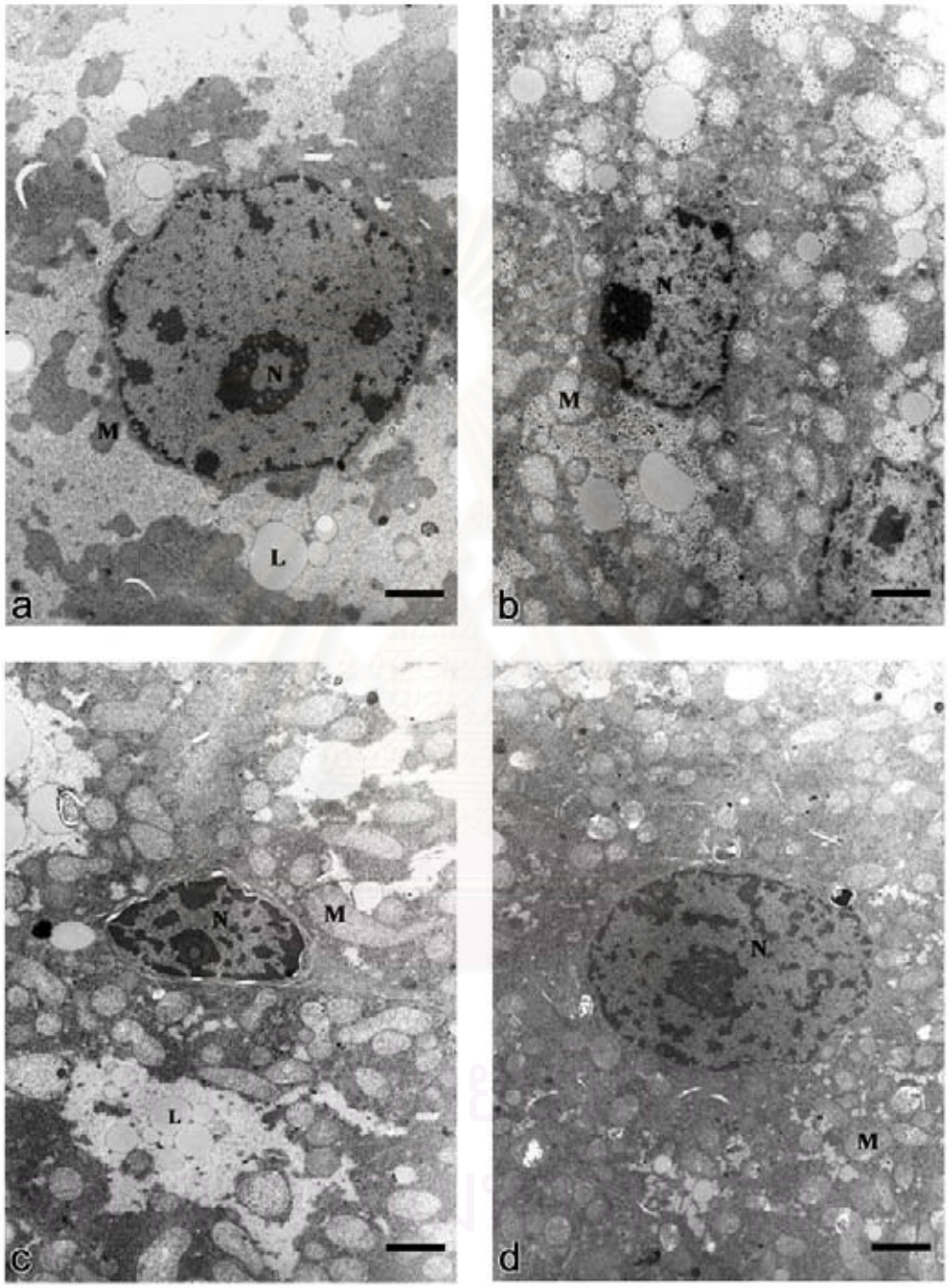
a
N
M
L
b
N
M
c
N
M
L
d
N
M

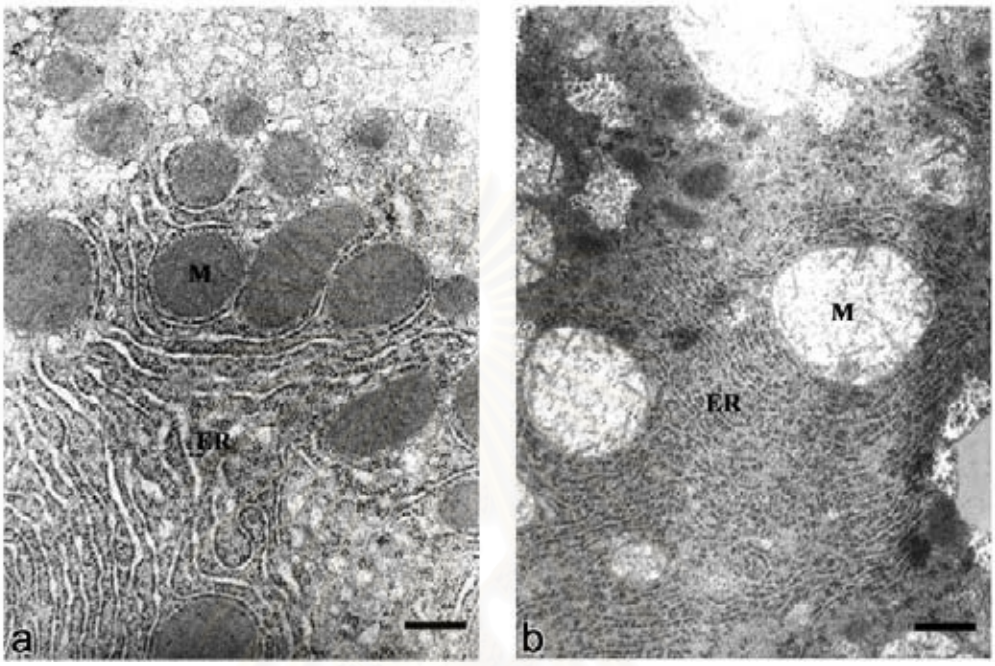

Fig. 26. Electron micrographs of mouse liver treated with a single dose of 200 mg/kg barakol at 48 hours.

a Normal ultrastructure of hepatocyte in control mouse. Rough ER with well defined cisternae were easily identified and mitochondria were normal looking with cristae.

b Rough ER appeared to increase in number and densely packed together with swollen mitochondria.

a-b Magnification X 20,400; M, mitochondria; ER, endoplasmic reticurum.

Experiment II. Subacute Toxicity Study

Blood Sampling for Clinical Biochemistry Analysis

Food consumption and body weight were recorded at the beginning and at the end of different time points (Table 4). Food intake was markedly decreased after treated with 200 and 300 mg/kg/day barakol for 7 days. After 14 days, the food consumption of the 200 mg/kg/day barakol-treated mice were increased and trended to elevate until 28 days. The final body weight of the 300 mg/kg/day barakol-treated mice was markedly decreased after 14, 21, and 28 days.

The activities of AST, ALT, and the levels of total bilirubin in all barakol-treated groups were elevated more than 50 % at all different time points, except that in the 100 mg/kg/day barakol-treated mice whose AST and ALT levels started to increase on day 4 of treatment (Figs. 27-29). In contrast, blood cholesterol, triglyceride and glucose concentrations were decreased more than 50 % beginning on day 1 to day 28 in 200 and 300 mg/kg/day barakol-treated mice, and day 4 to day 28 in 100 mg/kg/day barakol-treated group (Figs. 30-32).

Table 4. Effects of barakol on food consumption, body weight, liver weight, and relative liver weight in subacute toxicity study.

Repeated Doses of Barakol (mg/kg/day)	Food Intake (g/day/animal)	Initial Body Weight (g)	Final Body Weight (g)	Liver Weight (g)	Normalized Liver Weight per g BW
Control					
2 d	4.69 ± 0.18	35.21 ± 1.25	35.93 ± 1.11	2.31 ± 0.09	6.44 ± 0.10
4 d	4.30 ± 0.36	34.88 ± 0.65	36.63 ± 0.78	2.27 ± 0.04	6.40 ± 0.20
7 d	4.44 ± 0.11	31.50 ± 0.45	34.10 ± 0.61	2.20 ± 0.05	6.57 ± 0.09
14 d	4.55 ± 0.06	31.10 ± 0.21	35.95 ± 0.54	2.22 ± 0.04	6.38 ± 0.15
21 d	4.55 ± 0.04	30.67 ± 0.63	37.21 ± 0.70	2.23 ± 0.05	5.96 ± 0.08
28 d	4.50 ± 0.11	30.88 ± 0.41	38.29 ± 0.79	2.17 ± 0.07	5.60 ± 0.11
B100					
2 d	4.69 ± 0.12	33.69 ± 0.61	34.06 ± 0.61	2.12 ± 0.07	6.21 ± 0.17
4 d	4.63 ± 0.20	34.88 ± 0.78	36.94 ± 0.77	2.14 ± 0.06	5.79 ± 0.11
7 d	4.68 ± 0.02	32.13 ± 0.56	34.94 ± 0.83	2.15 ± 0.07	6.17 ± 0.14
14 d	4.66 ± 0.07	31.31 ± 0.56	35.38 ± 0.93	2.14 ± 0.06	6.06 ± 0.18
21 d	4.73 ± 0.07	32.00 ± 0.37	37.88 ± 0.65	2.27 ± 0.08	5.99 ± 0.21
28 d	4.39 ± 0.06	31.94 ± 0.27	39.56 ± .068	2.14 ± 0.06	5.41 ± 0.14
B200					
2 d	4.41 ± 0.28	35.06 ± 1.01	34.81 ± 0.81	2.00 ± 0.06	5.74 ± 0.09
4 d	4.77 ± 0.23	33.88 ± 0.86	36.00 ± 0.78	2.17 ± 0.05	6.02 ± 0.07
7 d	3.73 ± 0.16*	31.85 ± 0.50	33.05 ± 1.17	2.03 ± 0.09	6.20 ± 0.11
14 d	5.24 ± 0.14*	32.40 ± 0.48	35.60 ± 0.57	2.13 ± 0.05	6.23 ± 0.12
21 d	5.05 ± 0.11	31.40 ± 0.46	34.35 ± 0.82	2.03 ± 0.07	5.91 ± 0.12
28 d	5.23 ± 0.13	31.15 ± 0.47	37.10 ± 0.42	2.11 ± 0.05	5.70 ± 0.15
B300					
2 d	4.50 ± 0.29	35.00 ± 0.87	35.38 ± 0.88	2.05 ± 0.07	5.78 ± 0.12
4 d	4.41 ± 0.26	34.31 ± 0.63	35.25 ± 1.02	2.04 ± 0.07	5.83 ± 0.21
7 d	3.60 ± 0.13*	31.55 ± 0.54	32.20 ± 1.17	2.05 ± 0.11	6.36 ± 0.20
14 d	4.57 ± 0.14	31.15 ± 0.59	30.80 ± 1.34*	1.94 ± 0.13	6.13 ± 0.25
21 d	4.50 ± 0.24	31.71 ± 0.71	30.73 ± 1.72*	1.86 ± 0.13	5.79 ± 0.18
28 d	5.11 ± 0.19	31.64 ± 0.73	32.38 ± 0.82*	1.97 ± 0.07	5.69 ± 0.13

Mice were given daily dose of barakol (100, 200, and 300 mg/kg/day) for 28 days. Food consumption, initial body weight, terminal body weight, and liver weight were recorded at different time points. Data are presented as mean ± SEM. * $p<0.05$ considered significant different from control.

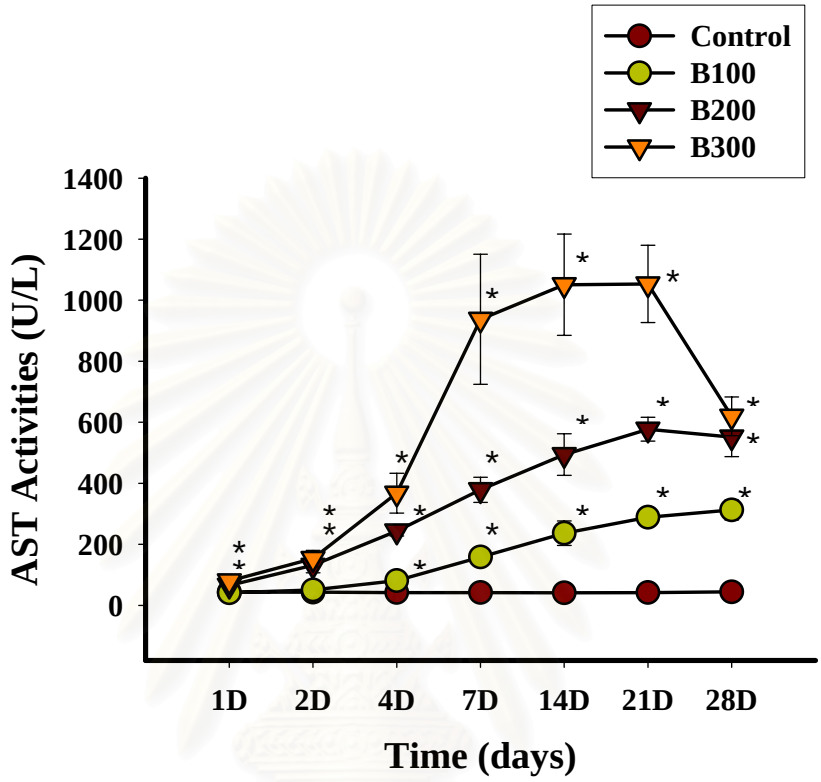

Fig. 27. Effect of barakol on aspartate aminotransferase (AST) activity in subacute toxicity study.

Mice received repeated doses of barakol (100, 200, and 300 mg/kg) and blood was collected at different time points (1, 2, 4, 7, 14, 21, and 28 days). Results are expressed as mean ± SEM (* $p < 0.05$).

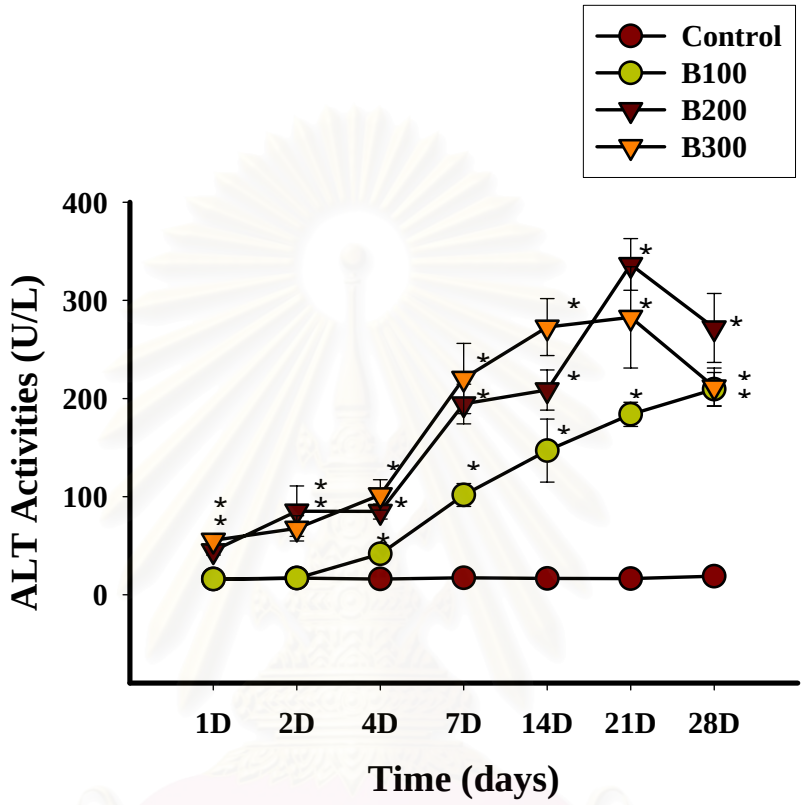

Fig. 28. Effect of barakol on alanine aminotransferase (ALT) activity in subacute toxicity study.

Mice received repeated doses of barakol (100, 200, and 300 mg/kg) and blood was collected at different time points (1, 2, 4, 7, 14, 21, and 28 days). Results are expressed as mean ± SEM (* $p < 0.05$).

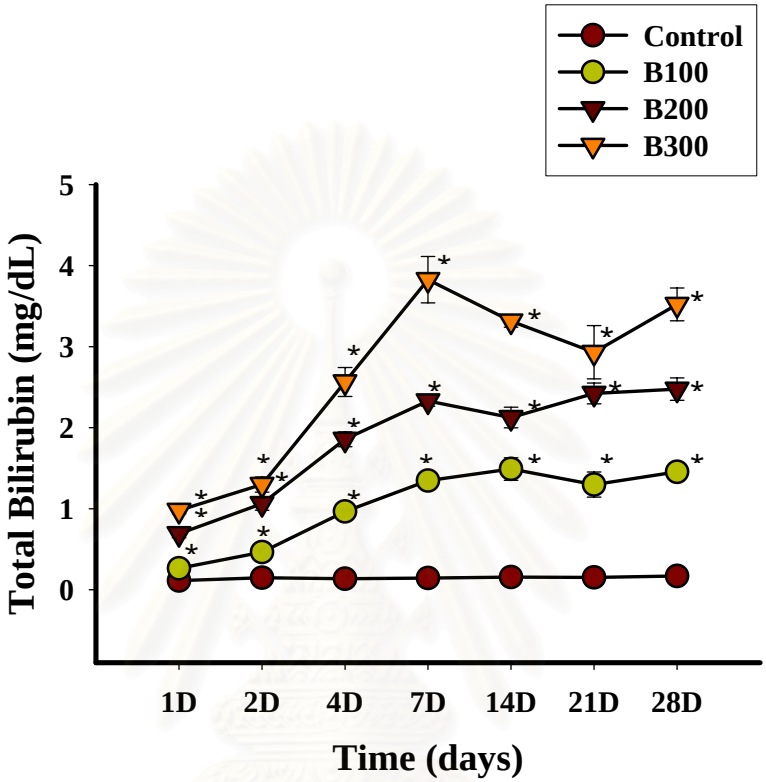

Fig. 29. Effect of barakol on total bilirubin level in subacute toxicity study.

Mice received repeated doses of barakol (100, 200, and 300 mg/kg) and blood was collected at different time points (1, 2, 4, 7, 14, 21, and 28 days). Results are expressed as mean ± SEM (* $p < 0.05$).

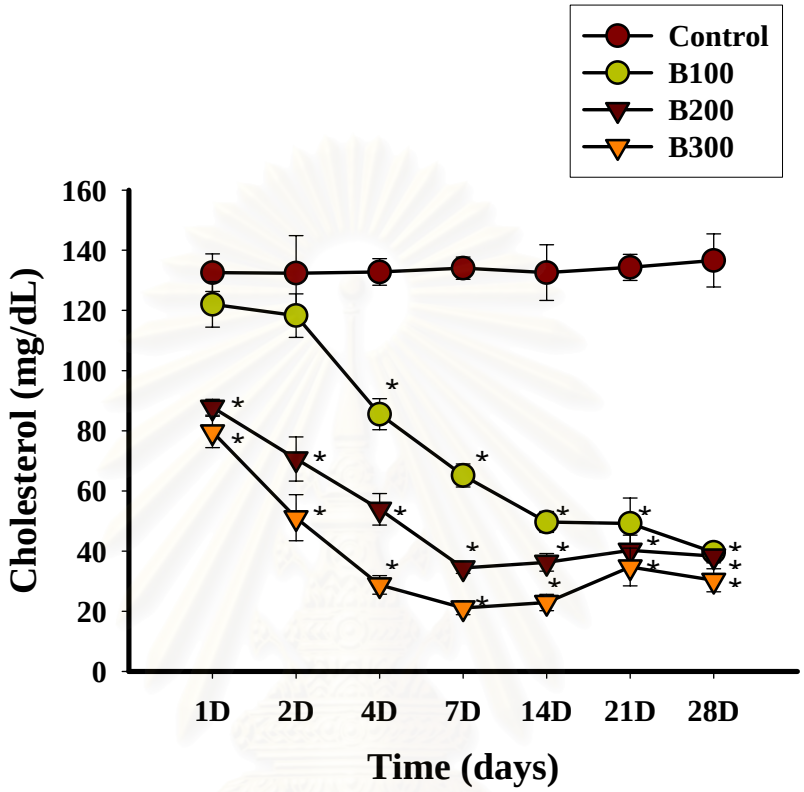

Fig. 30. Effect of barakol on cholesterol level in subacute toxicity study.

Mice received repeated doses of barakol (100, 200, and 300 mg/kg) and blood was collected at different time points (1, 2, 4, 7, 14, 21, and 28 days). Results are expressed as mean ± SEM (* $p < 0.05$).

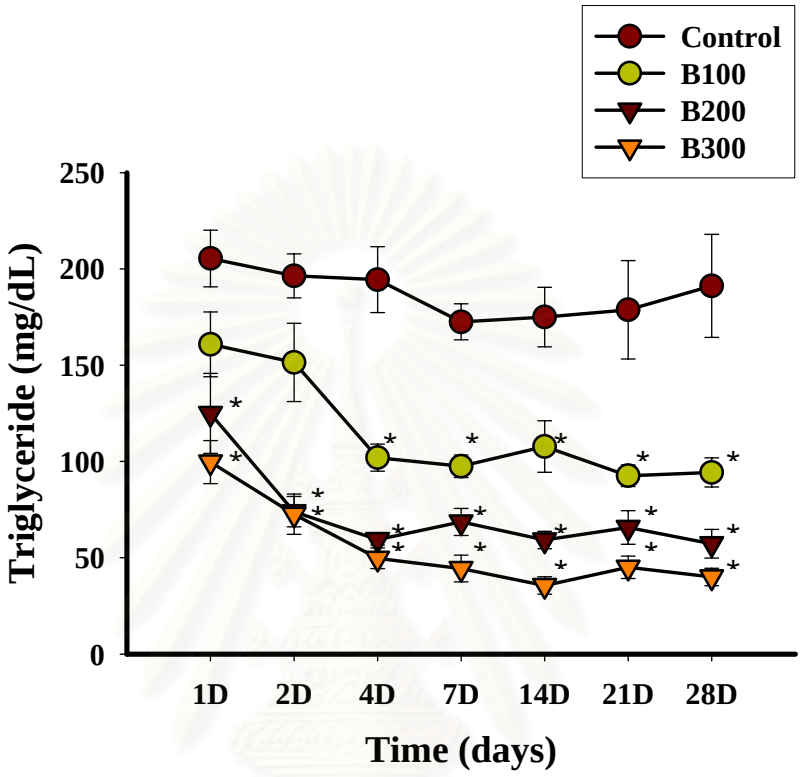

Fig. 31. Effect of barakol on triglyceride level in subacute toxicity study.

Mice received repeated doses of barakol (100, 200, and 300 mg/kg) and blood was collected at different time points (1, 2, 4, 7, 14, 21, and 28 days). Results are expressed as mean ± SEM (* $p < 0.05$).

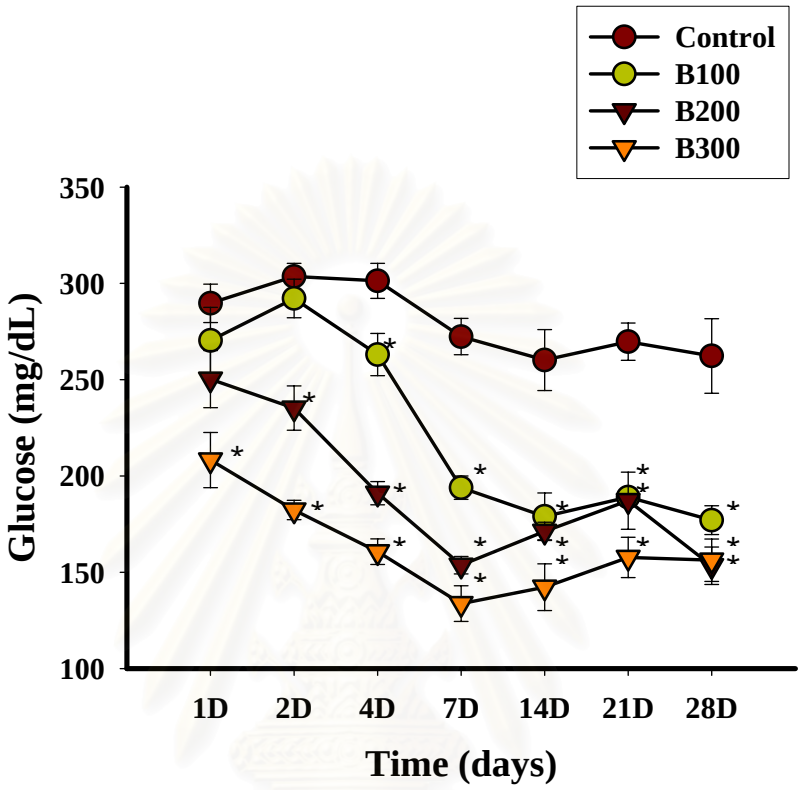

Fig. 32. Effect of barakol on glucose level in subacute toxicity study.

Mice received repeated doses of barakol (100, 200, and 300 mg/kg) and blood was collected at different time points (1, 2, 4, 7, 14, 21, and 28 days). Results are expressed as mean ± SEM (* $p < 0.05$).

Histopathological Findings

The histopathological finding in this experiment is summarized in Table 5. The lowest dose of barakol (100 mg/kg/day) caused swelling of hepatocytes located at pericentral zone after treatment for 4–21 days, together with diffuse hepatic necrosis and mitotic figure (Fig. 34). In addition, hepatocytes death in the form of apoptosis were also found at days 7-28 with a marked increase at 14 days of treatment (Fig. 35). The distribution of apoptotic cells at various time points is shown in Fig. 36. In 200 mg/kg/day barakol-treated mice, centrilobular hepatic swelling occurred at day 2 and 4 and widely spreaded to intermediate zone after 7, 14 and 21 days. At 28 days, it spreaded from pericentral zone to periportal (peripheral) zone (Figs. 37 and 38). Scattered necrosis and mitotic figure were also detected since day 1 to day 28. The apoptotic cells were shown markedly exhibited from pericentral zone to peripheral zone at day 14. The distribution of cell death was shown in Fig. 39. Scattered necrosis and mitotic figure were found in mice treated with highest dose of barakol (300 mg/kg/day) at different time points. Area of hepatocyte swelling spreaded from pericentral zone, intermediate zone and pericentral zone to peripheral zone at 2, 4-7, and 14-28 days post treatment, respectively (Figs. 40 and 41). The apoptotic cells were shown from pericentral zone to peripheral zone after treatment for 7 to 28 days, and the distribution of cell death was illustrated in Fig. 42. Based on apoptotic mapping index (AMI) calculation from area measurement and apoptotic count under the microscope, it was clear that lower doses of barakol increased AMI which peaked at day 14, and decreased progressively marking a crescendo-decrescendo profile. However, at higher doses of barakol, AMI appeared to increase vigorously beyond the time frame of this study (Fig. 43).

Mouse liver cell death in type of apoptosis found in tissue sections stained with H&E was confirmed by TUNEL assay. Slides were randomly selected from 100 mg/kg barakol-treated mice for 14 days. They showed positive nuclei compared with apoptotic bodies at the same area in the same specimen that was

previously stained with H&E (Fig. 44). The states of morphological changes in apoptosis were presented in Fig. 45.

All treated groups showed brown pigment in sinusoid and in Kupffer cell after 14 to 28 days in 100 and 200 mg/kg/day barakol-treated mice and 7-28 days in 300 mg/kg/day treated group. Slides randomly selected from 300 mg/kg barakol-treated mice, exhibited the hemosiderin pigment located in Kupffer cell confirmed by Thurnbull blue staining (Fig. 46). Slides selected from 300 mg/kg/day barakol-treated mice at 28 days, hemosiderin accumulation was markedly observed in the red pulp in spleen when compared to control group (Fig. 47).

In addition, after treating mice with barakol for 14 days, there was the red brown-color (fat accumulation) in cytoplasm of hepatocytes from pericentral zone to periportal zone. Low dose of barakol showed the positive color at pericentral zone which spreaded to periportal zone when treating with higher doses (Fig. 48).

Table 5. Histopathological findings of mouse liver after treating with various doses of barakol at different time points in subacute toxicity study.

Repeated Doses of Barakol (mg/kg/day)	Histopathological Findings									
	Necrosis	Hydropic Degeneration			Apoptotic Body			Iron Pigment		
		C	I	P	C	I	P	C	I	P
Control (Fig. 33)	-	-	-	-	-	-	-	-	-	-
Barakol 100 (Figs. 34-36)										
2 d	-	-	-	-	-	-	-	-	-	-
4 d	+	+	-	-	-	-	-	-	-	-
7 d	+/M	+	-	-	+	+	-	-	-	-
14 d	+/M	+	-	-	+	+	+	+	+	-
21 d	+/M	+	-	-	+	+	-	+	-	-
28 d	+/M	-	-	-	+	-	-	+	-	-
Barakol 200 (Figs. 37-39)										
2 d	+	+	-	-	-	-	-	-	-	-
4 d	+/M	+	-	-	-	-	-	-	-	-
7 d	+/M	+	+	-	+	+	+	-	-	-
14 d	+/M	+	+	-	+	+	+	-	+	+
21 d	+/M	+	+	-	+	+	+	+	+	+
28 d	+/M	+	+	+	+	+	+	+	+	+
Barakol 300 (Figs. 40-42)										
2 d	+	+	-	-	-	-	-	-	-	-
4 d	+	+	+	-	-	-	-	-	-	-
7 d	+/M	+	+	-	+	+	+	-	+	+
14 d	+/M	+	+	+	+	+	+	+	+	+
21 d	+/M	+	+	+	+	+	+	+	+	+
28 d	+/M	+	+	+	+	+	+	+	+	+

Mice received repeated doses of barakol (100, 200, and 300 mg/kg), and livers were taken at different time points (2, 4, 7, 14, 21, and 28 days) for histopathological examination. C, pericentral zone; P, peripheral zone; I, intermediate zone; +, present; -, not present; +/M, present with mitotic figure.

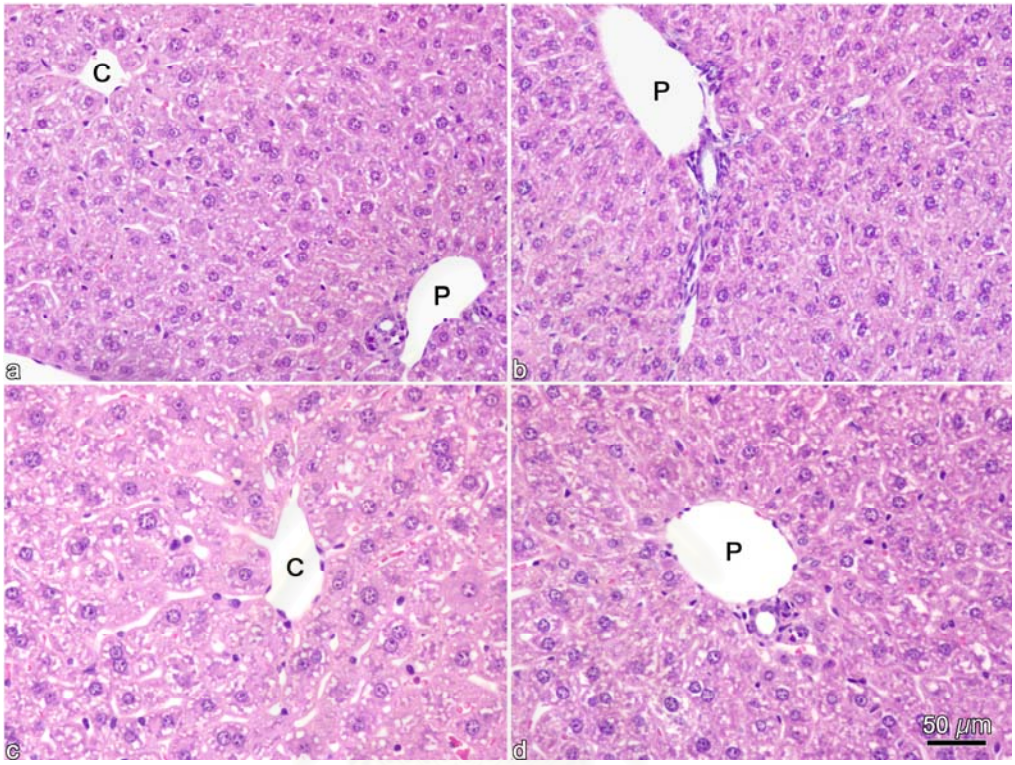

Fig. 33. Light micrographs of control mouse liver stained with H&E.

Mice received distilled water only. Normal liver is shown (a-d).
C, central vein; P, portal vein

Fig. 34. Light micrographs of mouse liver after treating with barakol (100 mg/kg/day) at different time points (2, 4, and 7 days) and stained with H&E.

a and b Liver section at day 2, no swelling of hepatocytes.

c Liver section at day 4, showing swelling of hepatocytes and scattered necrosis presented by neutrophil infiltration at pericentral zone (arrow).

d Liver section at day 4, showing scattered necrosis presented by neutrophil infiltration at peripheral zone and single cell necrosis (pyknotic nuclei, intact cell membrane, absence of inflammation) (arrow).

e-h Liver section at day 7, showing swelling of hepatocytes at pericentral zone, scattered necrosis presented by neutrophil infiltration (arrow) and liver undergoing mitosis (arrowhead).

C, central vein; P, portal vein.

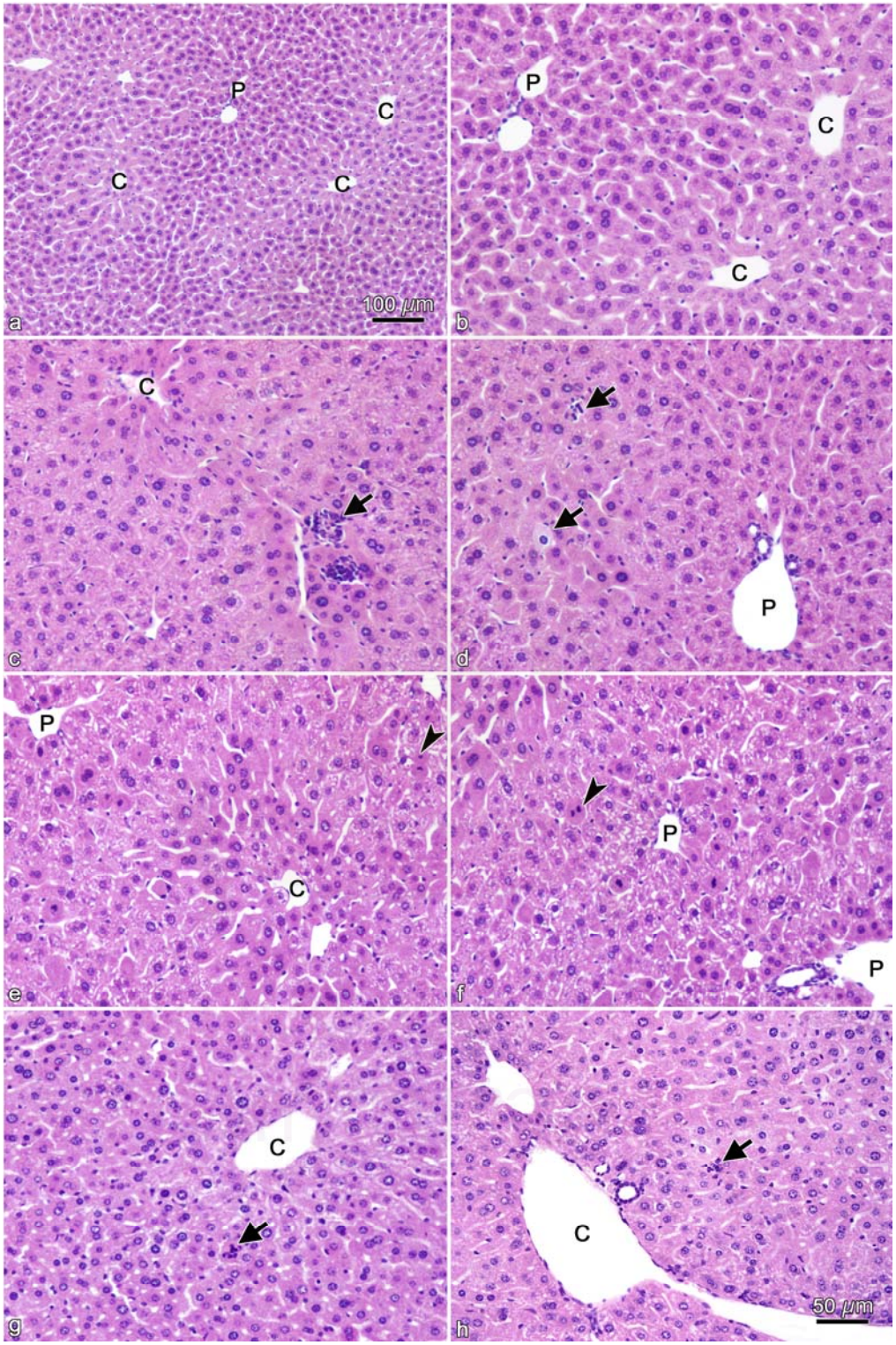
P
C
C
C
100 µm
a
P
C
C
b
C
c
P
d
P
C
e
P
P
f
C
g
C
50 µm
h

Fig. 35. Light micrographs of mouse liver after treating with barakol (100 mg/kg/day) at different time points (14, 21, and 28 days) and stained with H&E.

a-d Liver section at day 14, showing swelling of hepatocytes and scattered necrosis presented by neutrophil infiltration at pericentral zone (solid arrow), apoptotic cells with nuclear change (condensation and fragmentation) (open arrow), and liver cell undergoing mitosis (arrowhead).

e and f Liver section at day 21, showing degeneration, scattered necrosis presented by neutrophil infiltration (solid arrow), apoptotic cells with binucleated nuclear change (condensation and fragmentation) (open arrow).

g and h Liver section at day 28, showing degeneration, swelling of hepatocytes, apoptotic cells with nuclear change (open arrow).

C, central vein; P, portal vein.

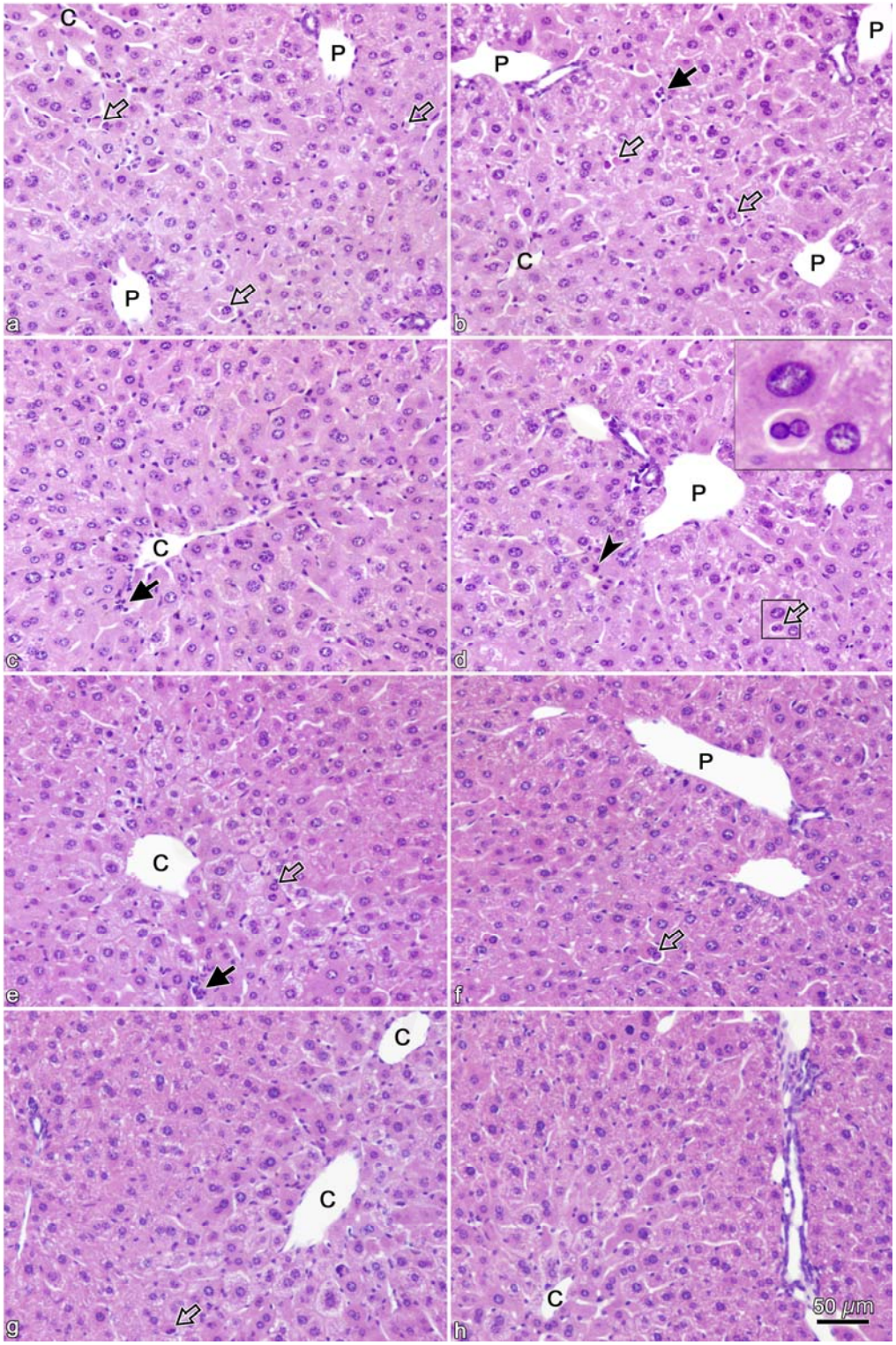
C
P
P
a
P
P
C
P
b
C
c
P
d
C
e
P
f
C
C
g
C
50 µm
h

Fig. 36. The distribution of apoptotic cells was observed in mapping of mouse liver sections after treating with barakol (100 mg/kg/day) at 7, 14, 21, and 28 days and stained with H&E.

7D Liver mapping at day 7, showing scattered apoptotic cells at pericentral zone to intermediate zone.

14D Liver mapping at day 14, showing apoptotic cells increased and widely spreaded from pericentral zone to peripheral zone.

21D Liver mapping at day 21, showing apoptotic cells at pericentral zone to intermediate zone.

28D Liver mapping at day 28, showing scattered apoptotic cells at pericentral zone to intermediate zone.

Yellow, central vein; Red, portal vein; Blue dot, apoptotic body.

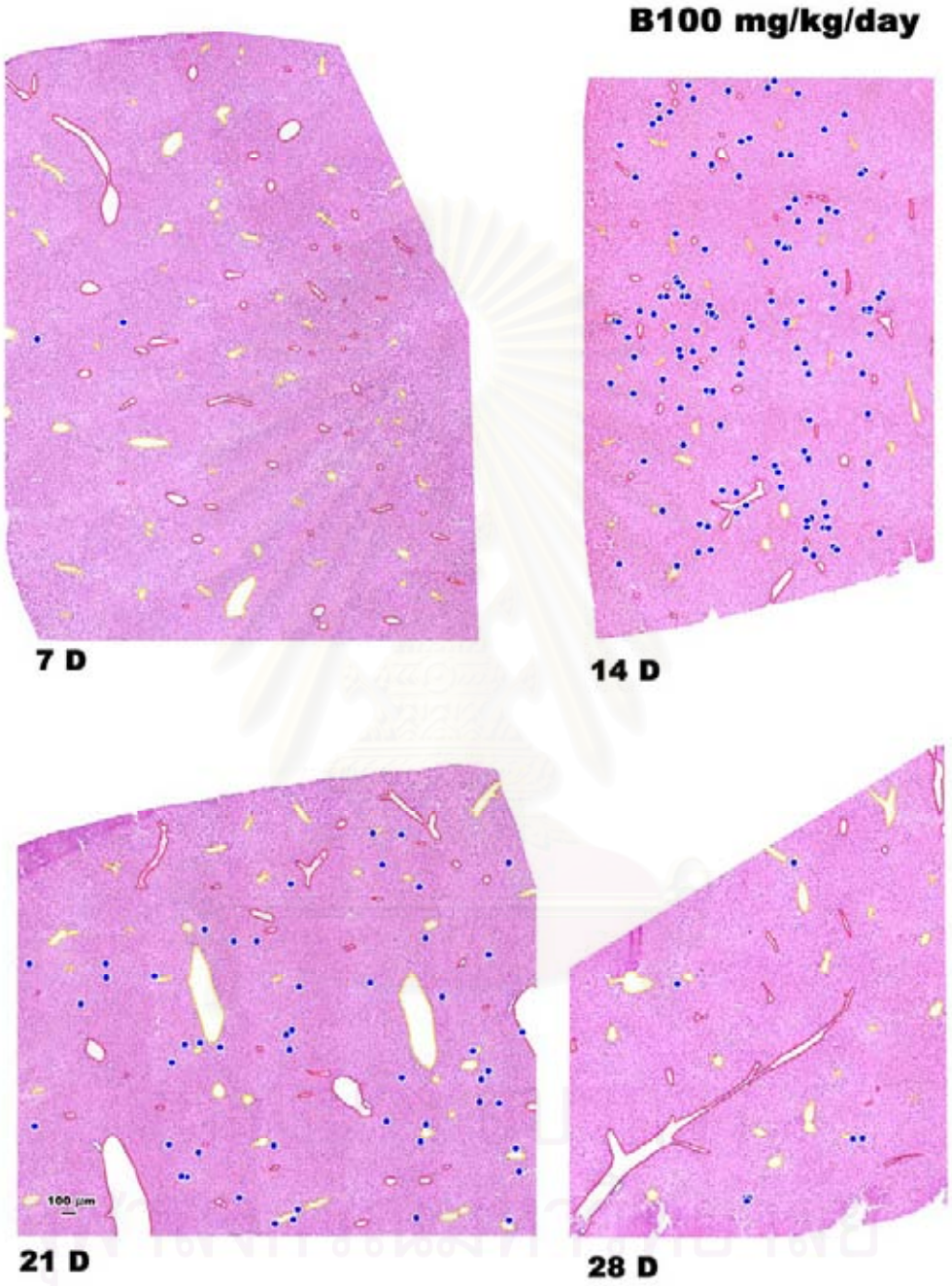
B100 mg/kg/day
7 D
14 D
21 D
28 D
100 µm

Fig. 37. Light micrographs of mouse liver after treating with barakol (200 mg/kg/day) at different time points (2-14 days) and stained with H&E.

a and b Liver section at day 2, no swelling of hepatocytes, scattered necrosis presented by neutrophil infiltration and single cell necrosis (pyknotic nuclei, intact cell membrane, absence of inflammation) (solid arrow).

c Liver section at day 4, showing swelling of hepatocytes at pericentral zone.

d Liver section at day 4, showing liver cell undergoing mitosis (arrowhead).

e and f Liver section at day 7, showing swelling of hepatocytes, scattered necrosis presented by neutrophil infiltration (solid arrow) and apoptotic cells (intracellular apoptotic bodies showing chromatin condensation and increased eosinophilia) (open arrow).

g and h Liver section at day 14, showing swelling of hepatocytes and apoptotic cells (intracellular apoptotic bodies showing chromatin condensation and increased eosinophilia) (open arrow).

C, central vein; P, portal vein.

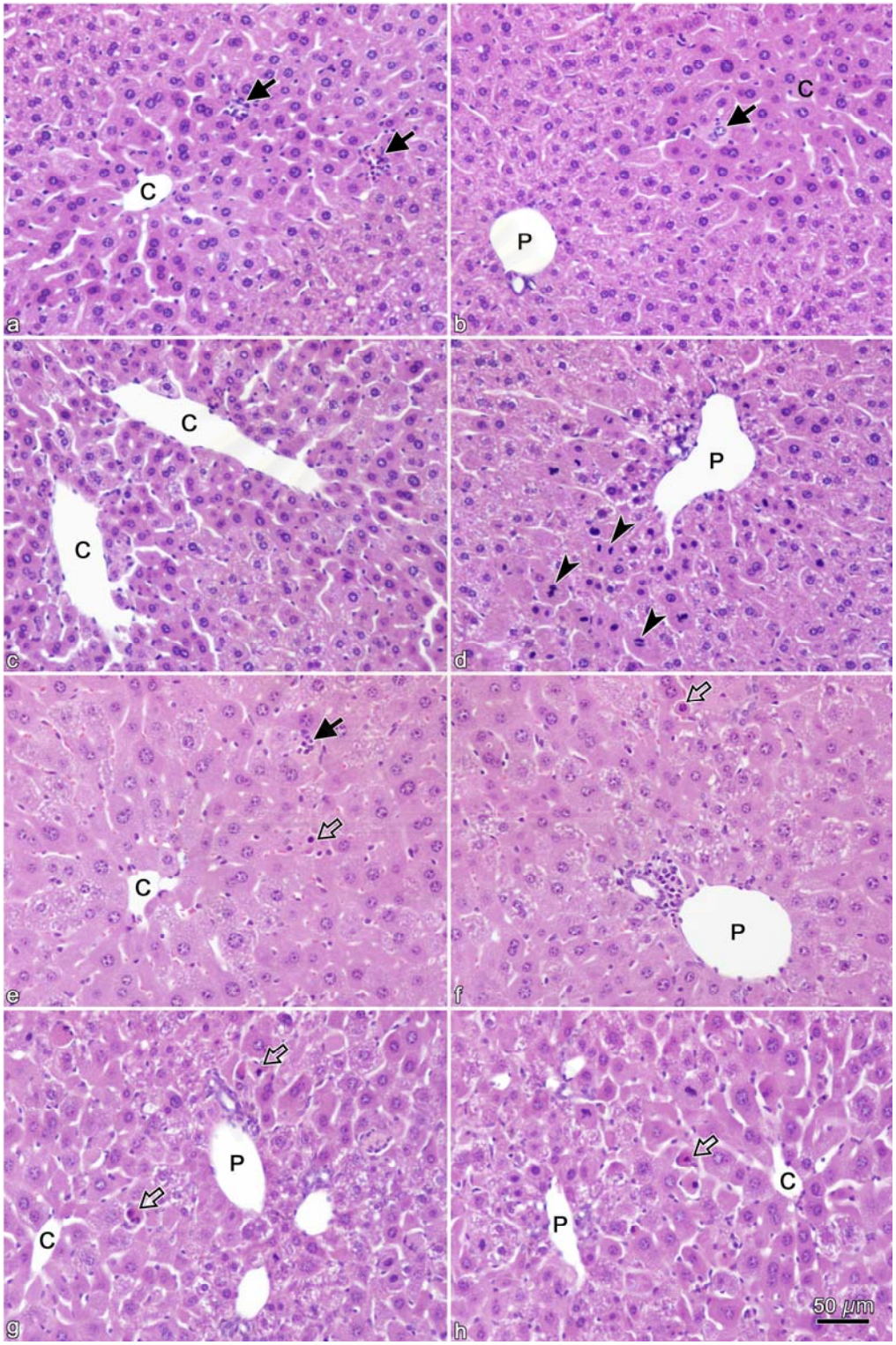
a
C
b
C
P
c
C
C
d
P
e
C
f
P
g
P
C
h
C
P
50 µm

Fig. 38. Light micrographs of mouse liver after treating with barakol (200 mg/kg/day) at different time points (7-28 days) and stained with H&E.

a and b Liver section at day 7, showing swelling of hepatocytes and apoptotic cells (intracellular apoptotic bodies showing chromatin condensation and increased eosinophilia) (arrow).

c and d Liver section at day 14, showing swelling of hepatocytes, apoptotic cells (intracellular apoptotic bodies showing chromatin condensation and increased eosinophilia) (arrow), and brown pigment in Kupffer cell.

e and f Liver section at day 21, showing swelling of hepatocytes, apoptotic cells (intracellular apoptotic bodies showing chromatin condensation and increased eosinophilia), apoptotic bodies were phagocytosed by Kupffer cell (arrow) and brown pigment in Kupffer cell.

g and h Liver section at day 28, showing swelling of hepatocytes and apoptotic cells (increased eosinophilia) (arrow) and brown pigment in Kupffer cell.

C, central vein; P, portal vein.

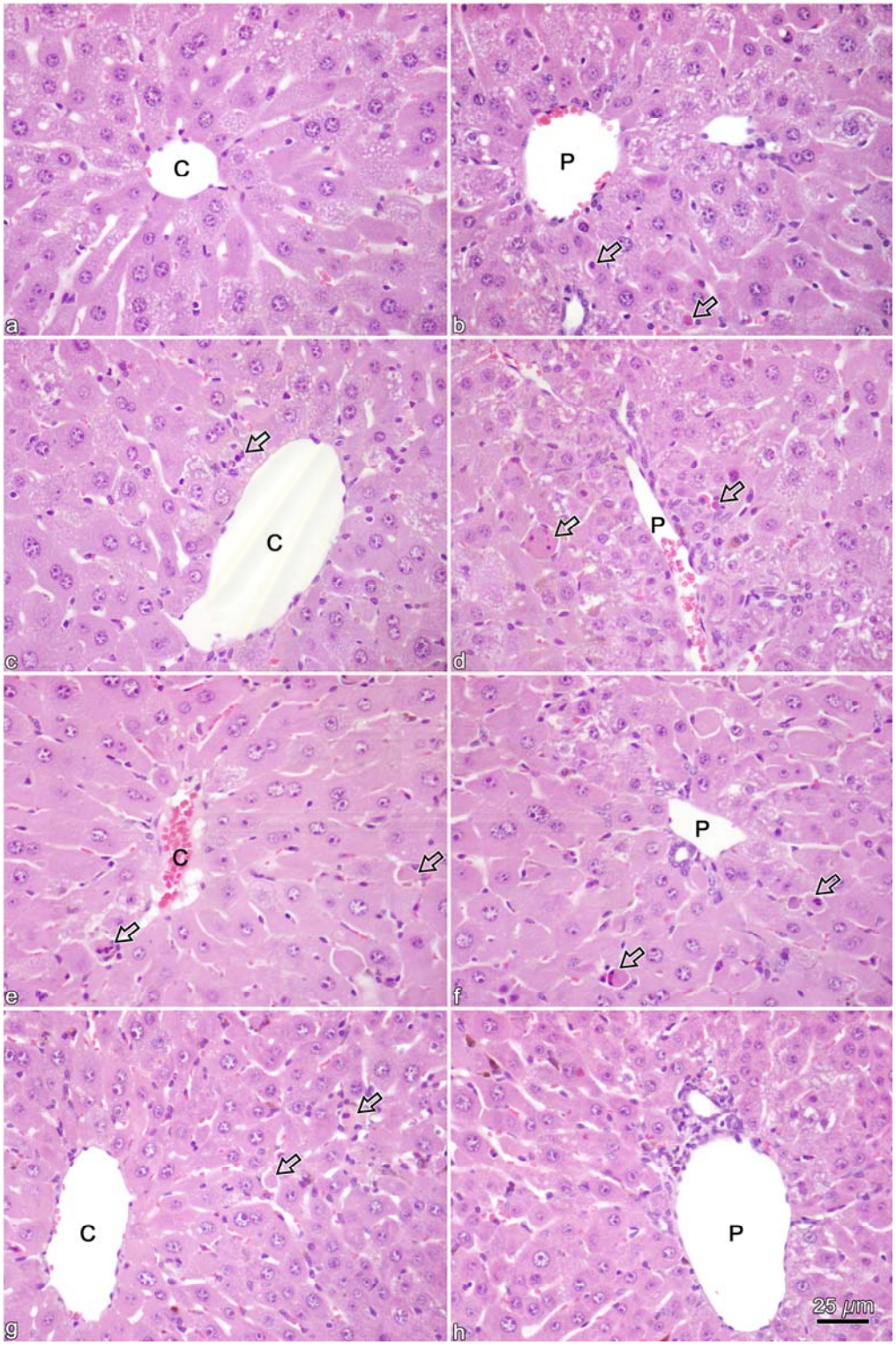
a
C
b
P
c
C
d
P
e
C
f
P
g
C
h
P
25 µm

Fig. 39. The distribution of apoptotic cells was observed in mapping of mouse liver sections after treating with barakol (200 mg/kg/day) at 7, 14, 21, and 28 days and stained with H&E.

7D Liver mapping at day 7, showing scattered apoptotic cells from pericentral zone to periportal (peripheral) zone.

14D Liver mapping at day 14, showing the increased apoptotic bodies and widely spreaded from pericentral zone to peripheral zone.

21D Liver mapping at day 21, showing apoptotic cells observed from pericentral zone to periportal zone.

28D Liver mapping at day 28, showing scattered apoptotic cells from pericentral zone to periportal zone.

Yellow, central vein; Red, portal vein; Blue dot, apoptotic body.

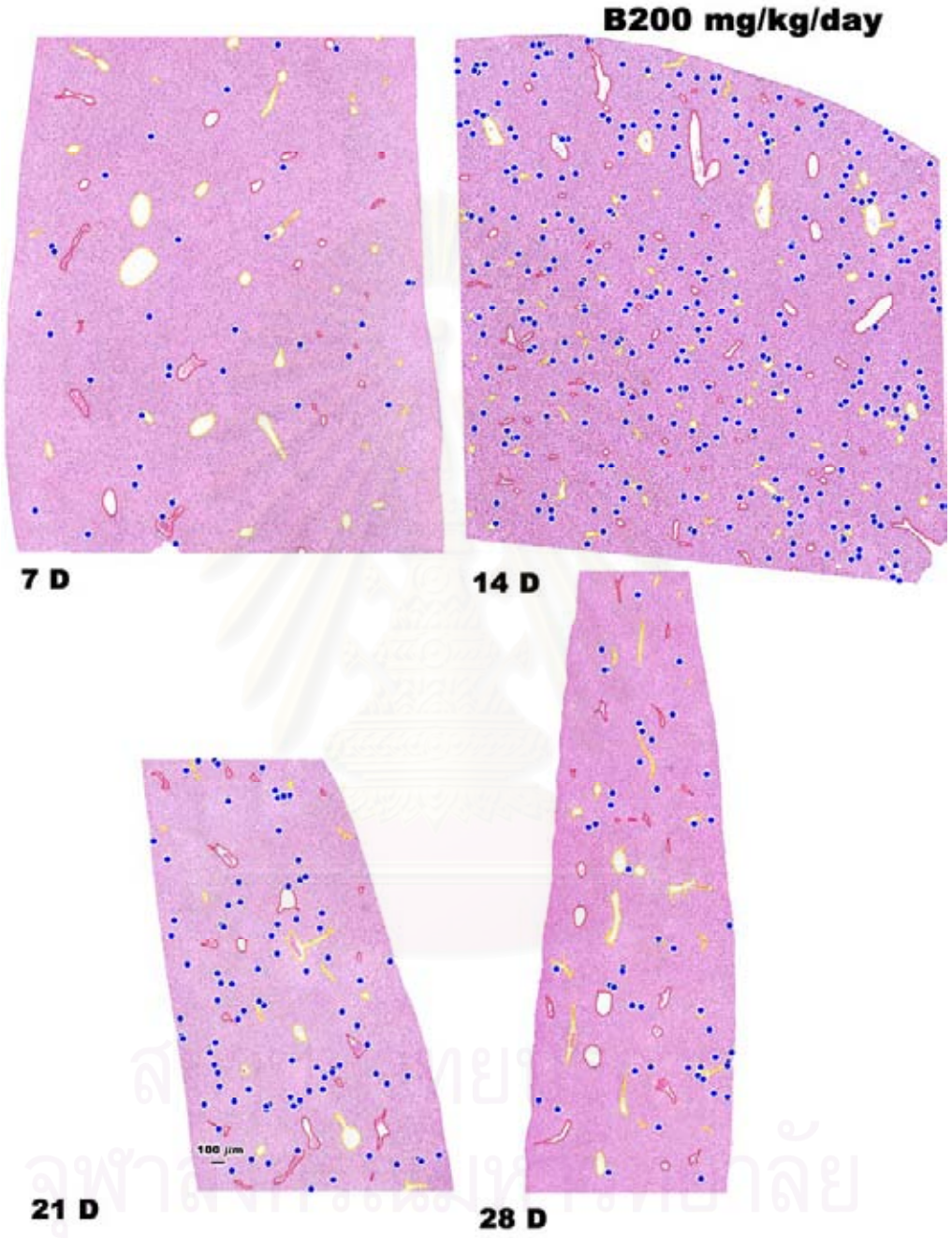
B200 mg/kg/day
7 D
14 D
21 D
28 D
100 µm

Fig. 40. Light micrographs of mouse liver after treating with barakol (300 mg/kg/day) at different time points (2-14 days) and stained with H&E.

a and b Liver section at day 2, showing degeneration, scattered necrosis presented by neutrophil infiltration (solid arrow).

c and d Liver section at day 4, showing degeneration, scattered necrosis presented by neutrophil infiltration (solid arrow).

e and f Liver section at day 7, showing swelling of hepatocytes and apoptotic cells (intracellular apoptotic bodies showing chromatin condensation, fragmentation and increased eosinophilia) (open arrow).

g and h Liver section at day 14, showing swelling of hepatocytes, apoptotic cells (intracellular apoptotic bodies showing chromatin condensation and increased eosinophilia) (open arrow) and brown pigment in Kupffer cell.

C, central vein; P, portal vein.

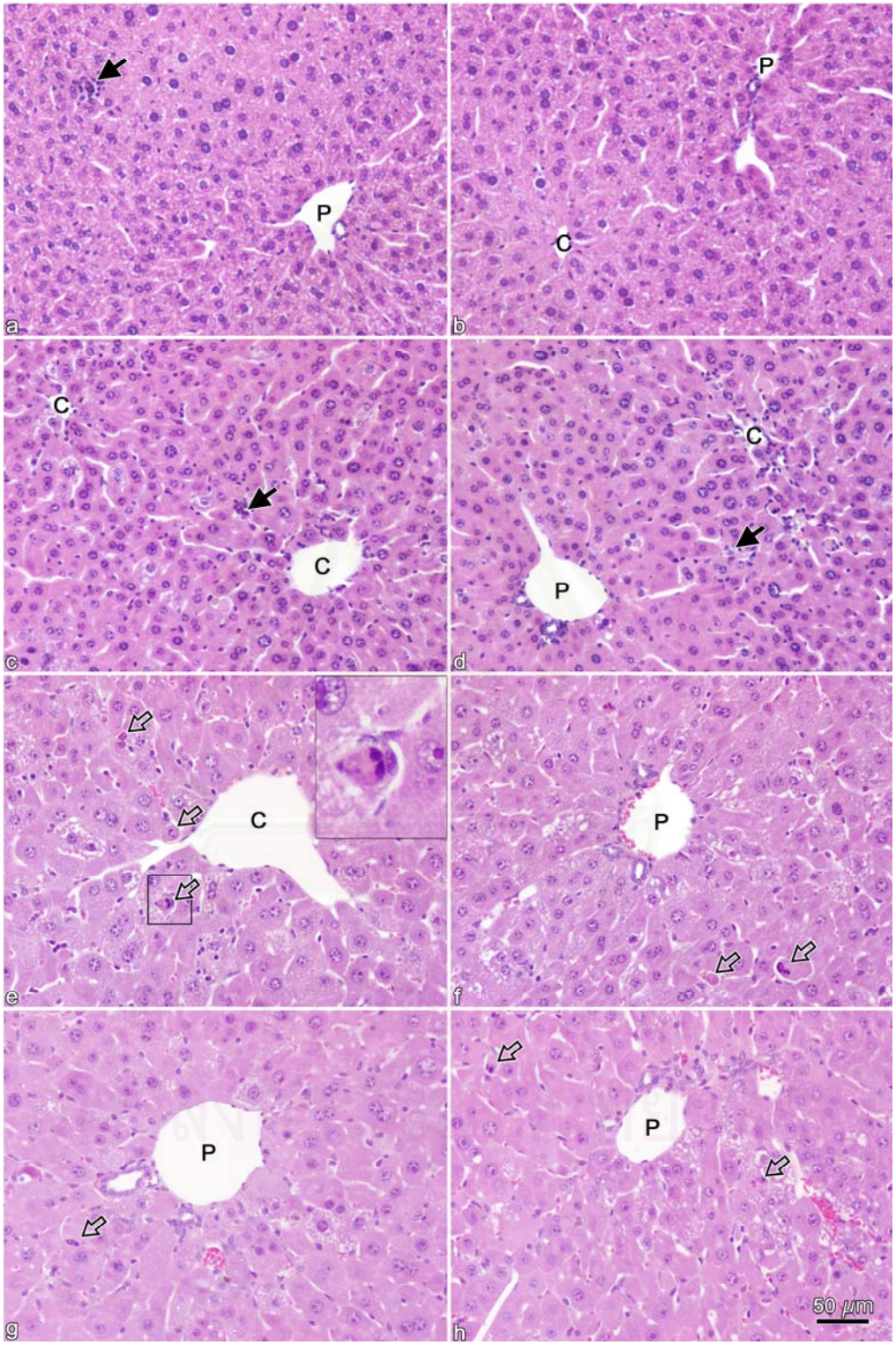
a
P
b
P
C
c
C
C
d
C
P
e
C
f
P
g
P
h
P
50 µm

Fig. 41. Light micrographs of mouse liver after treating with barakol (300 mg/kg/day) at different time points (21 and 28 days) and stained with H&E.

a and b Liver section at day 21, showing degeneration of liver cells with ground glass appearance of cytoplasm, swelling of hepatocytes, apoptotic cells (intracellular apoptotic bodies showing chromatin condensation and increased eosinophilia), and increasing brown pigment in Kupffer cell.

c and d Liver section at day 28, showing swelling of hepatocytes, apoptotic cells (increased eosinophilia) (open arrow) and brown pigment in Kupffer cell.

e and f High magnification of liver section at day 21, showing apoptotic cells (intracellular apoptotic bodies showing chromatin condensation and increased eosinophilia), apoptotic bodies were phagocytosed by Kupffer cell (open arrow) and brown pigment in Kupffer cell.

g and h High magnification of liver section at day 28, showing apoptotic cells (intracellular apoptotic bodies showing chromatin condensation and increased eosinophilia), apoptotic bodies were phagocytosed by Kupffer cell (open arrow) and brown pigment in Kupffer cell.

C, central vein; P, portal vein.

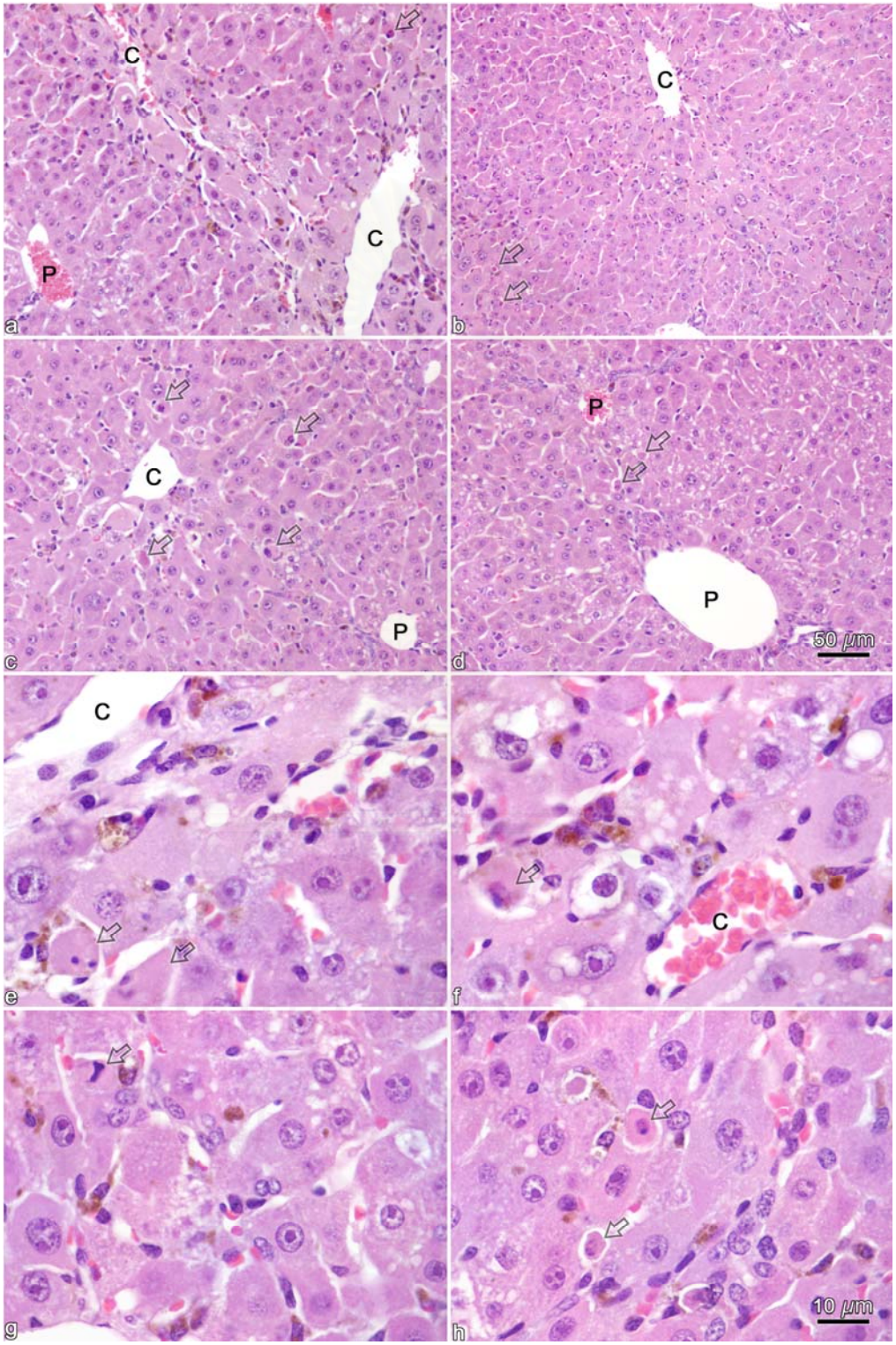
C
C
P
a
C
b
C
P
c
P
P
50 μm
d
C
e
C
f
g
10 μm
h

Fig. 42. The distribution of apoptotic cells was observed in mapping of mouse liver sections after treating with barakol (300 mg/kg/day) at 7, 14, 21, and 28 days and stained with H&E.

7D Liver mapping at day 7, showing apoptotic cells from pericentral zone to periportal zone.

14D Liver mapping at day 14, showing apoptotic cells from pericentral zone to periportal zone.

21D Liver mapping at day 21, showing apoptotic cells, prominent from pericentral zone and observed from pericentral zone to periportal zone.

28D Liver mapping at day 28, showing scattered apoptotic cells, prominent and widely spreaded from pericentral zone to periportal zone.

Yellow, central vein; Red, portal vein; Blue dot, apoptotic body.


B300 mg/kg/day
7 D
14 D
21 D
28 D
100 µm

A

Barakol 100 (mg/kg/day)	Apoptotic Count	Sectional Area (μm^2)	AMI (count / 1 mm^2)
7d	2	1.28×10^7	0.16
14d	126	9.08×10^6	13.88
21d	50	1.10×10^7	4.55
28d	7	6.97×10^6	1.00

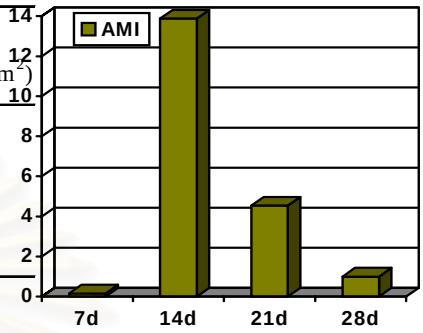

B

Barakol 200 (mg/kg/day)	Apoptotic Count	Sectional Area (μm^2)	AMI (count /1 mm^2)
7d	34	1.13×10^7	3.01
14d	327	1.25×10^7	26.22
21d	87	5.27×10^6	16.50
28d	48	5.69×10^6	8.43

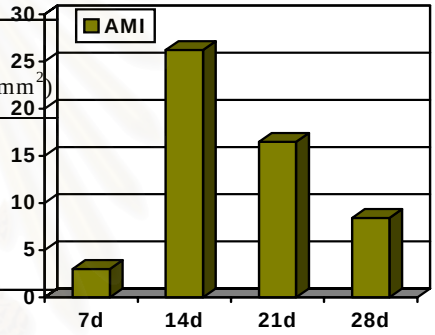

C

Barakol 300 (mg/kg/day)	Apoptotic Count	Sectional Area (μm^2)	AMI (count /1 mm^2)
7d	138	8.15×10^6	16.93
14d	60	6.19×10^6	9.70
21d	198	6.92×10^6	28.61
28d	356	6.85×10^6	51.94

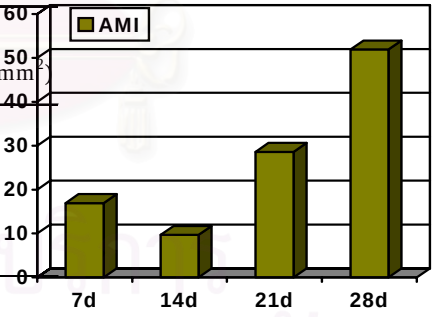

Fig. 43. Calculation of apoptotic mapping index (AMI) based on area measurement conducted by a Nikon on Cosmozone 1SA on an NEC work station. A, barakol 100 mg; B, barakol 200 mg; C, barakol 300 mg.

Fig. 44. Fluorescence micrographs of mouse liver showing results of TUNEL assay as compared to the same slides previously stained with H&E.

a Liver section of control mice, showing no positive nuclei.

b Liver section of control mice treated with DNAse I, showing the distribution of nuclei with greenish fluorescence of TUNEL-positive nuclei.

c, e, g Liver section at day 14, showing nuclei with greenish fluorescence of TUNEL-positive nuclei.

d, f, h Liver section at day 14 stained with H&E, showing apoptotic cells (intracellular apoptotic bodies showing chromatin condensation and increased eosinophilia) (arrow) at the same location of nuclei with greenish fluorescence of TUNEL-positive nuclei in pictures c, e, and g.

P, portal vein.

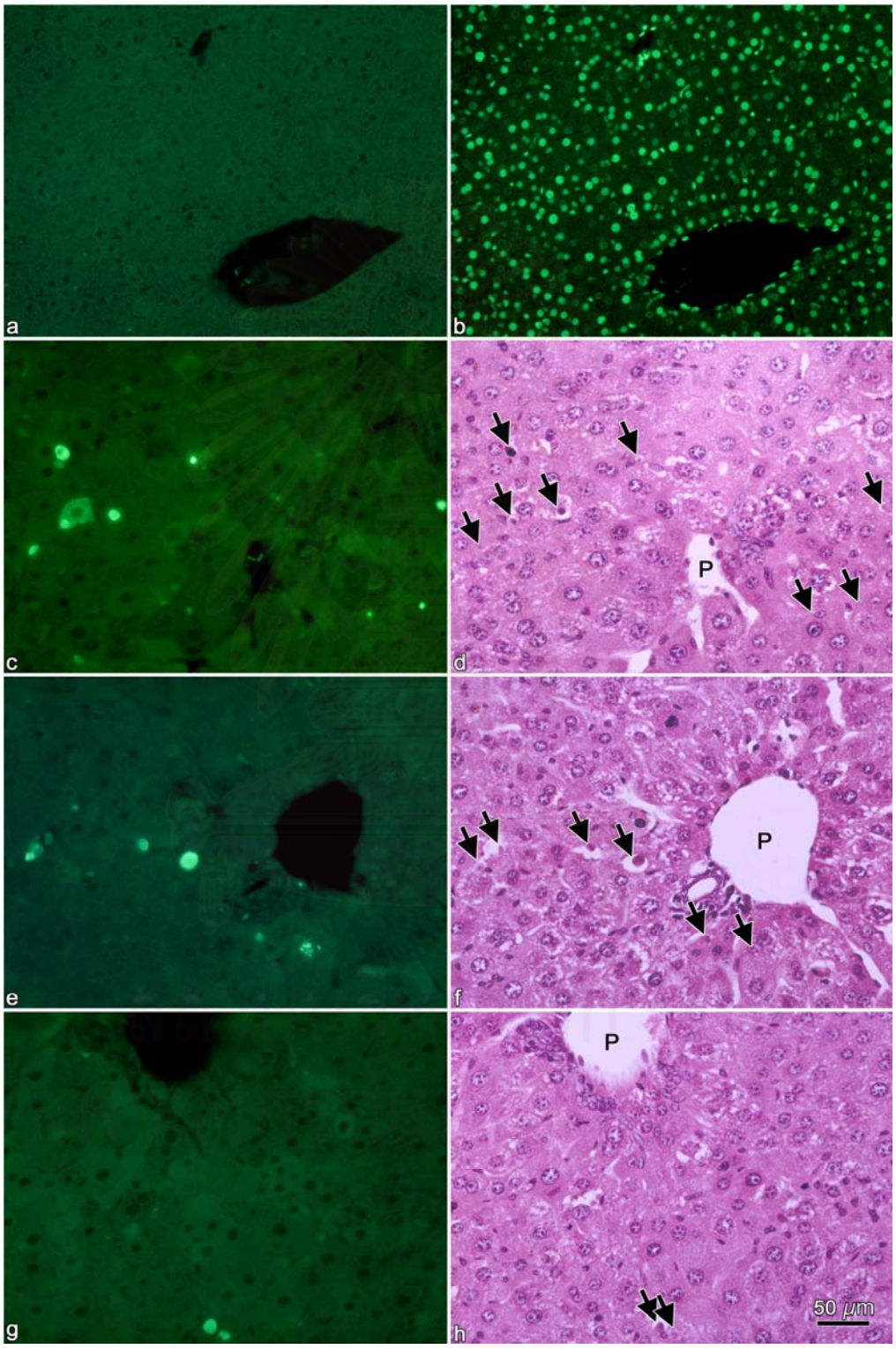
a
b
c
d
P
e
f
P
g
h
P
50 μm

Fig. 45. Light micrographs of mouse liver, showing morphologic characteristics of apoptosis at various stages as seen in preparations.

a Apoptotic cells showing chromatin condensation.

b Apoptotic cells showing nuclear fragmentation, condensation, and convolusion of cell membrane.

c Apoptotic cells showing nuclear event changing, convolusion of cell membrane and blebbing.

d Apoptotic cells showing nuclear event changing pronounced pyknosis and convolusion of cell membrane.

e Intracellular apoptotic bodies showing chromatin condensation, increased acidophilicity, and reduced cytoplasmic volume.

f Apoptotic bodies were phagocytosed by neighboring hepatocytes.

g and h Apoptotic bodies were phagocytosed by Kupffer cells.

C, central vein.

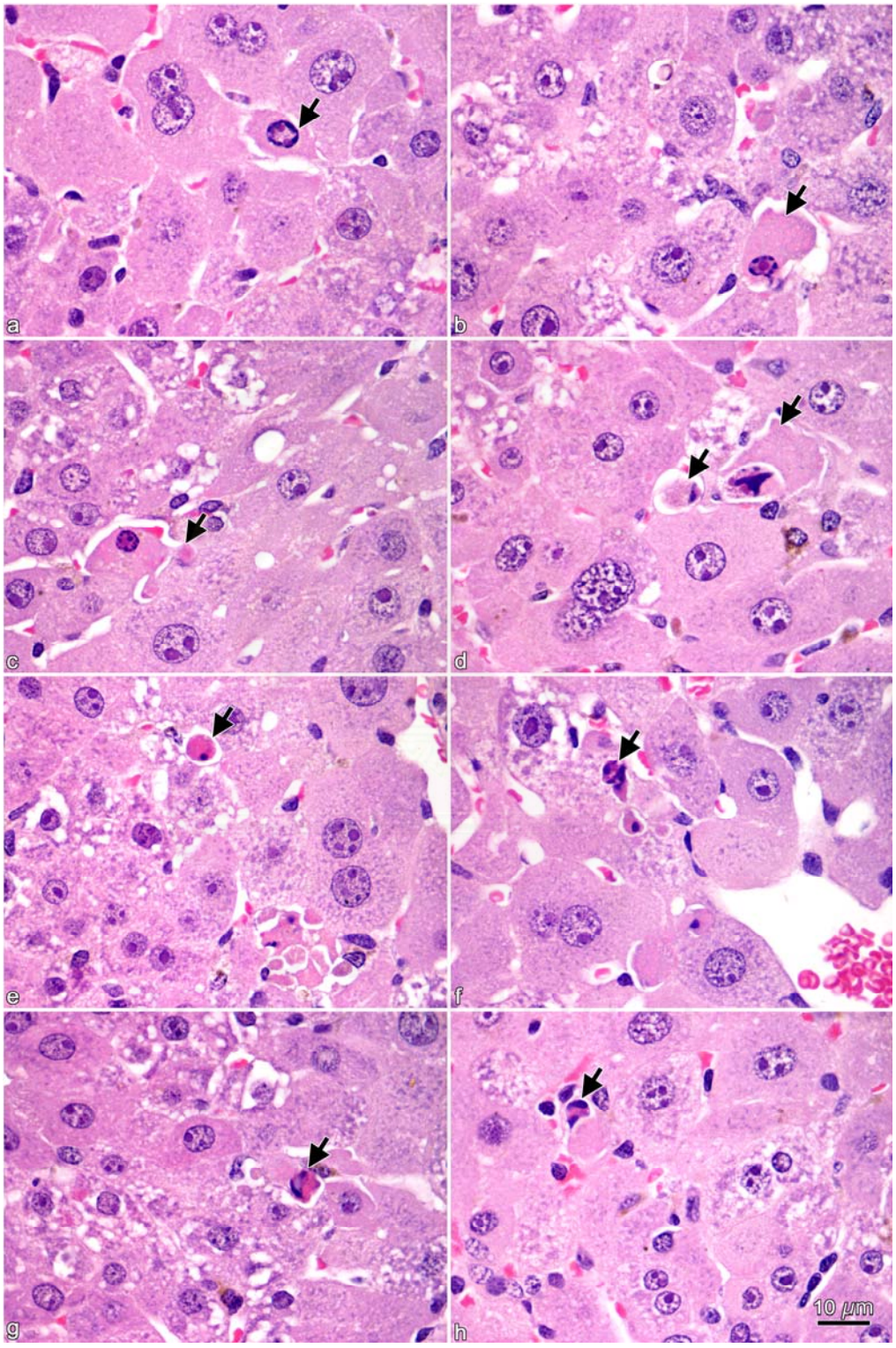
a
b
c
d
e
f
g
h
10 µm

Fig. 46. Light micrographs of mouse liver, showing results of Turnbull blue staining.

a Liver section of control mouse, showing scattered foci of positive pigments (blue).

b Liver section at day 7, showing the distribution of positive pigments (blue) at periportal zone to pericentral zone.

c Liver section at day 14, showing the distribution of positive pigments (blue) at periportal zone to intermediate zone.

d Liver section at day 14, showing the distribution of positive pigments (blue) at periportal zone to pericentral zone.

e and f High magnification of liver section at day 21, showing the distribution of positive pigments (blue) at periportal zone to pericentral zone.

g and h High magnification of liver section at day 21, (same sample as picture e and f) stained with H&E showing brown pigment in Kupffer cells.

C, central vein; P, portal vein.

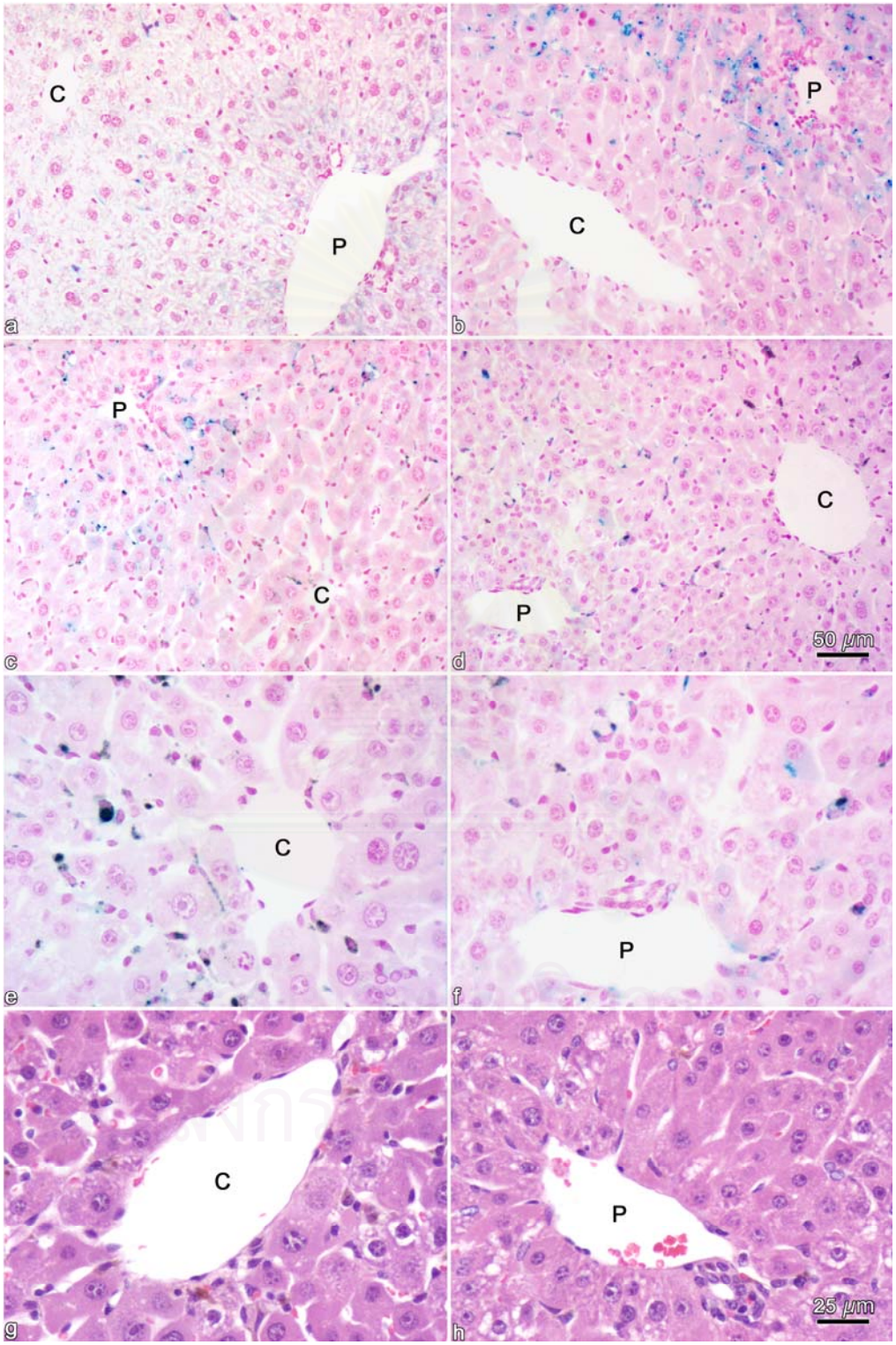
C
P
a
P
C
b
P
C
c
C
P
50 μm
d
C
e
P
f
C
g
P
25 μm
h

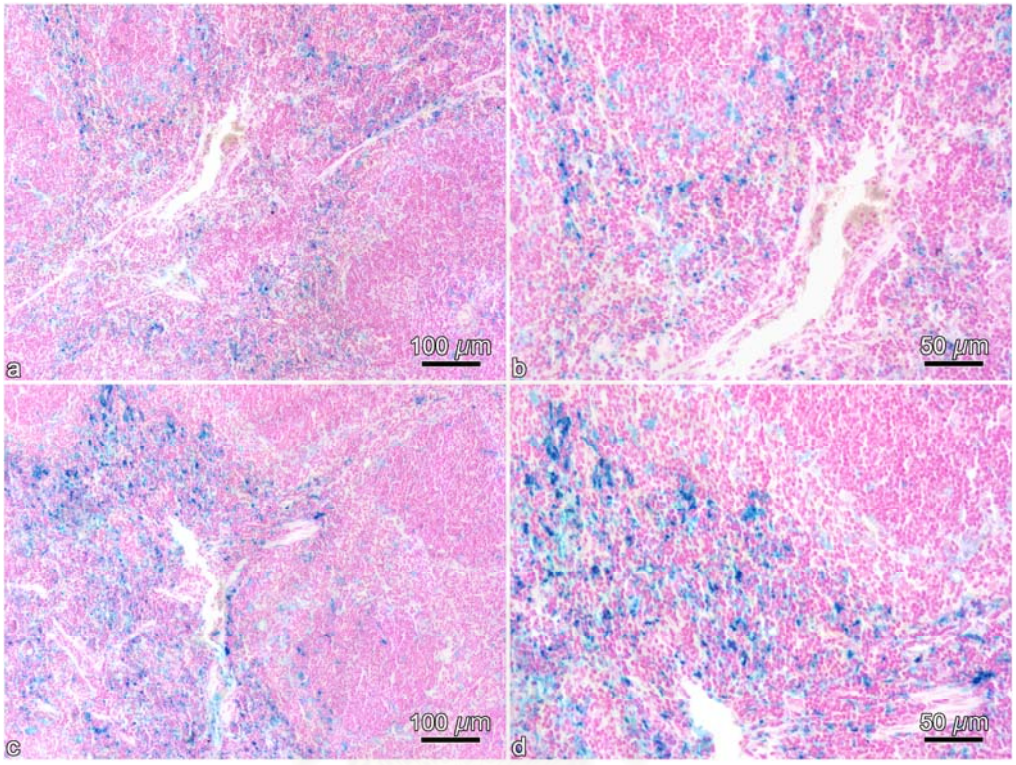

Fig. 47. Light micrographs of mouse spleen, showing results of Turnbull blue staining.

a and b Liver section of control mouse, showing positive pigment (blue) in red pulp.

c and d Liver section at day 28, showing the distribution of positive pigment (blue) in red pulp.

Fig. 48. Light micrographs of mouse liver, showing results of Sudan III staining.

a and b Liver section of control mice, showing no red brown color in hepatocytes.

c and d Liver section at day 14 (100 mg/kg barakol), showing the red brown color in hepatocytes at pericentral zone.

e and f Liver section at day 14 (200 mg/kg barakol), showing the red brown color in hepatocytes from pericentral zone to periportal zone.

g and h Liver section at day 14 (300 mg/kg barakol), showing the red brown color in hepatocytes from pericentral zone to periportal zone.

C, central vein; P, portal vein.

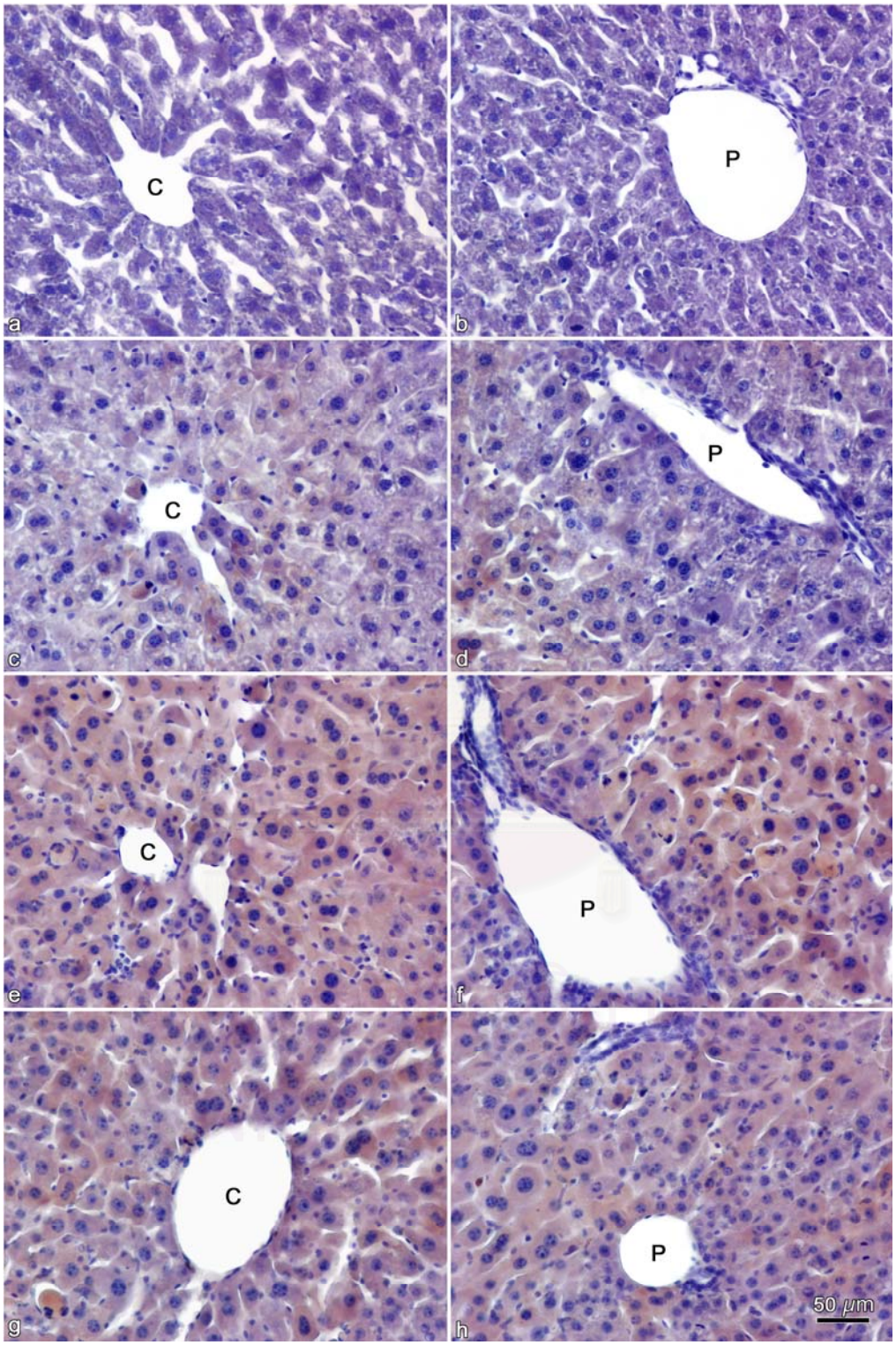
C
P
a
b
C
P
c
d
C
P
e
f
C
P
50 µm
g
h

Part B : Possible Mechanisms of Barakol-Induced Hepatotoxicity, *Ex Vivo* and *In Vi*tro Studies

Ex Vivo Study

Effects of Barakol on Hepatic Microsomal Contents and Protein Expression

Total Cytochrome P450 Contents

In acute toxicity study, the total cytochrome P450 contents decreased in 300 and 400 mg/kg barakol-treated mice after 24 and 48 hours and tended to go back to normal at 72 and 96 hours (Fig. 49).

In subacute toxicity study, the total cytochrome P450 contents decreased to approximately 50 % of control value in barakol (200 and 300 mg/kg/day)-treated groups after 7, 14, 21, and 28 days of treatment (Fig. 50).

CYP 3A1 and CYP 2E1 Protein Expression

The protein expression of CYP 3A1 and CYP 2E1 were detected in two groups of barakol-treated mice (200 and 300 mg/kg/day) after treatment for 14 days. Western blot analysis showed no difference in relative intensity of CYP 3A1 and CYP 2E1 proteins compared with control group at the same time point (Figs. 51 and 52).

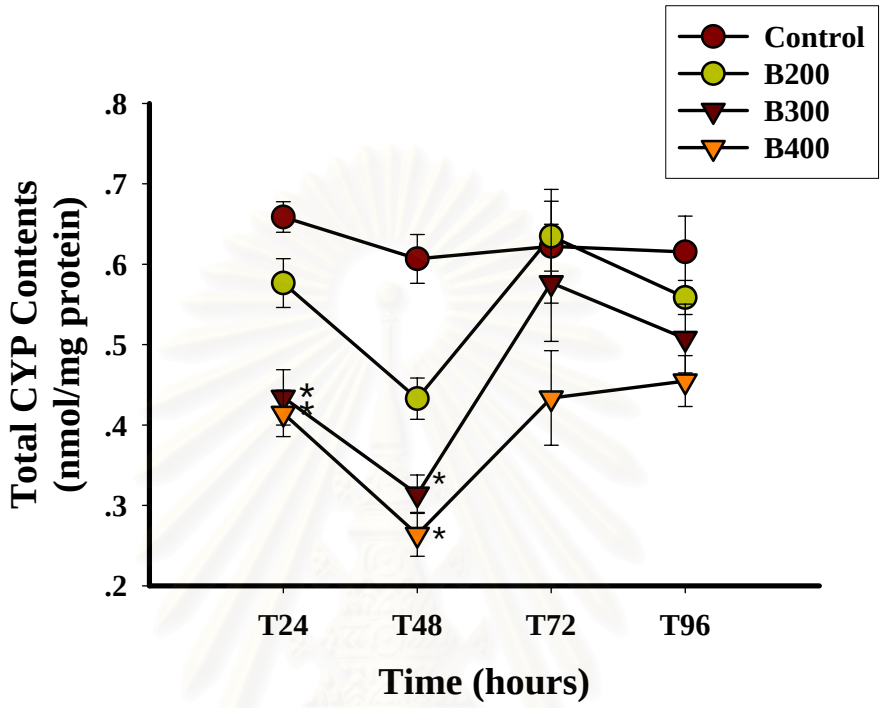

Fig. 49. Effect of barakol on mouse total hepatic microsomal cytochrome P450 contents (nmol/mg protein) in acute toxicity study.

The microsomal proteins were obtained from livers of barakol-treated mice (a single dose of 200, 300, and 400 mg/kg) after treatment for 24, 48, 72, and 96 hours. Results are expressed as mean ± SEM (* $p < 0.05$).

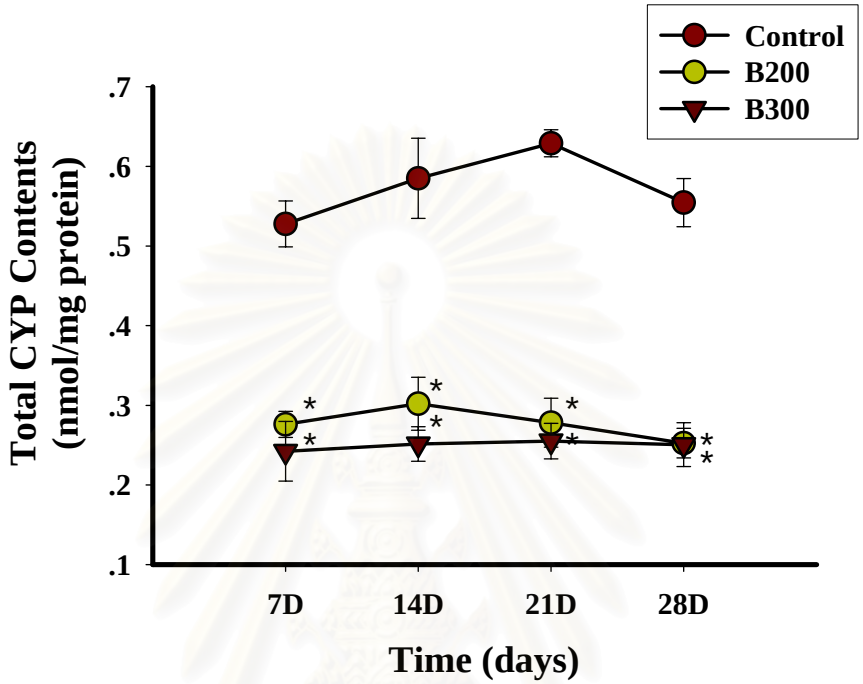

Fig. 50. Effect of barakol on mouse total hepatic microsomal cytochrome P450 contents (nmol/mg protein) in subacute toxicity study.

The microsomal proteins were obtained from livers of barakol-treated mice (repeated doses of 200 and 300 mg/kg) after treatment for 7, 14, 21, and 28 days. Results are expressed as mean ± SEM (* $p < 0.05$).

1

2

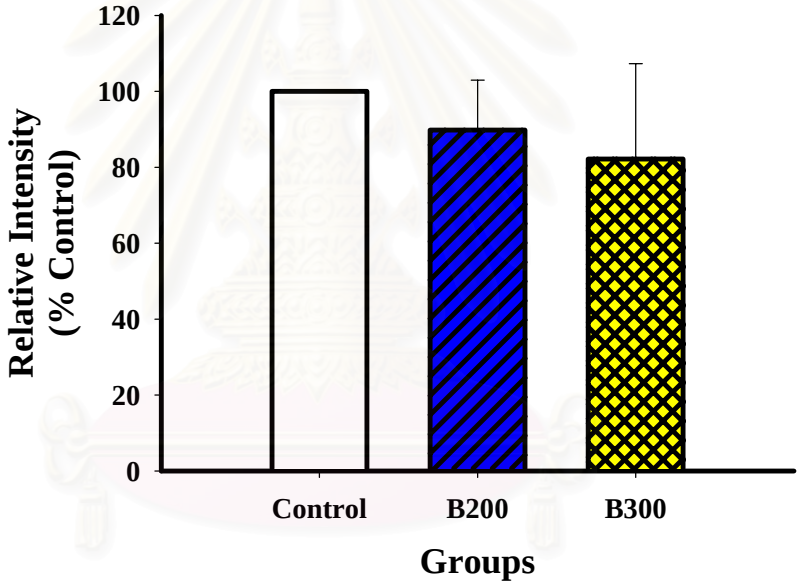

Fig. 51. Effect of barakol on CYP 3A1 protein levels.

(1) Western blot analysis of CYP 3A1, mice were given 200 and 300 mg/kg/day of barakol for 14 days. The positions of the molecular weight marker are indicated on the right (kDa). The lanes are as follows: 1, control; 2, barakol 200; 3, barakol 300. (2) The intensities of the bands from scanning densitometry of Western blot.

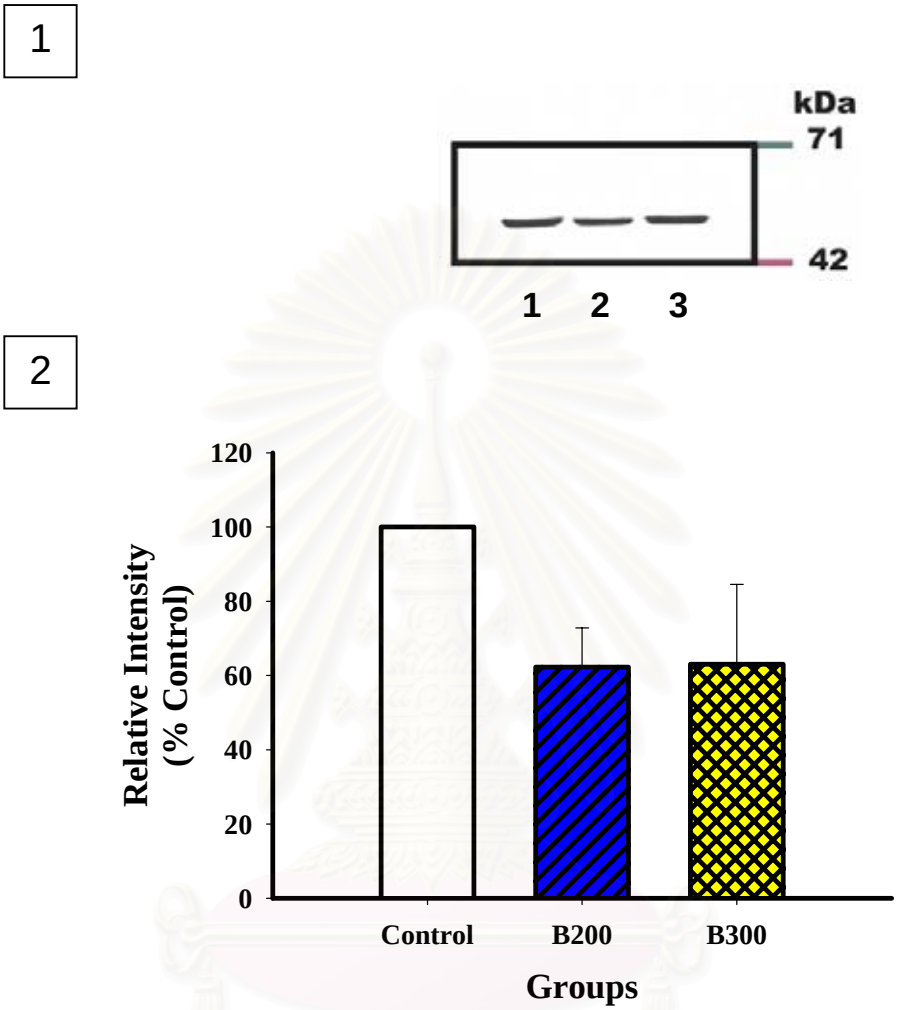

Fig. 52. Effect of barakol on CYP 2E1 protein levels.

(1) Western blot analysis of CYP 2E1, mice were given 200 and 300 mg/kg/day of barakol for 14 days. The positions of the molecular weight marker are indicated on the right (kDa). The lanes are as follows: 1, control; 2, barakol 200; 3, barakol 300. (2) The intensities of the bands from scanning densitometry of Western blot.

***In Vitro* Study**

Effects of Barakol on Respiration of Mouse Liver Mitochondria Using Glutamate Plus Malate as Substrates.

Rate of States 3 and 3u Respiration

Various concentrations of barakol (0.075–3 mM) decreased respiration of mouse liver mitochondria, especially rates of states 3 and 3u respiration to less than 50 % (Figs. 54 and 55). Barakol at low concentrations (0.075, 0.15 mM) caused a transient reduction of respiration. At higher concentrations (9.6 and 12 mM), barakol completely inhibited rate of state 3 respiration (Fig. 53).

Effect of Barakol on P/O Ratio and RCI Value

The RCI values decreased by all concentrations of barakol, especially at high concentrations (>50 %) (Fig. 56). ADP/O ratio did not change at all concentrations of barakol (Fig. 57).

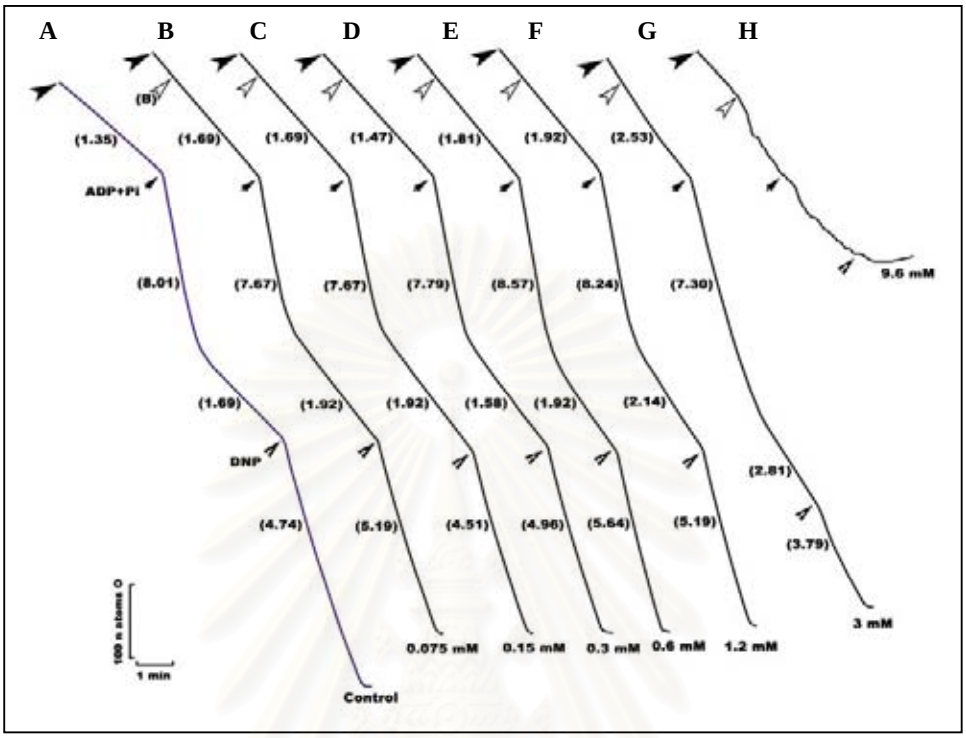

Fig. 53. Tracings demonstrated dose-response of barakol on oxidative phosphorylation in isolated mouse liver mitochondria.

Mouse liver mitochondria were incubated in a medium containing 40 mM HEPES, 2 mM $MgCl_2$, and 92 mM KCl (pH 7.4) in the presence of 1 M glutamate plus 1 M malate, 0.3 M ADP plus 0.6 M Pi, 50 mM DNP and barakol as indicated at 37 °C. The average mitochondrial protein was 32.01 mg/ml. Total volume was 1.91 ml. Barakol was added after glutamate plus malate as substrates, then, ADP plus Pi were added. DNP was added during state 4 respiration. Curve A, control; B, barakol 0.075 mM; C, barakol 0.15 mM; D, barakol 0.3 mM; E, barakol 0.6 mM; F, barakol 1.2 mM; G, barakol 3 mM; H, barakol 9.6 mM. The arrows indicated additions of substances as follows: , glutamate plus malate as substrate; , various concentrations of barakol; , ADP+ Pi; , DNP. The numbers next to the tracings indicated the specific respiratory rate as ng atoms of oxygen per minute per mg protein.

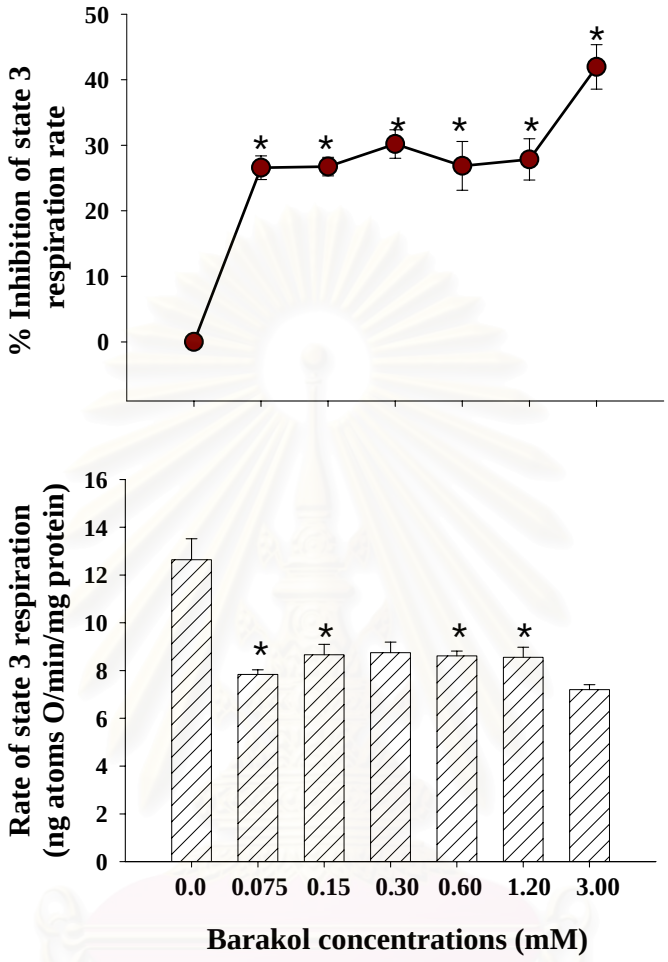

Fig. 54. Effect of barakol on rate of state 3 respiration and % inhibition of state 3 respiration rate in isolated mouse liver mitochondria with glutamate plus malate as substrates.

Mouse liver mitochondria were incubated in a medium containing 40 mM HEPES, 2 mM $MgCl_2$, and 92 mM KCl (pH 7.4) in the presence of 1 M glutamate plus 1 M malate, 0.3 M ADP plus 0.6 M Pi, 50 mM DNP and barakol as indicated at 37 $^{\circ}$C. The average mitochondrial protein was 32.01 mg/ml. Total volume was 1.91 ml. Various concentrations of barakol were added after glutamate plus malate as substrates, then, ADP plus Pi were added. DNP was added during state 4 respiration. Results are expressed as mean ± SEM, n=4 (* p <0.05).

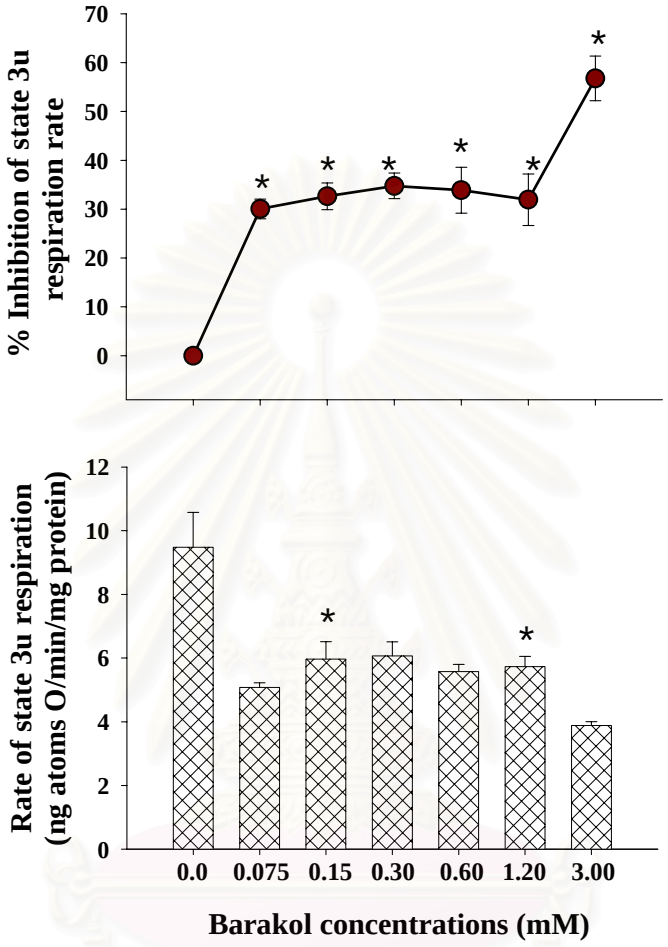

Fig. 55. Effect of barakol on rate of state 3u respiration and % inhibition of state 3u respiration rate in isolated mouse liver mitochondria with glutamate plus malate as substrates.

Mouse liver mitochondria were incubated in a medium containing 40 mM HEPES, 2 mM $MgCl_2$, and 92 mM KCl (pH 7.4) in the presence of 1 M glutamate plus 1 M malate, 0.3 M ADP plus 0.6 M Pi, 50 mM DNP and barakol as indicated at 37 $^{\circ}$C. The average mitochondrial protein was 32.01 mg/ml. Total volume was 1.91 ml. Various concentrations of barakol were added after glutamate plus malate as substrates, then, ADP plus Pi were added. DNP was added during state 4 respiration. Results are expressed as mean ± SEM, n=4 (* p <0.05).

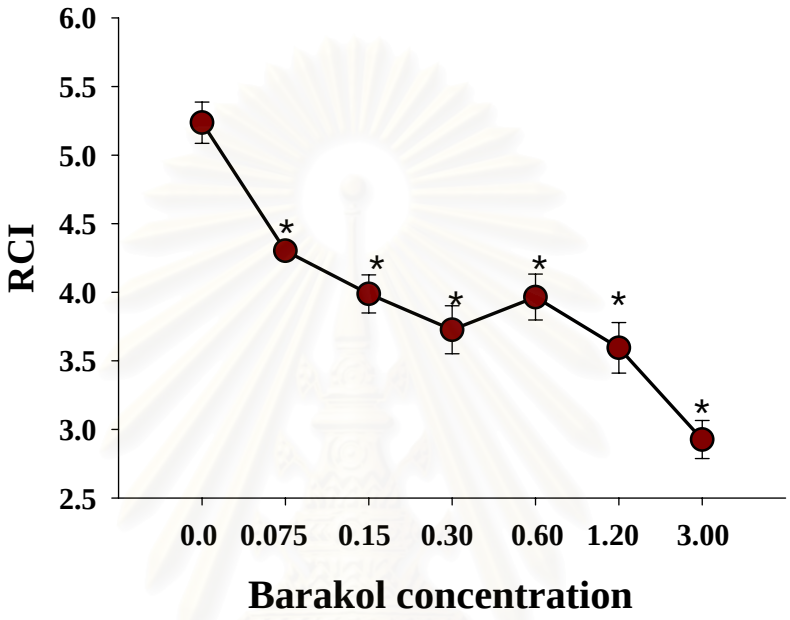

Fig. 56. Effect of barakol on respiratory control index (RCI) value in isolated mouse liver mitochondria with glutamate plus malate as substrates.

Mouse liver mitochondria were incubated in a medium containing 40 mM HEPES, 2 mM $MgCl_2$, and 92 mM KCl (pH 7.4) in the presence of 1 M glutamate plus 1 M malate, 0.3 M ADP plus 0.6 M Pi, 50 mM DNP and barakol as indicated at 37 $^{\circ}$C. The average mitochondrial protein was 32.01 mg/ml. Total volume was 1.91 ml. Various concentrations of barakol were added after glutamate plus malate as substrates, then, ADP plus Pi were added. DNP was added during state 4 respiration. Results are expressed as mean ± SEM, n=4 (* p <0.05).

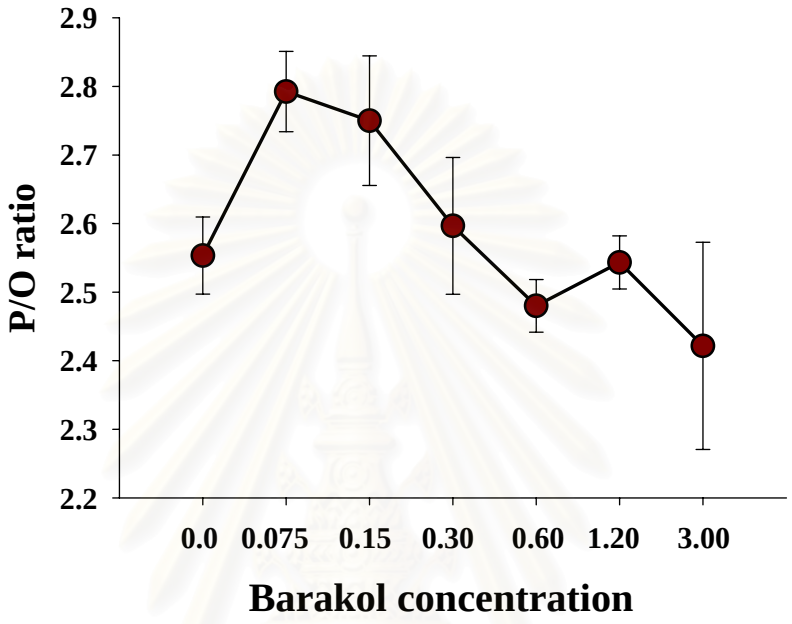

Fig. 57. Effect of barakol on P/O ratio in isolated mouse liver mitochondria with glutamate plus malate as substrates.

Mouse liver mitochondria were incubated in a medium containing 40 mM HEPES, 2 mM $MgCl_2$, and 92 mM KCl (pH 7.4) in the presence of 1 M glutamate plus 1 M malate, 0.3 M ADP plus 0.6 M Pi, 50 mM DNP and barakol as indicated at 37 °C. The average mitochondrial protein was 32.01 mg/ml. Total volume was 1.91 ml. Various concentrations of barakol were added after glutamate plus malate as substrates, then, ADP plus Pi were added. DNP was added during state 4 respiration. Results are expressed as mean ± SEM, n=4.

CHAPTER IV

DISCUSSION AND CONCLUSIONS

The present study demonstrated the extent of hepatotoxicity of barakol in mice in acute and subacute studies, which were dose- and time-dependent. The liver injury was evaluated from the alteration of blood chemical biochemistry parameters and histopathological examinations. The possible mechanisms of hepatotoxicity induced by barakol on target organelles, including the endoplasmic reticulum and mitochondria, were focused. The effects of barakol on hepatic cytochrome P450 and mitochondrial oxidative phosphorylation were also determined using both *ex vivo* and *in vitro* models.

Barakol dose ranging in this experiment was selected from the preliminary study in mice as manifested by the elevation of serum AST and ALT. The doses of barakol used ranged from 100-300 mg/kg which are nearly 150-450 times of the human hepatotoxic dose (40 mg in 60 kg man) reported by Hongsirinirachorn *et al.*, in 2003. Although the dose of barakol used was higher than that of a median lethal dose (LD50) (342.09 mg/kg, ip) (Jantarayota, 1987), no mice treated with barakol at this level died during the experimental period. It is suggested that the liver injury from *C. siamea* tablets in human might involve the other constituents of *C. siamea* leaves and flowers. On the other hand, barakol is not the only chemical compound induced toxicity in *C. siamea*.

***In Vivo* Study**

Serum AST and ALT activities and histopathological examinations were used as markers for evaluation of hepatotoxicity. Hepatocytes recovered from

inflammation occurred between 48 to 96 hours depending on the administered doses of barakol and related to the decrease in serum AST and ALT activities in acute toxicity study. In subacute toxicity study, histopathological findings are very interesting in showing details of event occurred step by step after increasing dose and time of barakol exposure. It started with swelling of hepatocytes and diffuse centrilobular hepatic necrosis together with the mitotic figure. The area of hydropic degeneration of hepatocytes and necrotic cells spreaded wider to periportal zone when the doses of barakol increased. Apoptotic cells were found at pericentral zone to periportal zone, and markedly detected at 14 days of barakol treatment.

Lysed debris of necrotic cells can persist for days when large amount of cells die. The concurrent plasma membrane leakage is suggested by the increased levels of ALT and AST. Apoptosis of damaged cells has a full value for tissue repair process, especially tissues that are made up from constantly renewing cells or dividing cells, and the apoptotic cells are readily replaced. Progression of cell injury by necrosis can be intercepted by two repair mechanisms, working in apoptosis and cell proliferation. Injured cells can initiate apoptosis, which counteracts the progression of cell injury. Occurrence of apoptosis prevents necrosis of injured cells and the consequences of inflammatory response such as the release of cytotoxic mediators. Therefore, apoptosis plays an elimination role to preserve the structural and functional integrity of the liver (Habeebu *et al*., 1998). Tissue necrosis occurs when injury overwhelmed and disable the repair mechanisms, including repair of damaged molecules, elimination of damaged cells by apoptosis, and replacement of lost cells by cell division. These observations corresponded with our findings that stimulation of mouse liver regeneration after sublethal doses of barakol appeared to be the protective mechanism, using apoptosis for the elimination of damaged cells. This adaptation mechanism enabled mouse liver to overcome liver injury inflicted by low doses of barakol given for a short period of time.

Barakol-induced mouse liver cell injury by both necrosis and apoptosis. The ultimate outcome of hepatotoxicity by barakol depended on the balance between the extent of damage and repair processes. In all doses of barakol treatment, there were signs of liver regeneration and recovery from injury. The outcome of hepatotoxicity induced by barakol at high dose was dose- and time-related, together with autoprotection in extent of tissue repair and elimination of damaged cells. Apoptotic cell death may be the mechanism of the damaged cell elimination.

In this study, animals were not fasted before collecting blood samples to mimic the barakol like drug effect in human. However, without fasting, the levels of cholesterol, triglyceride, and glucose markedly dropped, liver cell injury induced by barakol might affect its normal function in transportation and synthesis of biomolecules. In acute toxicity study, the serum levels of AST and ALT, cholesterol, triglyceride, glucose, and total bilirubin returned to normal within 96 h. These findings showed the dose-related manner of hepatic injury produced by various single doses of barakol. The degree of severity is dose- and time-dependent. In repeated doses study, loss of liver cell function was indicated by the alteration in hepatic functions, including the increase (>50 %) in total serum bilirubin, AST and ALT activities with the decrease (>50 %) in cholesterol, triglyceride, and glucose in all treated groups similar to the results obtained in acute study. The alterations of these parameters correlated with abnormalities of microscopic features showing centrilobular necrosis after treatment for 2 and 4 days. The death of cell by both centrilobular necrosis and apoptosis spreaded from pericentral zone to periportal zone during the observation. Apoptotic cell death prominently occurred and peaked at 14 days. It decreased at 28 days in low barakol dose (100 mg/kg/day) but still persisted with higher doses of barakol. Apoptotic bodies were eliminated by Kupffer cells and adjacent hepatocytes. Although, apoptosis was more difficult to detect histologically due to rapid removal of the affected cells (Corcoran *et al*., 1994), in this study, apoptosis was simply demonstrated during 7–28 days. Necrosis and apoptosis can co-exist,

especially in subacute injury (Mehendale *et al*., 1994). In addition, hepatocytic mitosis was observed throughout 28 days following barakol treatment. This regeneration was probably to compensate the cell loss caused by necrosis and apoptosis. However, such compensation was less in terms of functional integrity as evidenced by the continuing decrease in the levels of serum cholesterol, triglyceride, and glucose throughout 28 days of treatment. The decrease in circulating triglyceride could also be related to the fat deposit in pericentrol zone which was confirmed by Sudan III staining (Fig. 48).

In subacute toxicity study, final body weight in mice given 300 mg/kg/day barakol was reduced at 14, 21 and 28 days after the treatment with no change in food consumption and liver weight. The reduction in food intake and body weight might be associated with the sedative effect of barakol which has been reported for its anxiolytic activity in elevated plus-maze model by Thongsaard and colleagues in 1996. The livers weight which were not different from the control group might involve the mechanism of liver to balance homeostasis between cell death and regeneration process that maintain the liver structural integrity.

Hyperbilirubinemia was evident in high dose of barakol treated animals. Destruction of effete red blood cells by the macrophages occurs in the splenic red pulp, bone marrow, and liver. The main products of broken hemoglobin are heme and the protein fraction globin. Globin is cleaved to its constituent amino acids. Heme is degraded to iron, which is returned to the body's iron stores, and bilirubin is transported to the liver complexed with albumin. Because free iron is toxic, it is bound to a plasma protein known as transferrin. Storage of iron occurs in most cells, especially those of the liver, spleen, and bone marrow. In normal situation, hepatocytes maintain the homeostasis of iron by extracting this metal from the sinusoid by the receptor-mediated endocytosis and stored as protein ferritin. When iron is excessive, it is stored as hemosiderin, a form of ferritin complexed with additional iron that cannot readily be mobilized. Accumulation of excess iron is initially evident in periportal zone where active phagocytic Kupffer cells are most

abundant (Wake *et al.*, 1989). In the liver, bilirubin is conjugated with glucuronic acid and is excreted in the bile. Although heme from cytochromes and myoglobin also undergoes conversion to bilirubin, the major source of this bile pigment is hemoglobin. Abnormalities arising at various stages may lead to the accumulation of the pigments. Bilirubin concentrations rise as a consequence of one or more of the 3 major processes; overproduction, defective plasma clearance, and liver disorder. Overproduction of bilirubin is a feature of hemolysis and ineffective erythropoiesis; unconjugated bilirubin predominates. Defective bilirubin removal from plasma will result in unconjugated hyperbilirubinemia. Liver cell damage causes a decrease in elimination of conjugated bilirubin (Govan *et al.*, 1991; Marks *et al.*, 1996). Histopathological examinations also reveal the brown pigments of hemosiderin (iron pigment deposit) in Kupffer cells at periportal zone in liver which was confirmed by Turnbull Blue staining. In the spleen, hemosiderin accumulation was accentuated in the red pulp of animals treated (300 mg/kg/day) for 28 days (Fig. 47). This result is related to the hyperbilirubinemia induced by high doses of barakol. Similar finding was reported by Chivapat *et al*. (2001) in which chronic administration of 2000 mg/kg *Cassia siamea* tablets (containing 1.19% anhydrobarakol) causing the reduction of erythrocytes in female rats. Although, in this study, the hematological parameters were not examined, the presence of hemosiderosis in liver and spleen suggested the increased hemolysis in the barakol-induced liver cell injury.

***Ex Vivo* Study**

In the present study, endoplasmic reticulum and mitochondria were two organelles affected by barakol treatment as clearly seen in the electron micrographs. In acute toxicity study, the level of hepatic cytochrome P450 contents decreased at 24 and 48 hours after barakol treatment and returned to near normal within 96 hours. These findings corresponded to the profile pattern of blood biochemical parameters and microscopic appearance. In addition, in subacute toxicity study, the hepatic cytochrome P450 contents markedly decreased

approximately by 50 %, in the barakol-treated mice compared to the control group after 28 days of treatment. Cytochrome P450 enzymes are present in all zones of hepatic lobules but predominantly located at pericentral zone where cytochrome P450 was abundantly bound to the membrane of the endoplasmic reticulum (smooth endoplasmic reticulum; SER). When barakol caused hepatic cell death by both necrosis and apoptosis at pericentral zone, it is not surprised to find the decrease in total cytochrome P450 contents or CYP isozymes both in the acute and subacute studies. It was reported that after partial hepatectomy in rats, hepatic homeostasis was quite well-preserved, even though the cytochrome P450 contents of the residual liver were reduced by approximately 50 % (Starkel *et al*., 2000). Hepatocytes are involved in metabolism of a great variety of chemical substances by CYP isozymes. The level of CYP activities is decreased several hours after partial hepatectomy, and some isozymes may be selectively affected (Iversen *et al*., 1985; Marie *et al*., 1988). Barakol may have affected some CYP isozymes, for example, CYP 3A (most abundant in the liver) and CYP 2E1 (associated with metabolism of a wide range of compounds).

To explore the effect of barakol on the protein levels of CYP3A1 and CYP2E1, Western immunoblotting was conducted to determine the alteration of the immunoreactive protein levels. Results from the immunoblotting studies showed that administration of barakol (200 and 300 mg/kg/day) for 14 days did not affect the CYP3A1 and CYP2E1 protein levels as compared to the control. These results suggested the non-specific destruction of the endoplasmic reticulum. In addition, CYP isozymes, which are responsible for the conversion of xenobiotics to their metabolites, were explored. From the previous studies, the activities of aniline hydroxylase (ANH) and aminopyrine-N-demethylase (AMD) decreased, but the activities of UGT and GST increased after feeding rats with 5 % dietary *Cassia siamea* for 14 days (Tepsuwan *et al*., 1997, 1999). After treating rats with barakol for 90 days in normal and high cholesterol conditions, the activities of CYP 1A2 and CYP 1A1 decreased in both conditions. The activities of CYP 2B1/2B2, CYP 2E1, and GST did not change in the high cholesterol diet after the treatment

with barakol (Maniratanachote, 2001). Barakol induced an increase in AMD and GST activities in isolated rat hepatocytes, which may due to its metabolite(s) formed by CYP 2B and CYP 2C (Chirdchupunsare *et al*., 2003). In general, the zonality of necrosis appeared to be related to the mechanism of injury of some drugs such as acetaminophen, in which CYP isozymes were responsible for its conversion to hepatotoxic metabolite. A number of xenobiotics are direct toxins, whereas the toxicity of other is due largely to their metabolites. Formation of many reactive metabolites is catalyzed mainly by cytochrome P450. Detoxification, elimination of ultimate toxicant, or prevention of reactive metabolite formation required several pathways, depending on chemical nature of toxic substances. Our *in vivo* study showed that barakol caused centrilobular hepatic necrosis. Therefore, the barakol-induced centrilobular necrosis may be associated with barakol itself or cytochrome P450 enzymes for conversion to intermediate metabolite(s).

***In Vitro* Study**

From the preliminary study, the direct effect of barakol on mitochondrial respiration in isolated mouse liver mitochondria showed that barakol inhibited state 3 respiration when using glutamate plus malate as substrates (complex I; NADH dehydrogenase), while they had no inhibitory effect when respiring with succinate (complex II; Succinate dehydrogenase). Therefore, barakol may affect the mitochondrial respiration at complex I more than complex II of the electron transport chain. All concentrations of barakol inhibited states 3 and 3u respiration in the isolated mouse liver mitochondria and the percentage of inhibition was less than 50 %. Barakol at 0.075 and 0.15 mM inhibited states 3 and 3u respiration by approximately 30 %. The decrease in RCI value was observed in all concentrations. These effects were dose-dependent, whereas the ADP/O ratio did not change after each concentration of barakol was added. The ADP/O ratio, the capacity of mitochondria in ATP synthesis, tended to increase at low concentration of barakol. This effect might involve the reduction in energy waste of

mitochondria and seemed to be similar to the effect of ethanol studied in rat liver mitochondria, showing the decrease in energy conservation at site I of the electron transport chain (Bottenus *et al.*, 1982). Therefore, there was a mild inhibition of complex I electron transport chain with no change in ADP/O ratio or ATP synthesis. The concentrations of barakol (0.075 to 3 mM) in this study were higher than those of barakol (0.025 to 0.15 mM) that induced cytotoxicity in isolated rat hepatocytes which contain enzymes in both phase I and phase II reactions (Chirdchupunsare *et al*., 2003). This finding demonstrated that the inhibition of mitochondrial respiration may not be the initial step of mouse liver cell injury, and barakol metabolite(s) may involve in hepatotoxicity induced by barakol.

In conclusion, barakol at high doses induced hepatotoxicity in mice by causing necrosis and apoptosis. Its hepatotoxic expression was not severe even with doses that were much higher than human hepatotoxic dose. The possible hepatotoxic mechanism(s) may involve barakol itself or its metabolite(s). Inhibition of mitochondrial respiration was not the initial step of liver cell injury. Finally, barakol-induced hepatotoxicity may in part be associated with hemolysis.

Further studies should be performed to confirm the involvement of reactive metabolite(s) in barakol-induced hepatotoxicity using enzyme inducers and enzyme inhibitors. The role of Kupffer cell in liver injury produced by barakol may be assessed using some chemicals such as gadolinium chloride. The association of hemolysis with hepatotoxic effect of barakol should be studied in detail. In addition, the possibility of long-term exposure to barakol in causing hepatic fibrosis or cirrhosis should also be investigated.

REFERENCES

Thai

ป่าไม้, กรม. 2491. ชื่อพรรณไม้แห่งประเทศไทย. หน้า 103-105. พระนคร: โรงพิมพ์ บริษัท สุรีย์รัตน์.

พร้อมจิต ศรลัมพ์, รุ่งระวี เต็มศิริฤกษ์กุล, วงศ์สถิตย์ ฉั่วกุล และ อาทร ริ้วไพบูลย์. 2532. สมุนไพรและยาที่ควรรู้. พิมพ์ครั้งที่ 1. กรุงเทพมหานคร: สำนักพิมพ์ อาร์ ดี พี.

ภูมิพิชญ์ สุธาวรรณ. 2535. พืชสมุนไพรใช้เป็นยา เล่ม 2. กรุงเทพมหานคร: บริษัทอักษา นิพัฒน์ จำกัด.

สมบัติ ตรีประเสริฐสุข, มงคล หงษ์ศิรินิรชร และ อนุชิต จูฑะพุทธิ. 2543. ภาวะตับอักเสบจากสมุนไพร “ขี้เหล็ก” บทเรียนเพื่อการพัฒนาสมุนไพรไทย. คลินิก. 186: 385-390.

English

Arunlukshana, O. 1949. Studies of indigeneous drugs: 1. Pharmacological studies of the leaves of Cassia siamea. Siriraj Hosp. Gaz. 1: 434-444.

Bottenus, R.E., Spach, P.I., Filus, S., and Cunningham, C.C. 1982. Effect of chronic ethanol consumption of energy-linked processes associated with oxidative phosphorylation: proton translocation and ATP-Pi exchange. Biochem. Biophys. Res. Commun. 105(4): 1368-1373.

Bulyalert, D. 1992. Effect of barakol on the central nervous system: quantitative analysis of EEG in the rat. Chiang Mai Med. Bull. 32: 191-196.

Bycroft, B.W., Hassanali-Walji, A., Johnson, A.W., and King, T.J. 1970. The structure and synthesis of barakol: a novel dioxaphenalene derivative from Cassia siamea. J. Chem. Soc. 12: 1686-1689.

Cascales, M., Alvarez, A., Gasco, P., Fernandez-Simon, L., Sanz, N., and Bosca, L. 1994. Cocaine-induced liver injury in mice elicits specific changes in DNA ploidy and induces programmed death of hepatocytes. Hepatology. 20: 992-1001.

Chaichantipyuth, C. 1979. A phytochemical study of the leaves of Cassia siamea and Cassia spectabilis DC. Master's Thesis, Department of Pharmacognosy, Faculty of Pharmaceutical Sciences, Graduate School, Chulalongkorn University.

Chance, E., and Williams, G.R. 1956. The respiratory chain and oxidative phosphorylation. Advance Enzymology. 17: 65-134.

Chirdchupunsare, H., Pramyothin, P., and Chaichantipyuth, C. 2003. Effect of barakol on cytochrome P450, UDP-glucuronyltransferase and glutathione S-transferase in isolated rat hepatocytes. Thai J. Pharmacol. 25: 125-133.

Chivapat, S., Chavalittumrong, P., Sunyasootcharee, B., Rattanajarasroj, S., and Punyamong, S. 2001. Chronic toxicity of Cassia siamea Tablet. Bull. Dept. Med. Serv. 26: 485-497.

Cooper, B.J. 2002. Disease at the cellular level. In D. O. Slauson and B. J. Cooper (eds.), Mechanisms of disease: a textbook of comparative general pathology, pp 16-75. Missouri: Mosby.

Corcoran, G.B., and Ray, S.D. 1992. The role of the nucleus and other compartments in toxic cell death produced by alkylating hepatotoxicants. Toxicol. Appl. Pharmacol. 113: 167-183.

Corcoran, G.B., Fix, L., Jones, D.P., Moslen, M.T., Nicotera, P., Oberhammer, F.A., and Buttyan, R. 1994. Apoptosis: Molecular control point in toxicity. Toxicol. Appl. Pharmacol. 128: 169-181.

Dahm, L.J., and Jones, D.P. 1996. Mechanisms of chemically induced liver disease. In D. Zakim, and T.D. Boyer (eds.), Hepatology a textbook of liver disease, p 875. New York: W. B. Saunders.

Daugas, E., Susin, S.A. , Zamzami, N., Ferri, K.F., Irinopoulou, T., Larochette, N., Prevost, M.C., Leber, B., Andrews, D., Penninger, J., and Kroemer, G. 2000. Mitochondrio-nuclear translocation of AIF in apoptosis and necrosis. FASEB J. 14: 729-739.

Ekataksin, W., and Kaneda, K. 1991. Liver microvascular architecture: An insight into the pathophysiology of portal hypertension. Semin. Liver Dis. 19: 359-382.

Estabrook, R.W. 1967. Mitochondrial respiratory control and the polarographic measurement of ADP: O ratios. In S.P. Colowick, and N.O. Kaplan (eds.), Methods in Enzymology, pp 41-47. New York: Academic Press.

Gbeassor, M., Kossou, Y., Amegbo, K., Souza, C.De., Koumaglo, K., and Denke, A. 1989. Antimicrobial effects of eight african medicinal plants. J. Ethnopharmaco. 25: 115-118.

Gores, G.J., Herman, B., and Lemasters, J.J. 1990. Plasma membrane bleb formation and rupture: A common feature of hepatocellular injury. Hepatology. 11: 690-698.

Govan-Alasdair, D.T., Macfarlane, P.S., and Callander, R. 1991. Pathology illustrated. 3rd ed. pp. 21-22. New York: Churchill Livingstone.

Gritsanapan, W., Mekmance, R., and Chulasiri, M. 1989. Antimicrobial activity and effect on isolated guinea pig ileum of barakol. J. Pharm. Sci. 16: 27-31.

Green, D.R., and Reed, J.C. 1998. Mitochondria and apoptosis. Science. 281: 1309-1312.

Habeebu, S.S.M., Liu, J., and Klaassen, C.D. 1998. Cadmium-induced apoptosis in mouse liver. Toxicol. Appl. Pharmacol. 149: 203-209.

Hassanali-Walji, A., King, T.J., and Wallwork, S.C. 1969. Barakol, a novel dioxaphenalene derivative from Cassia siamea. J. Chem. Soc. Chem. Commun. 12: 678.

Hinkle, P.C. 1995. Oxygen, proton and phosphate fluxes, and stoichiometries. In G.C.

Brown, and C.E. Cooper (eds), Bioenergetics a practical approach, p 2. New York: IRL Press.

Hogeboom, G.H. 1955. Fractionation of cell components of animal tissues. In S.P. Colowick, and N.O. Kaphan (eds), Methods in Enzymology, pp 16-19. New York: Academic Press.

Hongsirinirachorn, M., Threeprasertsuk, S., and Chutaputti, A. 2001. Hepatitis associated with barakol: case report. Thai J. Gastroenterology. 2: 17-21.

Hongsirinirachorn, M., Threeprasertsuk, S., and Chutaputti, A. 2003. Acute hepatitis associated with barakol. J. Med. Assoc. Thai. 86 (Suppl 2): S484-S489.

Iversen, P.L., Liu, Z., and Franklin, M.R. 1985. Selective changes in cytochrome P-450 and UDP-glucuronyltransferase sub-population following partial hepatectomy in rat. Toxicol. Appl. Pharmacol. 78: 10-18.

Jaeschke, H., and Lemasters, J.J. 2003. Apoptosis versus oncotic necrosis in hepatic ischemis/reperfusion injury. Gastroenterology. 125: 1246-1257.

Jantarayota, P. 1987. Actions of barakol on the central nervous system. Master's Thesis, Department of Physiology, Faculty of Pharmaceutical Sciences, Chulalongkorn University.

Kierszenbaum, A.L. 2002. Histology and cell biology: an introduction to pathology. pp 459-474. Missouri: Mosby.

Kroemer, G., Dallaporta, B., and Resche-Rigon, M. 1998. The mitochondrial death/life regulator in apoptosis and necrosis. Annu. Rev. Physiol. 60: 619-642.

Kroemer, G., Petit, P., Zamzami, N., Vayssiere, J.L., and Mignotte, B. 1995. The biochemistry of programmed cell death. FASEB J. 9: 1277-1287.

Kroemer, G., Zamzami, N., and Susin, S.A. 1997. Mitochondrial control of apoptosis. Immunol. Today. 18: 44-51.

Kusamran, W.R., Tepsuwan, A., and Kupradinum, P. 1998. Antimutagenic and anticarcinogenic potentials of Thai vegetables. Mutat. Res. 402: 247-258.

Laemmli, U. 1970. Cleavage of structural protein during the assembly of the head of bacteriophage T4. Nature. 227: 680-685.

Lake, B.G. 1987. Preparation and characterization of microsomal fractions for studies on xenobiotic metabolism. In K. Snell, and B. Mullock (eds.), Biochemical toxicology: A practical approach, pp. 183-125. Oxford: IRL Press.

Laskin, D.L. 1990. Nonparenchymal cells and hepatotoxicity. Semin. Liver Dis. 10: 293-304.

Lemasters, J.J. 1999. Mechanisms of hepatic toxicity V. Necrapoptosis and the mitochondrial permeability transition: shared pathways to necrosis and apoptosis. Am. J. Physiol. 276: G1-G6. Review.

Lemasters, J.J., Nieminen, A.L., Qian, T., Trost, L.C., Elmore, S.P., Nishimura, Y., Crowe, R.A., Cascio, W.E., Bradham, C.A., Brenner, D.A., and Herman, B. 1998. The mitochondrial permeability transition in cell death: a common mechanism in necrosis, apoptosis and autophagy. Biochem. Biophys. Acta. 1366: 177-196.

Lowry, O.H., Rosebrough, N.J., Farr, A.L., and Randall, R.J. 1951. Protein measurements with the Folin phenal reagent. J. Biol. Chem. 193: 265-275.

Maniratanachote, R., Kijsanayotin, P., Phivthong-ngam, L., Thongsaard, W., Niwattisaiwong, N., and Lawanprasert, S. 2002. Subchronic effects of barakol on blood clinical biochemistry parameters in rats fed with normal and high cholesterol diets. Thai J. Pharmacol. 24: 101-111.

Marie, I.J., Dalet, C., Blanchard, J.M., Astre, C., Szawlowski, A., Aubert, B.S., Joyeux, H., and Maurel, P. 1988. Inhibition of cytochrome P-450p (P450IIIA1) gene expression during liver regeneration from two-thirds hepatectomy in the rat. Biochem. Pharmacol. 37: 3515-3521.

Marks, D.B., Marks, A.D., and Smith, C.M. 1996. Basic Medical Biochemistry: A clinical approach. pp 626-630. Maryland: Williams & Wilkins.

Masini, A., Gallesi, D., Giovannini, F., Trenti, T., and Ceccarelli, D. 1997. Membrane potential of hepatic mitochondria after acute cocaine administration in rats-the role of mitochondrial reduced glutathione. Hepatology. 25: 385-390.

Mehendale, H.M., Routh, R.A., Gandolfi, A., Klaunig, J.E., Lemaster, J.J., and Curtis, L.R. 1994. Novel mechanisms in chemically induced hepatotoxicity. FASEB J. 8: 1285-1295.

Meyer, S.A., and Kulkarni, A.P. 2001. Hepatotoxicity. In E. Hodgson, and R.C. Smart (eds.), Introduction of biochemical toxicology, pp 487-491. New York: John Wiley and Sons.

Mokhasmit, M., Sawasdimongkol, K., and Sartravaha, P. 1971. Toxicity study of some Thai medicinal plants. Bull. Dep. Med. Sci. 12: 36-65.

Myers, D.K., and Slater, E.C. 1957. The enzyme hydrolysis of adenine triphosphate by liver mitochondria I: activities at difference pH value. Biochem. J. 67: 558-572.

Omura, T., and Sato, R. 1964. The carbon monoxide-binding pigment of liver microsome I. Evidence for its hemoprotein nature. J. Biol. Chem. 239: 2370-2377.

Petit, P.X., Susin, S., Zamzami, N., Mignotte, B., and Kroemer, G. 1996. Mitochondria and programed cell death: Back to the future. FEBS Lett. 196: 7-13.

Plaa, G.L. 2000. Chlorinated methane and liver injury: Highlights of the past 50 years. Annu. Rev. Pharmacol. Toxicol. 40: 43-65.

Rai, P.P. 1977. Anthraquinones in Cassia siamea. Curr. Sci. 46: 814-815.

Smith, M.T., Loveridge, N., Wilis, E.D., and Chayen, J. 1979. The distribution of glutathione in the rat liver lobule. Biochem. J. 182: 103-108.

Sordahl, L.A., Johnson, C., Blailock, Z.R., and Schwartz, A. 1971. The mitochondrion. In A. Schwartz (ed.), Methods in Pharmacology, pp 247-286. New York: Merdith Corporation.

Starkel, P., Laurent, S., Petit, M., Van Den Berge, V., Lambotte, L., and Horsmans, Y. 2000. Early down-regulation of cytochrome P450 3A and 2E1 in the regeneration rat liver is not related to the loss of liver mass or the process of cellular proliferation. Liver. 20: 405-410.

Sukma, M., Chaichantipyuth, C., Murakami, Y., Tohda, M., Matsumoto, K., and Watanabe, H. 2002. CNS inhibitory effects of barakol, a constituent of Cassia siamea Lamk. J. Ethnopharmaco. 83: 87-94.

Susin, S.A., Zamzami, N., Castedo, M., Hirsch, T., Marchetti, P., Macho, A., Daugas, E., Geuskens, M., and Kroemer, G. 1996. Bcl-2 inhibits the mitochondrial release of an apoptogenic protease. J. Exp. Med. 184: 1331-1341.

Susin, S.A., Lorenzo, H.K., Zamzami, N., Marzo, I., Snow, B.E., Brothers, G.M., Mangion, J., Jacotot, E., Costantini, P., Loeffler, M., Larochette, N., Goodlett, D.R., Aebersold, R., Siderovski, D.P., Penninger, J.M., and Kroemer, G. 1999. Molecular characterization of mitochondrial apoptosis-inducing factor. Nature. 397: 441-446.

Suwan, G., Sudsuang, R., Dhamma-upakorn, P., and Werawong, C. 1992. Hypertensive effects of barakol extracted from leaves of Cassia siamea Lam. in rats and cats. Thai J. Physiol. Sci. 5: 53-65.

Tepsuwan, A., and Kusamran, W.R. 1997. Effect of the leaves of Siamese Cassia, Indian Mulberry and Asiatic Pennywort on the metabolizing enzymes of chemical carcinogens in rat liver. Bull. Dept. Med. Serv. 22: 425-437.

Tepsuwan, A., Kupradinum, P., and Kusamran, W.R. 1999. Effect of Siamese cassia leaves on the activities of chemical carcinogen metabolizing enzymes and on mammary gland carcinogenesis in the rat. Mutat. Res. 428: 363-373.

Thongsaard, W., Bennett, G.W., and Marsden, C.A. 1995. Barakol inhibits striatal dopamine release in vitro. Br. J. Pharmacol. 114: 383P.

Thongsaard, W., Deachapunya, C., Pongsakorn, S., Boyd, E.A., Bennett, G.W., and Marsden, C.A. 1995. The dioxaphenalene derivative barakol extracted form Cassia siamea: a natural anxiolytic?. Br. J. Pharmacol. 114: 284.

Thongsaard, W., Deachapunya, C., Pongsakorn, S., Boyd, E.A., Bennett, G.W., and Marsden, C.A. 1996. Barakol: a potent anxiolytic extracted from Cassia siamea. Pharmacol. Biochem. Behav. 53: 753-758.

Thongsaard, W., Pongsakorn, S., Sudsuang, R., Bennett, G.W., Kendall, D.A., and Marsden, C.A. 1997. Barakol, a natural anxiolytic, inhibit striatal dopamine release but not uptake in vitro. Eur. J. Pharmacol. 319: 157-164.

Thongsaard, W., Shainakul, S., Bennett, G.W., and Marsden, C.A. 2001. Determination of barakol extracted from Cassia siamea by HPLC with electrochemical detection. J. Pharm. and Biomed. Anal. 25: 853-859.

Treinen-Moslen, M. 2001. Toxic responses of the liver. In C.D. Klaassen (ed.), Casarett and Doull's toxicology: The basic science of poisons, pp 471-489. New York: McGraw-Hill.

Tsutsumi, M., Lasker, J.M., Shimizu, M., Rosman, A.S., and Lieber, C.S. 1989. The intralobular distribution of ethanol-inducible P450IIE1 in rat and human liver. Hepatology. 10: 437-446.

Wagner, H., EI-Sayyad, S.M., Seligmann, O., and Chari, V.M. 1978. Chemical constituents of Cassia siamea. I. 2- methyl- 5- acetonyl- 7- hydroxychromone (cassiachromone). Planta. Med. 33: 258-261.

Wake, K., Decker, K., Kirn, A., Knook, D.L., McCuskey, R.S., Bouwens, L., and Wisse, E. 1989. Cell biology and kinetics of Kupffer cells in the liver. Int. Rev. Cytol. 118: 173-229.

Wyllie, A.H., Kerr, J.F.R., and Currie, A.R. 1980. Cell death: The significance of apoptosis. Int. Rev. Cytol. 68: 251-300.

Zimmerman, H.J. 1999. Hepatotoxicity: the adverse effects of drugs and other chemicals on the liver toxicity. 2nd ed. pp 11-145. Philadelphia: Williams & Wilkins.

APPENDIX

Table A1. Effects of barakol on aspartate and alanine aminotransferase activities in acute toxicity study.

Single dose of barakol (mg/kg; po)	AST activities (U/L)		ALT activities (U/L)	
	T24	T48	T24	T48
Control	43.50 ± 0.73	42.00 ± 1.24	16.00 ± 1.00	16.38 ± 1.65
B50	40.63 ± 1.95	48.29 ± 4.63	17.13 ± 4.49	16.86 ± 2.08
B100	41.50 ± 1.34	45.13 ± 0.93	15.88 ± 1.09	14.35 ± 1.48
B200	66.00 ± 3.58*	57.13 ± 1.98*	44.75 ± 4.28*	36.88 ± 3.68*
B300	80.38 ± 2.74*	70.50 ± 2.00*	55.38 ± 4.64*	46.88 ± 4.35*
B400	100.63 ± 5.62*	88.75 ± 4.15*	72.00 ± 7.27*	62.38 ± 7.38*
B600	105.29 ± 13.40*	114.17 ± 10.74*	40.71 ± 6.17*	50.83 ± 6.19*

Mice received various doses of barakol and blood was collected at 24 and 48 hours. Results are expressed as mean ± SEM (* $p< 0.05$).

Table A2. Effect of barakol on aspartate aminotransferase activity in acute toxicity study.

Single dose of barakol (mg/kg; po)	AST activities (U/L)			
	T24	T48	T72	T96
Control	43.50 ± 0.73	42.00 ± 1.24	43.00 ± 1.60	42.00 ± 1.49
B100	41.50 ± 1.34	45.10 ± 0.93	43.90 ± 1.67	47.30 ± 1.88
B200	66.00 ± 3.58*	57.10 ± 1.98*	53.90 ± 2.89*	43.90 ± 1.51
B300	80.40 ± 2.74*	70.50 ± 2.00*	60.10 ± 4.41*	45.00 ± 1.24
B400	101.00 ± 5.62*	88.80 ± 4.15*	74.50 ± 6.57*	43.60 ± 2.22

Mice received single dose of barakol (100, 200, 300, and 400 mg/kg), and blood was collected at different time points (24, 48, 72, and 96 hours). Results are expressed as mean ± SEM (* $p < 0.05$).

Table A3. Effect of barakol on alanine aminotransferase activity in acute toxicity study.

Single dose of barakol (mg/kg; po)	ALT activities (U/L)			
	T24	T48	T72	T96
Control	16.00 ± 1.00	16.40 ± 1.65	16.50 ± 1.39	16.60 ± 1.56
B100	15.90 ± 1.09	14.30 ± 1.48	12.40 ± 0.86	14.90 ± 1.33
B200	44.80 ± 4.28*	36.90 ± 3.68*	23.00 ± 1.76	19.60 ± 1.89
B300	55.40 ± 4.64*	46.90 ± 4.35*	37.80 ± 4.63*	22.90 ± 2.52
B400	72.00 ± 7.27*	62.40 ± 7.38*	57.00 ± 7.19*	26.40 ± 3.18

Mice received single dose of barakol (100, 200, 300, and 400 mg/kg), and blood was collected at different time points (24, 48, 72, and 96 hours). Results are expressed as mean ± SEM (* $p< 0.05$).

Table A4. Effect of barakol on total bilirubin level in acute toxicity study.

Single dose of barakol (mg/kg; po)	Total bilirubin (mg/dL)			
	T24	T48	T72	T96
Control	0.11 ± 0.01	0.12 ± 0.01	0.12 ± 0.01	0.13 ± 0.01
B100	0.26 ± 0.02*	0.23 ± 0.02*	0.20 ± 0.02*	0.21 ± 0.01*
B200	0.69 ± 0.05*	0.45 ± 0.03*	0.37 ± 0.03*	0.29 ± 0.02*
B300	0.98 ± 0.04*	0.81 ± 0.09*	0.51 ± 0.04*	0.42 ± 0.02*
B400	1.16 ± 0.09*	0.97 ± 0.06*	0.52 ± 0.04*	0.54 ± 0.05*

Mice received single dose of barakol (100, 200, 300, and 400 mg/kg), and blood was collected at different time points (24, 48, 72, and 96 hours). Results are expressed as mean ± SEM (* $p< 0.05$).

Table A5. Effect of barakol on cholesterol level in acute toxicity study.

Single dose of barakol (mg/kg; po)	Cholesterol (mg/dL)			
	T24	T48	T72	T96
Control	133.00 ± 6.24	132.00 ± 6.43	135.00 ± 4.58	136.00 ± 7.44
B100	122.00 ± 7.59	128.00 ± 5.03	128.00 ± 2.96	133.00 ± 6.53
B200	87.80 ± 2.61*	111.00 ± 3.75	125.00 ± 3.55	127.00 ± 8.10
B300	79.60 ± 5.22*	82.30 ± 2.54*	96.80 ± 4.19*	109.00 ± 4.88*
B400	86.10 ± 7.89*	68.80 ± 3.38*	101.00 ± 7.12*	100.00 ± 3.61*

Mice received single dose of barakol (100, 200, 300, and 400 mg/kg), and blood was collected at different time points (24, 48, 72, and 96 hours). Results are expressed as mean ± SEM (* $p< 0.05$).

Table A6. Effect of barakol on triglyceride level in acute toxicity study.

Single dose of barakol (mg/kg; po)	Triglyceride (mg/dL)			
	T24	T48	T72	T96
Control	205.00 ± 14.70	209.00 ± 17.50	199.00 ± 08.56	205.00 ± 19.60
B100	161.00 ± 16.80	164.00 ± 11.40	198.00 ± 20.80	163.00 ± 06.60
B200	125.00 ± 20.80*	197.00 ± 20.40	162.00 ± 21.20	179.00 ± 21.30
B300	99.70 ± 11.20*	158.00 ± 13.10	162.00 ± 11.50	151.00 ± 14.80
B400	77.40 ± 05.44*	135.00 ± 08.77*	164.00 ± 21.30	146.00 ± 16.40

Mice received single dose of barakol (100, 200, 300, and 400 mg/kg), and blood was collected at different time points (24, 48, 72, and 96 hours). Results are expressed as mean ± SEM (* $p< 0.05$).

Table A7. Effect of barakol on glucose level in acute toxicity study.

Single dose of barakol (mg/kg; po)	Glucose (mg/dL)			
	T24	T48	T72	T96
Control	290.00 ± 09.97	285.00 ± 14.30	288.00 ± 08.36	285.00 ± 10.90
B100	270.00 ± 17.20	281.00 ± 13.20	308.00 ± 13.70	292.00 ± 10.50
B200	250.00 ± 14.90	288.00 ± 09.79	269.00 ± 11.10	279.00 ± 08.88
B300	208.00 ± 14.30*	254.00 ± 09.31	253.00 ± 11.20	277.00 ± 09.72
B400	247.00 ± 15.60*	251.00 ± 09.36	247.00 ± 09.64	248.00 ± 08.15

Mice received single dose of barakol (100, 200, 300, and 400 mg/kg), and blood was collected at different time points (24, 48, 72, and 96 hours). Results are expressed as mean ± SEM (* $p< 0.05$).

Table A8. Effect of barakol on aspartate aminotransferase activity in subacute toxicity study.

Repeated doses of barakol (mg/kg/day; po)	AST activities (U/L)						
	1D	2D	4D	7D	14D	21D	28D
Control	43.50 ± 0.73	43.50 ± 1.25	42.25 ± 1.57	42.25 ± 2.23	41.38 ± 2.39	42.38 ± 1.99	44.38 ± 1.10
B100	41.50 ± 1.34	50.88 ± 2.14	81.63 ± 7.77*	158.50 ± 16.88*	236.57 ± 40.18*	289.00 ± 22.63*	312.86 ± 32.91*
B200	66.00 ± 3.58*	131.57 ± 24.81*	244.00 ± 16.41*	378.88 ± 41.15*	494.25 ± 67.98*	577.63 ± 39.01*	551.75 ± 64.48*
B300	80.38 ± 2.74*	153.67 ± 27.10*	367.88 ± 65.20*	937.50 ± 212.85*	1050.63 ± 165.76*	1053.13 ± 126.59*	619.75 ± 63.34*

Mice received barakol (100, 200, and 300 mg/kg/day for up to 28 days), and blood was collected at different time points. Results are expressed as mean ± SEM (* $p < 0.05$).

Table A9. Effect of barakol on alanine aminotransferase activity in subacute toxicity study.

Repeated doses of barakol (mg/kg/day; po)	ALT activities (U/L)						
	1D	2D	4D	7D	14D	21D	28D
Control	16.00 ± 1.00	17.00 ± 1.52	16.00 ± 1.99	17.25 ± 1.58	16.63 ± 1.91	16.38 ± 2.93	18.88 ± 1.22
B100	15.88 ± 1.09	16.88 ± 0.90	41.63 ± 6.70*	101.63 ± 11.69*	146.86 ± 32.10*	183.71 ± 12.32*	209.29 ± 17.28*
B200	44.75 ± 4.28*	85.14 ± 25.78*	84.86 ± 7.65*	194.38 ± 20.23*	208.63 ± 20.46*	336.50 ± 26.37*	271.88 ± 35.09*
B300	55.38 ± 4.64*	67.67 ± 12.93*	101.75 ± 15.44*	220.38 ± 35.77*	272.75 ± 28.98*	282.63 ± 51.61*	211.75 ± 19.25*

Mice received barakol (100, 200, and 300 mg/kg/day for up to 28 days), and blood was collected at different time points. Results are expressed as mean ± SEM (* $p < 0.05$).

Table A10. Effect of barakol on total bilirubin level in subacute toxicity study.

Repeated doses of barakol (mg/kg/day; po)	Total bilirubin (mg/dL)						
	1D	2D	4D	7D	14D	21D	28D
Control	0.11 ± 0.01	0.15 ± 0.05	0.14 ± 0.01	0.14 ± 0.01	0.16 ± 0.02	0.15 ± 0.03	0.17 ± 0.02
B100	0.26 ± 0.02*	0.46 ± 0.06*	0.97 ± 0.08*	1.35 ± 0.08*	1.49 ± 0.14*	1.30 ± 0.15*	1.45 ± 0.07*
B200	0.69 ± 0.05*	1.06 ± 0.08*	1.86 ± 0.09*	2.33 ± 0.06*	2.13 ± 0.13*	2.42 ± 0.13*	2.48 ± 0.14*
B300	0.98 ± 0.04*	1.30 ± 0.09*	2.56 ± 0.18*	3.83 ± 0.29*	3.32 ± 0.08*	2.93 ± 0.33*	3.52 ± 0.20*

Mice received barakol (100, 200, and 300 mg/kg/day for up to 28 days), and blood was collected at different time points. Results are expressed as mean ± SEM (* $p < 0.05$).

Table A11. Effect of barakol on cholesterol level in subacute toxicity study.

Repeated doses of barakol (mg/kg/day; po)	Cholesterol (mg/dL)						
	1D	2D	4D	7D	14D	21D	28D
Control	132.55 ± 6.24	132.40 ± 12.49	132.80 ± 4.42	134.66 ± 3.69	132.58 ± 9.29	134.32 ± 4.32	136.63 ± 8.83
B100	122.06 ± 7.59	118.29 ± 7.22	85.51 ± 5.14*	65.15 ± 3.84*	49.67 ± 3.49*	49.18 ± 8.48*	39.58 ± 2.74*
B200	87.82 ± 2.61*	70.63 ± 7.35*	53.89 ± 5.24*	34.39 ± 1.78*	36.24 ± 2.93*	40.27 ± 5.04*	38.32 ± 2.20*
B300	79.62 ± 5.22*	51.07 ± 7.64*	28.77 ± 3.11*	21.11 ± 2.27*	22.92 ± 2.69*	34.70 ± 6.28*	30.30 ± 3.83*

Mice received barakol (100, 200, and 300 mg/kg/day for up to 28 days), and blood was collected at different time points. Results are expressed as mean ± SEM (* $p < 0.05$).

Table A12. Effect of barakol on triglyceride level in subacute toxicity study.

Repeated doses of barakol (mg/kg/day; po)	Triglyceride (mg/dL)						
	1D	2D	4D	7D	14D	21D	28D
Control	205.41 ± 14.70	196.42 ± 11.44	194.44 ± 17.16	172.51 ± 9.34	175.01 ± 15.45	178.74 ± 25.55	191.18 ± 26.72
B100	160.84 ± 16.84	151.47 ± 20.34	102.00 ± 7.08*	97.55 ± 5.85*	107.75 ± 13.37*	92.59 ± 5.60*	94.31 ± 7.55*
B200	124.95 ± 20.76*	73.95 ± 7.88*	59.43 ± 2.78*	68.59 ± 7.03*	59.21 ± 4.54*	65.74 ± 8.73*	57.29 ± 7.46*
B300	99.71 ± 11.21*	72.59 ± 10.49*	49.73 ± 5.35*	44.41 ± 6.93*	35.61 ± 4.53*	45.03 ± 5.83*	40.06 ± 4.53*

Mice received barakol (100, 200, and 300 mg/kg/day for up to 28 days), and blood was collected at different time points. Results are expressed as mean ± SEM (* $p < 0.05$).

Table A13. Effect of barakol on glucose level in subacute toxicity study.

Repeated doses of barakol (mg/kg/day; po)	Glucose (mg/dL)						
	1D	2D	4D	7D	14D	21D	28D
Control	289.68 ± 9.97	303.61 ± 6.74	301.33 ± 9.06	272.38 ± 9.45	260.2 ± 15.84	269.74 ± 9.68	262.31 ± 19.36
B100	270.39 ± 17.22	292.17 ± 10.02	263.05 ± 10.96*	193.91 ± 6.05*	179.02 ± 12.19*	188.98 ± 4.64*	177.05 ± 7.45*
B200	250.29 ± 14.87	235.23 ± 11.49*	191.03 ± 6.04*	153.65 ± 4.52*	171.23 ± 4.75*	187.15 ± 14.87*	153.36 ± 9.74*
B300	208.26 ± 14.33*	182.34 ± 5.07*	160.66 ± 6.68*	133.72 ± 9.29*	142.25 ± 12.12*	157.71 ± 10.43*	156.26 ± 11.03*

Mice received barakol (100, 200, and 300 mg/kg/day for up to 28 days), and blood was collected at different time points. Results are expressed as mean ± SEM (* $p < 0.05$).

Table A14. Effect of barakol on mouse total hepatic microsomal cytochrome P450 contents (nmol/mg protein) in acute toxicity study.

Single dose of barakol (mg/kg; po)	Hepatic microsomal total CYP contents (nmol/mg protein)			
	T24	T48	T72	T96
Control	0.66 ± 0.02	0.61 ± 0.03	0.62 ± 0.07	0.62 ± 0.04
B200	0.58 ± 0.03	0.43 ± 0.03	0.63 ± 0.04	0.56 ± 0.02
B300	0.43 ± 0.03*	0.31 ± 0.02*	0.58 ± 0.07	0.51 ± 0.04
B400	0.41 ± 0.03*	0.26 ± 0.03*	0.43 ± 0.06	0.45 ± 0.03

The microsomal proteins were obtained from barakol treated mice (a single dose of 200, 300, and 400 mg/kg) after treatment for 24, 48, 72, and 96 hours. Results are expressed as mean ± SEM (* $p < 0.05$).

Table A15. Effect of barakol on mouse total hepatic microsomal cytochrome P450 contents (nmol/mg protein) in subacute toxicity study.

Repeated doses of barakol (mg/kg/day; po)	Hepatic microsomal total CYP contents (nmol/mg protein)			
	7D	14D	21D	28D
Control	0.53 ± 0.03	0.58 ± 0.05	0.63 ± 0.02	0.55 ± 0.03
B200	0.28 ± 0.02*	0.30 ± 0.03*	0.28 ± 0.03*	0.25 ± 0.02*
B300	0.24 ± 0.04*	0.25 ± 0.02*	0.26 ± 0.02*	0.25 ± 0.03*

The microsomal proteins were obtained from barakol treated mice (200 and 300 mg/kg/day) after treatment for 7, 14, 21, and 28 days. Results are expressed as mean ± SEM (* $p < 0.05$).

Table A16. Effect of barakol on respiratory rates and respiratory control in isolated mouse liver mitochondria with glutamate plus malate as substrates.

Barakol Concentration (mM)	RCI	P/O	Rate of state 3 respiration	% inhibition of state 3 respiration rate	Rate of state 3u respiration	% inhibition of state 3u respiration rate
0	5.24 ± 0.15	2.55 ± 0.06	12.64 ± 0.88	0	9.48 ± 1.09	0
0.075	4.30 ± 0.06*	2.79 ± 0.06	7.84 ± 0.19*	26.59 ± 1.80*	5.08 ± 0.15*	30.06 ± 2.01*
0.15	3.99 ± 0.14*	2.75 ± 0.09	8.66 ± 0.44*	27.24 ± 1.93*	5.97 ± 0.55*	32.64 ± 2.74*
0.30	3.73 ± 0.18*	2.60 ± 0.10	8.75 ± 0.44*	30.19 ± 2.18*	6.07 ± 0.45*	34.77 ± 2.62*
0.60	3.97 ± 0.17*	2.48 ± 0.04	8.62 ± 0.20*	26.86 ± 3.71*	5.57 ± 0.23*	33.90 ± 4.70*
1.20	3.60 ± 0.18*	2.54 ± 0.04	8.56 ± 0.43*	27.84 ± 3.15*	5.73 ± 0.32*	31.94 ± 5.27*
3.00	2.93 ± 0.14*	2.42 ± 0.15	7.20 ± 0.21*	41.97 ± 3.39*	3.88 ± 0.12*	56.78 ± 4.56*

Mouse liver mitochondria were incubated in a medium containing 40 mM HEPES, 2 mM $MgCl_2$, and 92 mM KCl (pH 7.4) in the presence of 1 M glutamate plus 1 M malate, 0.3 M ADP plus 0.6 M Pi, 50 mM DNP and barakol as indicated at 37 °C. The average mitochondrial protein was 32.01 mg/ml. Total volume was 1.91 ml. Various concentrations of barakol were added after glutamate plus malate as substrate, then ADP plus Pi were added. DNP was added during state 4 respiration. Results are mean ± SEM, n=4 (* p <0.05). Rate of state 3 respiration and rate of state 3u respiration are expressed as ng atom oxygen consumed per min per mg protein.

VITAE

Mrs. Watcharaporn Devakul Na Ayutthaya was born on December 1, 1969 in Nongkhai province. She completed her B.N.S. from Faculty of Medicine Ramathibodi Hospital, Mahidol University in 1992. She received her M.Sc. in Pharmacology from Fuculty of Graduate School, Chulalongkorn University in 1996 and started working as a lecture at Rangsit University.